1989

Multinuclear Magnetic Resonance Studies of Lithium Binding and Transport in Human Erythrocytes

Maryceline Tiausas Espanol
Loyola University Chicago

MULTINUCLEAR MAGNETIC RESONANCE STUDIES OF LITHIUM BINDING AND TRANSPORT IN HUMAN ERYTHROCYTES

by

MARYCELINE TIAUSAS ESPANOL

A Dissertation Submitted to the Faculty of the Graduate School of Loyola University of Chicago in Partial Fulfillment of the Requirements for the Degree of Doctor of Philosophy

May 1989

ACKNOWLEDGEMENTS

I would like to thank Dr. Duarte Mota de Freitas, my research mentor, for his encouragement, patience and guidance during the course of this study. I am most grateful for the intellectual stimulation and challenge that he provided, and for the support, both moral and financial, all of which gave me the opportunity to work on this project and present my work in various meetings and conferences.

My grateful appreciation to Dr. David Crumrine, Dr. Kenneth Olsen and Dr. Leslie Fung, for all their suggestions and assistance in the experimental design of my project. Special thanks to Dr. Thomas V. O'Halloran.

Thanks to my fellow graduate students for their support, especially to Ravi, Aida, Lisa and Sandip.

I am most grateful for the help from Dr. Leslie Fung's graduate students, particularly Benito Manolo Kalaw, Yin Zhang, Cynthia LaBrake and Li Gang; and her former students Nachu Chavrakarthy and Opinya Ekabo. The use of the facility and equipment in Dr. Fung's lab is gratefully acknowledged. I would also like to thank Thao Yang for his help in the preparation of

hemoglobin; and Dave Rockliffe and Glen Noronha for their assistance in the use of their sonicator.

I would like to acknowledge the support of the Chemistry Department faculty and staff, most especially Hazel Olson and Theresa Luhrs. I would also like to thank the Graduate School and the Arthur Schmitt Fellowship Foundation for their financial support.

My special thanks to Ray Wiebolt and Greg Nemeth for their help with the NMR at Northwestern University. I would also like to thank Kim Moore and Bill Stevens for their help and suggestions with the NMR at Loyola University.

Thanks to my good friend Marie, who made all those late night hours at the NMR lab at Northwestern bearable.

Thanks to my dearest Ernie and Marielle, who have been very supportive and who accompanied me during my grave yard shifts on Friday nights. Thanks to my family who never lost faith in me.

And finally, thank you Lord for all of these blessings.

Vita

The author, Maryceline Tiausas Espanol, is the daughter of Dr. Ligaya Mendonez Tiausas and the late Charlie Constantino Tiausas. She was born January 15, 1959, in Manila, Philippines.

Her elementary and high school education were obtained from Malate Catholic School in Manila, Philippines.

In June 1975 she was awarded the Procter and Gamble Chemistry Scholarship at De La Salle University. In April 1979 she received her Bachelor of Science with a major Chemistry and a minor in Math-Physics from De La Salle University, Manila, Philippines.

In May 1979, she joined the faculty of the Chemistry Department of her alma mater, as a half-time Chemistry Lecturer and half-time Instrumentation Laboratory Manager. In 1981, she passed the National Board Examinations for Chemistry Certification in the Philippines.

In August 1982, she entered The University of Michigan, Ann Arbor to pursue graduate studies in Chemistry. In August 1984, she transferred to Loyola

University of Chicago to pursue graduate studies in Bioinorganic Chemistry. She was awarded Research Assistantships in Summer 1986 and from June to December 1987. In September 1988 she was awarded the Arthur Schmitt Dissertation Fellowship, enabling her to complete the Doctor of Philosophy Degree in 1989, under the supervision of Dr. Duarte Mota de Freitas.

Publications

"^{7}Li NMR Studies of Lithium Transport in Human Erythrocytes", M.C. Espanol and D. Mota de Freitas, Biophys. J., 49, 326a (1986).

"^{7}Li NMR Studies of Lithium Transport in Human Erythrocytes", M.T. Espanol and D. Mota de Freitas, Inorg. Chem., 26, 4356 (1987).

"Investigation of the Biological Action of Lithium by ^{7}Li NMR Spectroscopy", D. Mota de Freitas, M.T. Espanol and R. Ramasamy, Recueil Trav. Chim. Pays. Bas, 106, 389 (1987).

"^{7}Li NMR Studies of Li^{+} Transport in Red Cells of Manic-Depressive Patients and Normal Controls", in "Lithium: Inorganic Pharmacology and Psychiatric Use" (Birch, N.J., ed.) D. Mota de Freitas, M.T. Espanol and R. Ramasamy, IRL Press Limited, Oxford, pp. 281-284 (1988).

"Measurement of Lithium Transport across Human Erythrocyte Membranes by ^{7}Li NMR Spectroscopy", in "Biological and Synthetic Membranes" (Butterfield, A., ed.), M.T. Espanol, R. Ramasamy and D. Mota de Freitas, Alan Liss Inc., New York, pp. 33-43 (1989).

"Aqueous Shift Reagents for $^{7}Li^{+}$ NMR Studies in Cells", R. Ramasamy, M.T. Espanol, K.M. Long, C.F.G.C. Geraldes and D. Mota de Freitas, Inorg. Chim. Acta, in press (1989).

"Lithium Transport in Red Blood Cells from Bipolar Patients and Matched Controls", in "Lithium and Blood" (Gallicchio, V. , ed.), Lithium Theraphy Monographs, D. Mota de Freitas and M.T. Espanol, Karger Publications, Basel, in press (1989).

TABLE OF CONTENTS

LIST OF TABLES

Page

LIST OF FIGURES

LIST OF ABBREVIATIONS

AA	atomic absorption
ATP	adenosine triphosphate
CPID	ortho-carboxyphenyliminodiacetate
CPMG	Carl-Purcell-Meiboom-Gill
^{133}Cs	cesium isotope 133
18C6	18-crown-6
15C5	15-crown-5
C211	4,7,13,18-tetraoxa-1,10-diazabicyclo-(8.5.5)eicosane
C221	4,7,13,16,21-pentaoxa-1,10-diazabicyclo(8.5.5) tricosane
C222	4,7,13,16,21,24-hexaoxa-1,10-diazabicyclo(8.8.8)hexacosane
DSM-IIIR	Diagnostic and Statistical Manual, version III, revised
$Dy(PPP)_2^{-7}$	dysprosium (III) triphosphate
$Dy(TTHA)^{-3}$	dysprosium (III) tetraethylenehexaacetate
DIDS	4,4'-disothiocyanostilbene-2,2'-disulfonic acid
$\Delta\nu_{1/2}$	NMR signal linewidth at half-height
EDTA	ethylenediaminetetraacetate
FE	flame emission
f_{in}	fractional intracellular NMR window
f_{out}	fractional extracellular NMR window

HEPES	[4-(2 hydroxyethy)-1-piperazine-ethanesulfonic acid]
hct	hematocrit
ISO	inside out
^{39}K	potassium isotope 39
^{7}Li	lithium isotope 7
MRI	magnetic resonance imaging
MIR	modified inversion recovery
NMR	nuclear magnetic resonance
^{23}Na	sodium isotope 23
^{31}P	phosphorus isotope 31
PC	phosphatidylcholine
PI	phosphatidylinositol
PS	phosphatidylserine
0.3P7.6	0.3 mM sodium phosphate, pH 7.6
5PBS7.4	5 mM sodium phosphate - saline buffer, pH 7.4
5PBS8	5 mM sodium phosphate - saline, pH 8
5P8-1Mg	5 mM sodium phosphate, pH 8, with 1 mM Mg^{+2}
RBC	red blood cells
SA	spectrin-actin
SAM	spectrin-actin matrix
SUVs	small unilamellar vesicles
SR	shift reagent
T_1	spin-lattice relaxation time
T_2	spin-spin relaxation time

TRIS	tris(hydroxymethyl)aminomethane
UDA	uramildiacetate
VAL	valinomycin

CHAPTER I

INTRODUCTION

A. Chemistry of Lithium

Lithium was first discovered in 1817 by Arfvedson in the mineral petalite in Sweden (1). Lithium is found in trace quantities in water, soil and rocks. The current principal commercial source of lithium is the mineral spodumene ($LiAlSi_2O_6$) and is being mined by the Lithium Corporation of America near Kings Mountain in North Carolina (1).

Lithium belongs to Group I of the periodic table and is the lightest member of the alkali metals. It has two naturally occurring isotopes ^{6}Li and ^{7}Li and three radioactive isotopes ^{5}Li, ^{8}Li and ^{9}Li (2). The natural abundance of ^{6}Li and ^{7}Li are 7.42 and 92.58%, respectively (1). Lithium isotopes undergo thermonuclear reactions which release large amounts of energy,

$$^{7}_{3}Li + {}^{1}_{1}H \longrightarrow 2\ {}^{4}_{2}He$$

$$^{6}_{3}Li + {}^{3}_{1}H \longrightarrow 2\ {}^{4}_{2}He + {}^{1}_{0}\eta$$

^{6}Li is also an important tritium source (1),

$$^{6}_{3}Li + ^{1}_{0}\eta \text{ ----> } ^{3}_{1}H + ^{4}_{2}He$$

The chemical properties of lithium are similar to those of magnesium and calcium, which are members of Group II. The large decrease in size as one goes down each group and the large difference in effective nuclear charge and size as one goes through the first row of the periodic table contribute to what is known as the diagonal relationship shared between lithium and magnesium. The atomic and ionic radii and the polarizing power of lithium are much closer to those of magnesium and calcium (Table 1). Lithium also has a greater covalent character than other alkali metals. The free energy of hydration is high and the lithium ion has a large hydration sphere because of its small size. Lithium ion coordinates with four, five or six water molecules, the three species being in rapid equilibrium. The first coordination sphere or the primary hydration shell of Li^{+} is tetrahedral.

Group I cations form weak complexes with oxygen ligands. However, lithium ion has also been found to have a higher affinity for nitrogen and oxygen ligands compared to other members of Group I. This property of lithium is similar to that of the magnesium ion, which has a

Table 1

Properties of Some Alkali and Alkaline Earth Metals

Cation	Ionic Radius[a] /Å	Hydrated Radius[a] /Å	C.N.[b]	Charge Density[c] /10^{20}C Å^{-3}	Heat of Hydration[c] kJ/mol
Li^+	0.68	3.40	4,6	12.1	515
Na^+	0.95	2.80	6	4.46	406
K^+	1.33	2.32	6,8	1.62	322
Mg^{+2}	0.65	4.67	6	26.8	1940
Ca^{+2}	0.99	3.21	6,8	7.9	1600

[a] taken from ref. 1; [b] coordination number; [c] taken from ref. 2.

preference to bind nitrogen donors compared to other members of Group IIA cations which also prefer oxygen coor--dination. Uramildiacetate and orthocarboxyphenyl-iminodiacetate are examples of nitrogen containing ligands that bind Li^+ (3). The stability constants for some complexes of oxygen and nitrogen containing ligands and alkali and alkaline earth metal cations are shown in Table 2. Alkali metal ions also form stable complexes with macrocyclic (crown ethers and naturally occurring ionophore antibiotics like valinomycin and monensin) and cryptate (like C211, C221 and C222) ligands (4). The structures for some of these ligands are shown in Figure 1. The selectivity and the affinity of these ligands for the metal ion depends on how well the ion fits in the ligand cavity (Table 3). The oxygens and the nitrogens in these ligands are the metal chelating sites. Complexation of alkali metal ions by these ligands have been attributed to the electrostatic attraction between the cation's positive charge and the negative dipolar charge on the heteroatoms.

Crown ethers are polyethers. For example, in 18-crown-6, 18 refers to the number of ring atoms, crown refers to the class specification and 6 refers to the number of heteroatoms in the ring. Addition of an oligoether chain to the classic monocyclic crown ether results in what is called a cryptand. Conventional cryptands possess 2 bridgehead nitrogens which are joined

Table 2

Stability Constant in log K^j at 25°C

Ligand	Solvent	Li^+	Na^+	K^+	Mg^{+2}	Ref.
EDTA[a]	H_2O	2.8	1.7	1.0	-	3
$P_2O_7^{-4}$	H_2O	2.4	2.3	1.5	2.3	3
C211[b]	H_2O	5.3	2.8	<2	-	5
C221[c]	H_2O	2.5	5.4	3.9	-	5
C222[d]	H_2O	<2	3.9	5.4	-	5
18C6[e]	H_2O	-	0.3	2.06	-	5
15C5[f]	H_2O	-	0.7	0.74	-	5
UDA[g]	H_2O	4.9	2.7	1.2	8.1	3
CPID[h]	H_2O	2.1	0.9	-	6.9	3
Val[i]	CH_3OH	1.3	0.7	4.9	-	5

[a] ethylenediaminetetraacetate; [b] 4,7,13,18-tetraoxa-1,10-diazabicyclo-(8,5,5)eicosane; [c] 4,7,13,16,21-pentaoxa-1,10-diazabicyclo(8,8,5)tricosane; [d] 4,7,13,16,21,24-hexaoxa-1,10-diazabicyclo(8,8,8)hexacosane; [e] 18-crown-6; [f] 15-crown-5; [g] uramil-diacetate; [h] orthocarboxyphenyliminodiacetate; [i] valinomycin; [j] M^{-1}

Figure 1. Structure of Li^+ Ligands

(A) 18-Crown-6

(B) Uramildiacetate

(C) C211(l=1, m=n=0)
C221(l=m=1,n=0)
C222(l=m=n=1)

(D) o-carboxyphenyl-iminodiacetate

A

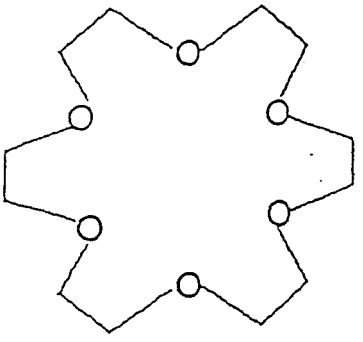

B

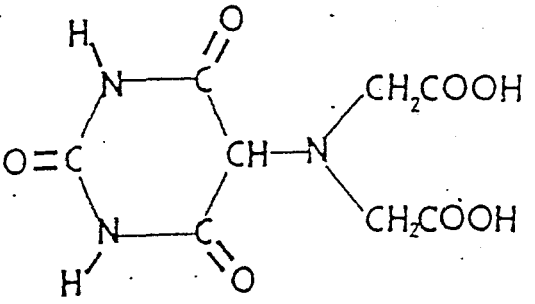
H
N
O
C
O=C
CH
N
CH2COOH
CH2COOH
N
C
H
O

C

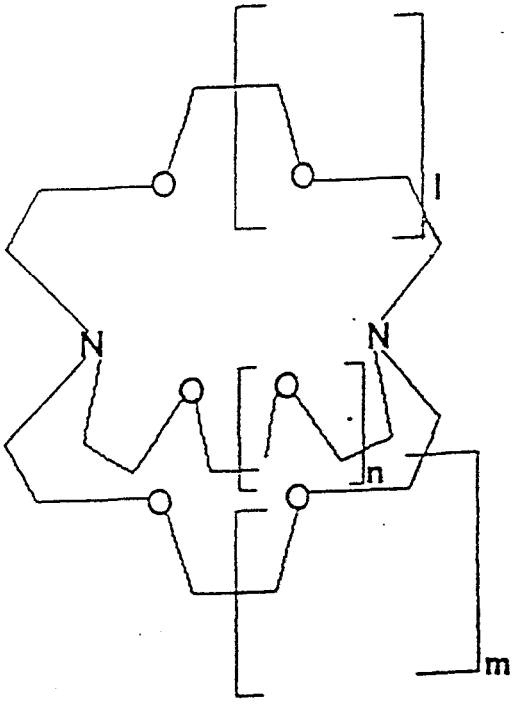
l
N
N
n
m

D

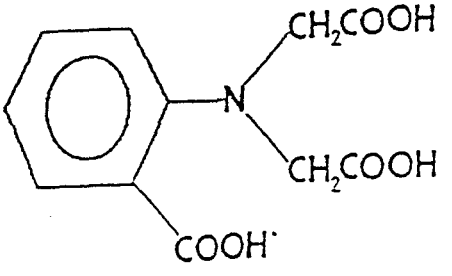
CH2COOH
N
CH2COOH
COOH

Table 3

Crown and Cryptate Ligand Selectivity

Ligand	Cavity Diameter/Å	Selectivity	Reference
12-Crown-4	1.2	$Li^+ > Na^+$	2
14-Crown-4	1.2-1.5	$Na^+ > K^+$	2
15-Crown-5	1.7-2.2	$Na^+, K^+ > Cs^+$	2
C211	0.8	$Li^+ > Na^+$	6
C221	1.2	$Na^+ > K^+$	6
C222	1.4	$K^+ > Cs^+$	6

by three oligooxachains of different lengths and number of donor atoms (4). Cryptands are actually better ligands for alkali metal ions because they have three-dimensional selectivity unlike crown ethers which only give two-dimensional selectivity.

In biological membranes, the lipid bilayer presents a hydrophobic barrier to the transport of hydrated cations of Group IA and IIA. The translocation of metal cations can occur either by an active transport involving an enzyme-linked ion pump which requires energy derived from adenosine triphosphate (ATP) or facilitated diffusion by an ion carrier or through an ion channel, following a concentration gradient. Crown ethers, cryptands and ionophore antibiotics can be used to study ion transport across cell membranes. Their complexation of alkali metal cations in organic solvent presumably mimic their activity in biological membranes (8). A characteristic feature of these macrocylic molecules is that they all have a cavity that will bind a cation with varying selectivity, while the resulting complex has a hydrophobic exterior that can cross or span the membrane. Therefore, they can be used as models for ion carriers and ion channels postulated to be present in natural membranes. This provides a unique experimental approach to the study of ion transport and the role of metal cation gradients on bioenergetics.

The chemistry and biochemistry of lithium have been

the subject of several reviews (2,7,8).

B. Nuclear Magnetic Properties of Lithium

The nuclear magnetic properties of lithium and other alkali metals are summarized in Table 4. The majority of these metals have nuclear spin quantum numbers ≥ 1 and relatively large quadrupole moments thus making quadrupolar relaxation the predominant mechanism. Both isotopes of lithium have low quadrupole moments and other competitive relaxation mechanisms like dipole-dipole and spin rotation are present as well. The most abundant isotope of lithium, ^{7}Li, is a high receptivity nucleus (1540 relative to ^{13}C). ^{7}Li isotope is a spin I=3/2 system, and three transitions are possible. In general, all three transitions are degenerate. However, in a situation where an asymmetrical electric field is present around the Li^{+} ion, this degeneracy is lifted and only the central +1/2 <——> -1/2 line may be visible resulting in an overall loss in resonance intensity of 60%. A loss of signal intensity by a factor other than 60% is generally indicative of Li^{+} binding. This makes ^{7}Li nuclear magnetic resonance (NMR) spectroscopy an important tool to monitor binding and transport of lithium ions in cell membranes. Paramagnetic and diamagnetic contributions to the chemical shift tend to cancel each other out for this isotope leading to a narrow chemical shift range for ^{7}Li NMR (9). The other isotope of

Table 4

Nuclear Properties of Alkali Metals

Isotope	^{6}Li	^{7}Li	^{23}Na	^{39}K	Ref.
Nat. Abundance (%)	7.42	92.6	100	93.1	9
Spin Number, I	1	3/2	3/2	3/2	9
Gyromagnetic Ratio (10^{7} rad $T^{-1}s^{-1}$)	3.9	10.4	7.1	1.3	9
Quadrupole Moment (10^{-28} m^{2})	-0.0008	-0.045	0.12	0.055	9
Receptivity relative to ^{13}C	3.6	1540	525	2.7	9
Chemical Shift (ppm)	5	5	30	30	10
Resonance Freq. (^{1}H - 300 MHz) MHz	44.2	116.6	79.4	7.7	-
T_1 (s)	10-80	0.3-20	$\leq$ 0.06	$\leq$ 1.33	10
$\Delta\nu_{\frac{1}{2}}$ (Hz)	1	1	14	13	10

lithium, ^{6}Li, has a natural abundance of 7.42% making its receptivity only 3.58 relative to ^{13}C. The two lithium isotopes have low quadrupole moments which explain the line width narrowness of the observed NMR signals. ^{6}Li behaves like a spin 1/2 nucleus. Studies with ^{6}Li spin-lattice relaxation time for aqueous LiCl solutions showed that the dipole-dipole and spin-rotation contribution account for 84 and 8%, respectively, at 40°C. The contribution of the quadrupolar mechanism is negligible. For aqueous LiI solution, the contribution of the dipolar mechanism accounts for 30% of the ^{7}Li spin-lattice relaxation time (9).

C. Lithium in Psychiatry

Lithium ion (Li^{+}) has been used extensively in psychiatry, particularly in the treatment of bipolar or manic-depressive patients (11). This disease is a bipolar affective disorder that is characterized by severe mood swings cycling from a manic to a depressive state. Symptoms of mania can include physical restless, increased talkativeness, racing thoughts and inflated self-esteem extending to delusions of grandeur. Depressive episodes are characterized by a mood of hopelessness, decreased energy, loss of interest and feelings of worthlessness, extending to thoughts of death. Bipolar disorder is not a rare disease. It is estimated that at least 1 in every

1000 individuals in the United States, Great Britain and Scandinavian countries are undergoing lithium therapy (11). Lithium is generally administered in the form of lithium carbonate and patients normally take between 200-1600 mg a day to maintain a therapeutic plasma Li^+ level of 0.5-1.2 mM. Lithium exerts its effect by controlling acute manic states as well as decreasing the frequency of relapses in bipolar patients. Moreover, lithium has found applications in other areas of medicine including control of herpes simplex virus related infections and in white blood cell count regulation during cancer chemotherapy (11).

D. Possible Mechanisms of Action of Lithium

Despite the fact that lithium has proven to be an effective psychotropic drug for more than a decade, the mechanism by which the Li^+ cation exerts its biological action still remains questionable. A number of reviews on the biological action of lithium and its use in psychiatry have been published (2,3,7,8,12,13). Several hypotheses for the biological action of lithium have evolved based on biochemical (14), genetic (15-17), bioinorganic (3) and physiological (18) studies. Lithium may exert its pharmacological effects by inhibiting neurotransmitter-stimulated activity of cerebral adenylate cyclase (14). The effect of lithium on this system is specific because it is not shared by other monovalent cations like sodium,

potassium, cesium and rubidium. It is also selective because only the hormone activated enzyme activity is affected. Thus lithium may be interfering with the adrenergically activated-adenylate cyclase by influencing one or more of these regulated processes. This mechanism could only explain the antimanic therapeutic effect of lithium.

At therapeutic concentrations (0.5-1.2 mM Li^+ in the plasma), lithium also blocks the cholinergically-activated phosphatidyl inositol turnover (19-21). Lithium inhibits the enzyme inositol-1-monophosphatase. The phosphoinositide system is a prominent second messenger for neurotransmitters (19). The inhibitory effect of lithium alters the phosphoinositide signal transduction by limiting the regeneration of inositol. The dampening action of lithium on the phosphoinositide-associated neurotransmission could prevent interaction of individual neurotransmitter systems with different phosphoinositide-linked transmitters separately involved in manic and depressive episodes. This may explain the normalizing action of lithium in the prophylactic treatment of both mania and depression. It was also found that lithium blocks the activity of two types of guanine nucleotide binding proteins (G proteins), G_s and G_i or G_o. These two different types of G proteins may provide a common site for both the antimanic and antidepressant therapeutic effects

of lithium (14). It is possible that the Li^+ ion may act by competing with Mg^{+2} ions, known to be required for GTP binding to G proteins. The mechanisms cited above also involve calcium dependent and/or calcium regulated enzyme systems. In a recent review (22), the dual hypothesis was put forward; bipolar illness may be a result of disorders in calcium regulated functions and lithium ion may reverse or counterbalance these dysfunctions.

Another proposed hypothesis linking lithium to manic-depression or bipolar illness is cell membrane dysfunction (18). This followed from studies carried out with red blood cells (RBCs). Evidence has accumulated in recent years lending support to this cell membrane theory. Some investigators have claimed that the therapeutic response of bipolar patients undergoing prophylactic lithium treatment can be monitored by looking at the steady state RBC/plasma lithium ratio. Patients who respond to lithium treatment had higher RBC/plasma ratios (23-26). A number of groups have also identified and characterized a component of erythrocyte lithium transport that is significantly different in a subgroup of manic-depressive patients compared to controls (23-27): the Na^+-Li^+ countertransport (or exchange) system. Although some groups have reported that the rate of Na^+-Li^+ exchange for bipolar patients are lower than that of normal controls (28,29), other investigators failed to find any significant

difference between rates for bipolar patients and controls (30-34).

Investigations on the abnormalities of lipid metabolism and composition in platelets and red blood cells revealed a significant alteration of the levels of phosphatidylcholine (PC) and phosphatidylserine (PS). There was an increase and decrease in both PC and PS levels, for schizophrenics and manic depressives, respectively (35). Data obtained from other studies indicated that lithium irreversibly blocks the transport of choline across the RBC membrane resulting in the accumulation of free choline in RBCs of manic-depressive patients on lithium therapy (36,37). In animal model studies, lithium has also been found to affect the brain's serotonergic system by altering the regional turnover of serotonin and increasing the availability of the serotonin precursor, tryptophan. This may be related to the biogenic amine hypothesis for affective disorders associating the therapeutic action of lithium with alterations in amine neurotransmission (38-41).

E. Lithium Transport in Red Blood Cells

In human RBCs the transport of Li^+ across the cell membranes (Figure 2) follows the same pathways as sodium (42). Li^+ is transported out of RBCs via the Na^+-Li^+ countertransport system and to a small extent by the sodium

Figure 2. The major pathways for Li^+ influx are through the Band 3 Protein and through the Leak mechanisms and the major pathway for Li^+ efflux is through the Na^+-Li^+ Countertransport system. The contributions of the Na^+-K^+ Pump and the Li^+-K^+ Cotransport in transport of Li^+ across the cell membrane are negligible under physiological conditions.

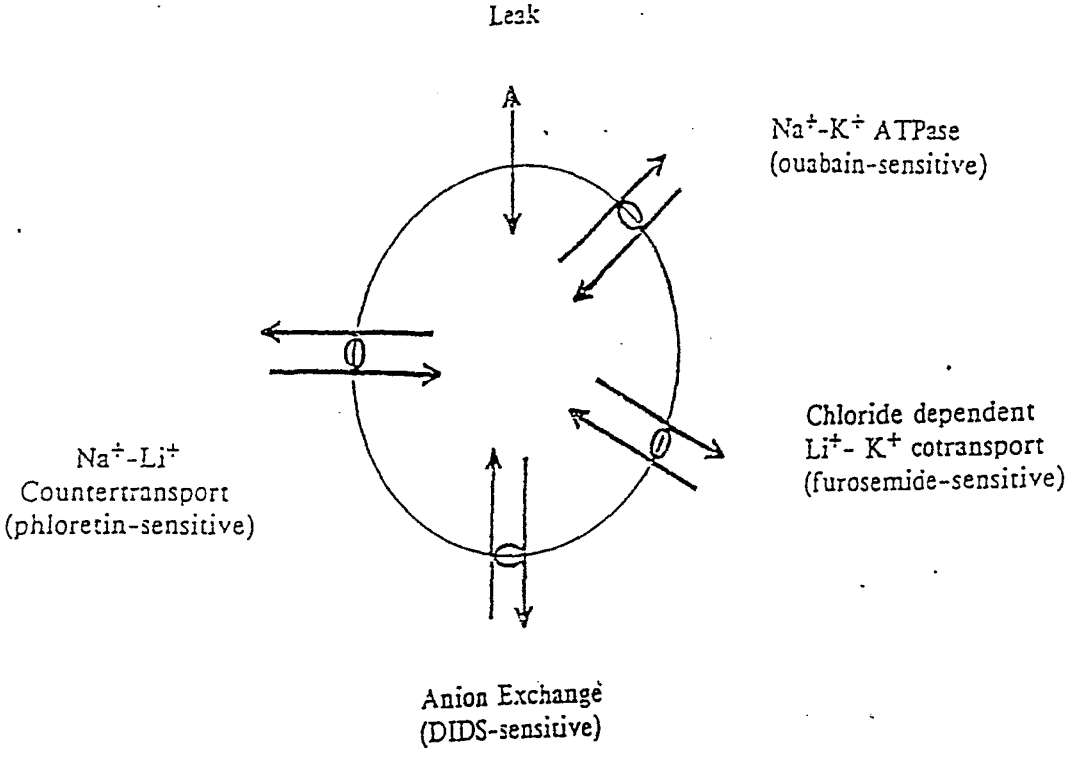
Leak
Na^+-K^+ ATPase
(ouabain-sensitive)
Chloride dependent
Li^+- K^+ cotransport
(furosemide-sensitive)
Na^+-Li^+
Countertransport
(phloretin-sensitive)
Anion Exchange
(DIDS-sensitive)

pump. On the other hand, Li^+ entry in human RBCs can proceed by passive leak across the RBC membrane and by a chloride dependent system that transports both sodium and potassium. In addition Li^+ entry is also mediated by the anion exchange protein, exchanging $LiCO_3^-$ for Cl^-. This last pathway is not shared by sodium.

1. Lithium Transport Pathways

a. The Na^+-K^+ Pump

The sodium pump is the ouabain inhibited (Na^+,K^+)-ATPase system and is responsible for maintaining the distribution of Na^+ and K^+ ions across the RBC membrane as well as across the neuronal membrane. Normally the intracellular potassium is high while the free intracellular sodium and calcium are low. Na^+ is transported out while K^+ is transported into the cell by the sodium pump at the expense of ATP (43). Cation transport mediated by the sodium pump is an active transport process because it utilizes energy and the ion movements are against the concentration gradients. Due to similarities in the chemical properties of Na^+ and Li^+ ions, it was originally thought that at therapeutic levels, Li^+ could mimic Na^+ and be actively transported out of the cell by the sodium pump. However, ouabain-sensitive Li^+ efflux from RBC only proceeds under conditions in which intracellular Na^+ and K^+ are absent (44,45). Similarly Li^+

may be transported into the cell via this pathway by mimicking potassium only under conditions in which extracellular Na^+ and K^+ are replaced by choline (46). Although the activity of the (Na^+,K^+)-ATPase system in RBCs has been found to be reduced in manic-depressive patient (47,48), other studies have shown elevated erythrocyte membrane Mg^{+2} and (Na^+,K^+)-ATPase activities in both depressive and manic-depressive patients compared to controls (49,50). However, lithium transport by this pump is not significant under physiological conditions (44,51).

b. The Li^+-K^+ Cotransport

Li^+ entry through the chloride-dependent Na^+-K^+ cotransport system is blocked by loop diuretics like furosemide and bumetanide (52). Experiments where the RBCs were loaded with three different cation pairs [Na^+ + K^+], [Li^+ + K^+] and [Na^+ and Li^+], demonstrated that Li^+ can replace Na^+ but not K^+, in the furosemide-sensitive Na^+-K^+ cotransport pathway. Extracellular Li^+ or K^+ was found to inhibit furosemide-sensitive effluxes of Na^+ or K^+. The magnitude of Li^+ efflux through this pathway increased as cell Li^+ increased and K^+ concentration decreased. Li^+ transport can also be driven against its electrochemical gradient by a K^+ gradient. When Cl^- was replaced by NO_3^-, inhibition of the furosemide sensitive Na^+-K^+ cotransport was observed.

c. The Na^+-Li^+ Countertransport

The distribution of lithium across the cell membrane, which results in lower intracellular lithium concentration relative to the extracellular lithium concentration, is maintained by the Na^+ - Li^+ countertransport pathway (53,54). This mechanism is analogous to those described for other cell system attributed to the Na^+-Na^+ exchange diffusion (55). This pathway is inhibited by phloretin, furosemide, quinine and quinidine and does not require ATP (42,51,54). At physiological conditions there is a tightly coupled 1:1 Na^+-Li^+ exchange where lithium is transported out and sodium is transported into the cell. This countertransport system has an affinity 15 to 18 times greater for lithium than for sodium (56). However, since the plasma sodium concentration is 140 times more than that of lithium, the transport sites on the outer leaf of the cell membrane will bind sodium predominantly. Lithium is then transported against an electrochemical gradient and the energy to drive the transport is derived from the large Na^+ gradient which is maintained by the sodium pump (57). It is important to note that the Na^+ electrochemical gradient found in nerves is the energy source for the flow of bioelectric currents necessary for neurotransmission (58). Increasing extracellular Na^+ stimulates Li^+ efflux through this pathway, reaching saturation at 150 mM Na^+ (54), and

reversing the Na^+ gradient reverses the direction of Li^+ transport (56).

Neither Ca^{+2}, Mg^{+2}, K^+, Rb^+, Cs^+ nor choline substitution for Na^+ induces an increase in Li^+ efflux. Na^+ efflux in Na^+ pre-loaded RBCs was significantly stimulated when extracellular Li^+ was substituted for K^+. This system then promotes Na^+-Li^+ exchange in both inward and outward directions. It is still not known whether this pathway is a mobile carrier or a spanning membrane protein ion channel (54,56). Both these models support a consecutive or simultaneous mechanism in which both the intra- and extracellular binding sites are complexed at the same time. The greater negative charge on the inner leaf due to phosphatidylserine headgroups may induce a concentration of the cations around the transport site. On the other hand, the negatively charged moieties of the sialic acid and glycophorin on the outer leaf of the red cell membrane are farther from the membrane surface and they may not significantly influence the local distribution of the cations around the extracellular transport site. Thus the difference in affinities on the inner and outer leaf of the RBC may also be partly due to excess negative charges on the inner leaf (56).

Sarkadi et al. (56) used a one variable analysis to look at the kinetics of Na^+-Li^+ countertransport fluxes. However the model did not discriminate among the different

molecular mechanisms. Garay and Hannaert (54) used a two-variable kinetic analysis, as a function of intra- and extracellular cation concentrations, and proposed a quantitative consecutive "ping-pong" model of Na^+-Li^+ countertransport. The rate-limiting step of the overall reaction is cation translocation. This is based on the carrier model (Figure 3) proposed by Sarkadi et al. (56) . Based on this assumption, the values of the equilibrium dissociation constants are independent of the extracellular cation concentrations and competitively modified by intracellular cation. This kinetic model confirmed that the rates of Li^+ efflux through this pathway appears two-threefold much faster than Na^+ efflux.

d. The Leak Pathway

The leak mechanism represents passive diffusion of lithium across the cell membrane probably through pores in the membrane. This is dependent on the cells resting potential. Under physiological conditions, this pathway contributes to both influx and efflux of lithium across the cell membrane (46). If passive diffusion is the only mechanism responsible for the distribution of lithium ions across the cell membrane, the intra- and extracellular Li^+ distribution should follow the Donnan equilibrium ratio of 1.2 observed for Cl^-. However, the RBC to plasma Li^+ ratio is always less than 1. Therefore other transport pathways are at play. Li^+ transport through this pathway does not

Figure 3. The Na^+ - Li^+ countertransport pathway is thought of as a carrier, represented as "C" in the diagram. Li^+ forms a complex with the carrier in the inner leaf and is transported out of the cell. Na^+ forms a complex with the carrier in the outer leaf and is transported into the cell.

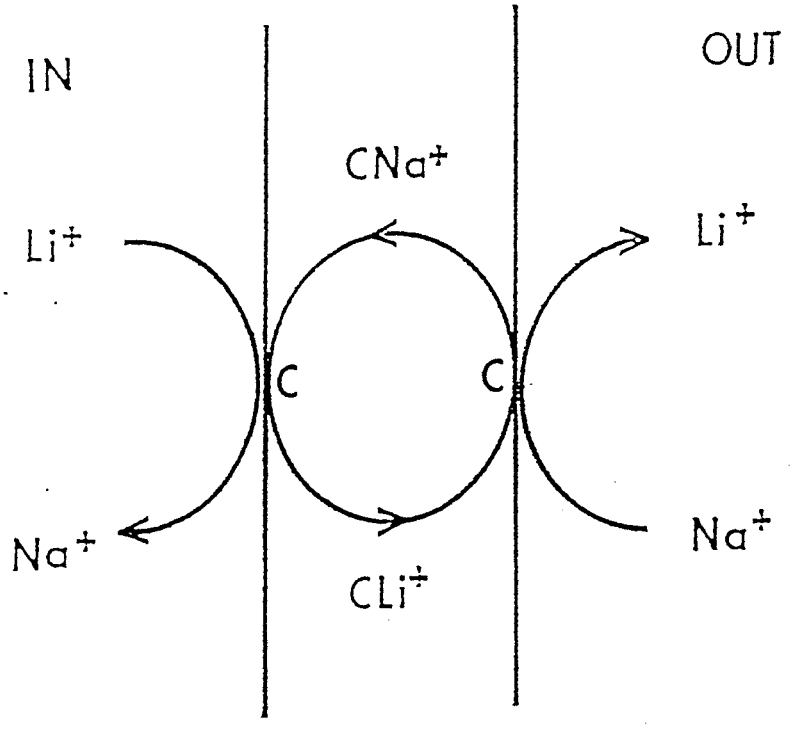
IN
OUT
CNa+
Li+
Li+
C
C
Na+
Na+
CLi+

seem to be affected by lithium treatment (51).

e. The Band 3 Protein

The bicarbonate sensitive pathway or the anion exchange pathway is different from the leak mechanism in that lithium is transported as a cation in the latter and as an anion in the former. The leak and the bicarbonate sensitive pathway account for 70 and 30%, respectively, of lithium influx into RBCs (46). The anion exchanger or the band 3 protein is a membrane spanning protein that allows the 1:1 exchange of Cl^- for Cl^- or Cl^- for HCO_3^- (59). A twelve-fold increase in the influx of lithium into RBCs was observed when bicarbonate was used instead of chloride in the suspension medium. This bicarbonate dependent lithium influx disappeared upon addition of 4,4' diisothiocyanostilbene-2,2'-disulfonic acid (DIDS) (59). DIDS is a well known inhibitor of the anion exchange protein, band 3. Thus the bicarbonate stimulated lithium influx is due to the complex formation of lithium with $CO_3^=$, to form a negatively charged ion pair (60).

Monovalent anions are ineffective because 1:1 ion pairs with alkali cations result in neutral species. On the other hand, ion pairs from trivalent anions and monovalent cations result in species with two negative charges. Transport through the anion exchange system requires 10^4 times as much divalent anion concentration compared to monovalent anions (42). Several divalent

inorganic as well as organic anions like succinate malonate, sulfate, maleate, monomethylphosphate, phthalate, phosphite, oxalate and sulfite have also been found to stimulate the DIDS-sensitive Li^+ transport (42). A preference for Li^+ over Na^+ in the transport as ion pairs was observed. In the dehydrated state, the diameter of the Li^+, Na^+ and K^+ cations increases from 1.4 to 1.9 to 2.6 Å. Due to its small size and high charge density, the Li^+ cation fits very well in the site between the anionic poles of bicarbonate and therefore is easily accommodated through the channel of the band 3 protein.

f. Other Pathways

Although Li^+ and Na^+ transport pathways in RBCs have been the subject of numerous studies, very little is known about the transport of divalent cations like Mg^{+2} or Ca^{+2}. The effects of Li^+ on Mg^{+2} or Ca^{+2} transport pathways have not been studied in detail. Because of the diagonal relationship between Li^+ and Mg^{+2} in the periodic table, similarities in their chemical properties may be such that plasma Li^+ could stimulate Mg^{+2} efflux from RBCs. Na^+, but not Li^+, has been found to stimulate Mg^{+2} transport in RBCs (63). Using ^{31}P NMR and optical spectroscopy, Ramasamy and Mota de Freitas found that Li^+ competes with Mg^{+2} for ATP in Li^+-loaded RBCs and that the released Mg^{+2} binds to the RBC membrane (64). Li^+ has also been found to activate the transport of Ca^{+2} (65).

Furthermore, abnormal calmodulin-activated Ca^{+2} - ATPase activity in RBCs from lithium carbonate treated and untreated bipolar patients, relative to normal controls, has been reported (65).

2. Abnormalities in Li^+ Transport in RBC from Bipolar Patients and Normal Controls

It has been established that bipolar disorder is a genetically inherited condition (14-17,23-26). Several studies have been conducted to determine whether the abnormalities observed in the Na^+-Li^+ countertransport rates in RBCs from bipolar patients can be used as genetic markers.

Although several groups have reported a decrease in Na^+-Li^+ countertransport rates in a subgroup of bipolar patients (23-26) and in some members of the patient's family (24), other investigators obtained no significant difference between bipolar patients and normal controls (30-34). Thus it is not clear at present whether a difference in RBC Na^+-Li^+ countertransport rates between bipolar patients and normal controls is related to the etiology of the disease. Intraindividual variation (66,67) as well as interindividual differences (30,31) have resulted in overlapping Na^+-Li^+ countertransport rates between patients and controls. Differences in RBC Na^+-Li^+ countertransport rates were observed between white and black populations; the rate constant for Li^+ efflux through

this pathway was found to be larger in whites than in blacks. Thus, some of the interindividual variations may be related to racial dissimilarities in the cellular metabolism involving cation transport (68). These observations seem to agree with genetic studies conducted on the Older Order Amish community in Eastern Pennsylvania. It was found that two marker genes near the tip of the shorter end of chromosome 11 have the same pattern of inheritance as does predisposition to develop the illness (15). Parallel studies (16,17) showed that for other populations the inheritance of bipolar disorder is not associated with the portion of chromosome 11 that contains the marker genes mentioned above. Therefore there may be several genetic defects that predispose an individual to develop bipolar disorder and these could account for the variations in the observed Na^+-Li^+ countertransport rates.

In clinical studies performed with manic-depressive patients initiating lithium therapy, it was found that it took about 1-4 days before Li^+ inhibition of RBC Na^+-Li^+ countertransport exchange can be detected and that it took about 4-7 days to achieve maximum inhibition (69,70). It has been claimed that the Na^+-Li^+ countertransport rates were also found to be lower during a manic-depressive episode than after remission and lower in mania than in depression compared to controls (27). During prophylactic lithium therapy, negative correlation was observed between

in vitro RBC Na^+-Li^+ countertransport rates and RBC to plasma Li^+ ratios. Higher RBC to plasma Li^+ ratios were correlated with low RBC Na^+-Li^+ countertransport rates, and vice versa (28,29). However, a separate study conducted with a large number (n=126) of randomly selected blood donors only showed a moderate negative correlation (r=-.61) between Na^+-Li^+ countertransport rates and Li^+ RBC/plasma ratios (31a). Some investigators claimed that not all bipolar patients respond to lithium therapy and patients who do respond to the treatment have been found to develop higher RBC to plasma Li^+ ratios. Thus, the ratio may be used as an indicator of patient response and the differences in Na^+-Li^+ countertransport activity in RBC results in variation in the extent of intracellular Li^+ accumulation. However, the higher Li^+ ratios, just like the lower Na^+-Li^+ countertransport rates, reported for manic-depressive patients do not appear to be statistically significant (31).

Most of the bipolar patients on lithium therapy at the time the measurements were made, exhibited lower Na^+-Li^+ countertransport rates compared to lithium free bipolar patients. The observed decrease in Na^+-Li^+ countertransport rates may be due to a slow inhibition of the transport process by Li^+ (69,70). This is an important factor because the assays for maximal Na^+-Li^+ countertransport rates were measured in a suspension medium

in the presence or absence of sodium. However, some of the measurements were conducted in the presence of extracellular Li^+ (26,71). The presence of both intra- and extracellular Li^+ has been found to inhibit the countertransport to a greater extent than having the same concentration of Li^+ on either side of the membrane alone (70). It is possible that the observed differences in RBC Li^+ transport are drug-induced effects (52), rather than disease related, since the Li^+ ion causes a slow inhibition of Na^+-Li^+ countertransport (70). Although the mechanism behind the slow inhibition of Na^+-Li^+ countertransport by Li^+ is still unknown, Ehrlich et al. (70) proposed several possible explanations: (1) the effect on countertransport may be due to alterations in membrane lipid composition, which may be affected in turn, by lithium's effect on the rate of choline production from membrane lipids; and, (2) Li^+ may be interacting with the membrane causing alterations on the rate of phospholipid flip-flop of the RBC membrane, thereby affecting countertransport or other membrane transport processes of other solutes.

Disagreement among observations made by several investigators may also be due to other factors (29). Methodological differences in defining the clinical criteria for treatment or diagnosis may be one factor. The affective state of the patients at the time of the sampling may contribute to the variations in the results obtained.

Differences in the RBC to plasma Li^+ ratios have been observed between bipolar and controls and between responders and nonresponders. Bipolar and unipolar patients who respond to Li^+ therapy exhibit higher RBC to plasma Li^+ ratios (71,72). The rates of RBC Na^+-Li^+ countertransport have been found to be lower for bipolar patients and higher for unipolar patients compared to controls (27).

RBC Na^+-Li^+ countertransport rates have also been proposed as markers of essential hypertension (73). Essential hypertension may also play an important role as a clinical variable in psychiatric patients because higher Na^+-Li^+ countertransport rates have been observed for hypertensive individuals compared to controls. Increased RBC Na^+-Li^+ countertransport rates were observed in patients with a major depressive disorder with personal or family histories of essential hypertension, compared to depressed patients or normal controls with no such histories (74).

Another problem is patient population sampling. If outpatients are involved, compliance with Li^+ medication may be inconsistent. This is apparent when measurements of RBC to plasma Li^+ ratios are taken from outpatients. Some of the studies on the Na^+-Li^+ countertransport rates were also obtained from a limited number of patients (23,26,32-34). Whether Na^+-Li^+ countertransport rates play a role in

the etiology of bipolar illness would require extensive studies on a larger population size of well defined bipolar patients, in a particular affective phase, who are on lithium therapy only, and who do not have any history of essential hypertension.

F. Techniques used for Measuring Li^+ Levels and Li^+ Transport in RBCs

Several analytical methods (75) have been used for monitoring Li^+ levels in the blood. They include atomic absorption, flame emission, spectrophotometry, fluorescence, ion-selective electrodes and neutron activation analysis. These techniques provide information about total intra- and extracellular Li^+ concentrations in RBCs. The advantages and disadvantages of analytical techniques used in the measurement of serum Li^+ levels have been the subject of a recent review (75). The use of neutron activation analysis for determination of serum Li^+ levels has also been described in the literature (76).

1. Conventional Analytical Methods

Conventional methods require physical separation of the intra- and extracellular compartments prior to chemical analysis. This usually involves subjecting the blood samples to centrifugation to separate the plasma from the cells. The cells are washed repeatedly in an isotonic non-Li^+ containing buffer, followed by cell lysis. The intra-

and extracellular Li^+ concentrations are then determined by comparing with standard Li^+ solutions with a composition similar to that of the blood samples being analyzed.

The sample processing required by most conventional methods makes the entire procedure time consuming. The invasive nature of conventional techniques may also lead to errors due to non-specific ion binding and additional ion transport during sample processing. One problem about this kind of approach is that when the two cell compartments are isolated, the ionic distribution may be different compared to intact cell systems where the two compartments are in contact with each other. This may be due to ionic equilibrium adjustments across the cellular membrane during sample processing in isolated systems. In intact cell systems, there is a steady state Li^+ distribution across the cell membrane.

Both flame emission (FE) and atomic absorption (AA) spectrometries generally use a flame as the atomization source. The lysed RBC and plasma samples are usually aspirated into the flame. Upon exposure to the flame, the samples are vaporized into free atoms, including Li atoms. A small portion of the free atoms will be in the excited state. As a result of the return of the excited free atoms to the ground state, light at specific wavelengths characteristic of each element is emitted. Alkali metals are excited at much lower temperature than most elements.

The atomic spectra of these alkali metals are also well resolved. This makes Li emission suitable for FE lithium determinations in blood samples. With AA, when a light beam produced from a hollow cathode lamp, with a wavelength characteristic of the lithium spectrum is passed through the vaporized sample, the ground state free Li atoms will absorb some of the light. The Li^+ concentration in the sample is directly proportional to the intensity emitted or absorbed radiation, measured by FE and AA respectively. AA is more specific than FE because a Li lamp is used and only the ground state free Li atoms will absorb the radiation. In recent years, the introduction of graphite furnaces (electrothermal or flameless atomization AA) or coupled plasmas (in inductively coupled plasma emission spectrometry) have considerably increased the sensitivities of AA and FE. Due to cost considerations and ease of operation, both AA and FE continue to be used, however, in clinical laboratories (77,78).

Spectrophotometric methods using optical and fluorescent dyes have also been used in the determination of Li^+ concentrations in biological fluids. Finding a reagent that is highly selective for Li^+ ions is a major problem with these techniques. In blood plasma, sodium ions are present at a one hundred-fold excess over Li^+. As a consequence of the similarities of the chemical properties of sodium and lithium ions, the affinities for

the optical and fluorescent dyes are almost the same.

Recently, highly selective Li^+ reagents such as crownazophenol-5 and 1,8-dihydroxyanthraquinone (79-81) have been developed. Lithium ion selective electrodes (82-85) are made by incorporating a Li^+ specific reagent (generally a 14-crown-4 derivative) into a liquid membrane. These electrodes have been used recently to monitor serum Li^+ levels in manic-depressive patients. Because the therapeutic level of Li^+ in the plasma is very near its toxic plasma concentration ($\geq$ 2.0 mM) there is a need for regular monitoring of serum Li^+ levels in manic-depressive patients. The advantages presented by low cost of instrumentation and ease of operation of both spectrophotometry or ion selective electrodes render these two techniques as the two most likely methods to be used by clinical laboratories in the near future.

The recently developed neutron activation analysis method allows determination of the Li^+ distribution in tissues (76). This involves subjecting ^6Li (7.4 % natural abundance) to neutron bombardment. This results in the formation of tritium and α particles. Lithium itself does not have any isotope with a relatively long half life to follow Li^+ distribution in tissues. However, tritium is a β-emitter and has a long half life (12.3 years). Thus, tritium activity can be used to probe Li^+ distributions in tissues. Undoubtedly, this method will open up the way for

imaging Li^+ distribution in the human body, particularly in the brain where Li^+ is presumed to exert its pharmacological effect (86).

2. Nuclear Magnetic Resonance Methods

Nuclear magnetic resonance (NMR) spectroscopy presents a noninvasive approach. ^1H NMR and magnetic resonance imaging (MRI) techniques have been applied to the study of manic-depression and related lithium treatment (87-91). Prior to lithium treatment, ^1H NMR studies of RBCs from six bipolar patients showed elevated water proton spin-lattice (T_1) relaxation times (434-547 ms) relative to normal matched controls (379-400 ms). The proton T_1 values of RBCs from five of the six bipolar patients normalized after one week of lithium treatment (87). Studies on proton T_1 of the frontal and temporal lobes of the brain of bipolar patients follows the same trend as that observed with work on RBCs (88). Based on these observations, it was proposed that lithium may be inducing changes in intracellular hydration and that changes in the tissue solvent structure may be associated with manic-depressive illness. ^1H NMR also showed that bipolar patients undergoing lithium treatment have a significantly higher RBC choline concentration compared to controls (37). Time dependent study on the lithium-inhibited choline transport showed that the choline levels returned to normal only for

young RBCs and that the inhibitory effect of lithium may be irreversible at the level of the individual RBC (89). Whether the accumulation of choline in RBCs is related to the mechanism of action of lithium is not clear at this time.

In vivo distribution of lithium was recently investigated by MRI techniques (90-92). The feasibility of looking at the brain and skeletal Li^+ levels by MRI using the ^7Li isotope has been demonstrated for normal volunteers who had taken both single and multiple doses of lithium carbonate (92). These studies may provide useful information on the tissue distribution of lithium and insights on lithium pharmacokinetics and thus complement those obtained by neutron activation analysis.

In NMR, ions in different environments generally give rise to different resonance signals. However, in RBC suspensions, the metal cations like Li^+, Na^+ and K^+ exist primarily as free hydrated ions in both intra- and extracellular compartments. This means that by looking at either ^7Li, ^{23}Na or ^{39}K resonances, only one signal is observed (93-98). This resonance signal is a composite of the intra- and extracellular signals. The metal cations are present in the two compartments as hydrated ions and hence are in the same chemical environment. ^{23}Na and ^{39}K have been used to look at sodium and potassium distribution in RBC suspensions (94,95,98). These studies showed that

the intra- and extracellular Na^+ and K^+ signals are not resolved. However, discrimination of the two metal cation pools can be achieved by addition of a membrane impermeable shift reagent like dysprosium(III)triphosphate $(Dy(PPP)_2^{-7}$ (94,95). The surface of the cell membrane bilayer is highly negative due to the polar headgroups of the phospholipid comprising the membrane. Thus the similarly highly negatively charged shift reagent is repelled by the membrane and renders it membrane impermeable.

The incorporation of a shift reagent in the RBC suspension resolves the resonance signal into intra- and extracellular resonances. This is because the extracellular metal cation experiences a lanthanide-induced shift. It is important to note that interaction of either Li^+ or Na^+ is electrostatic in nature and direct coordination to the shift reagent is not present (99). Since the two pools of lithium can be observed distinctly, time dependent changes in the intra- and extracellular signals can easily be visualized and monitored. ^{133}Cs NMR has also been used to look at Cs^+ distribution in Cs^+ loaded RBCs (100). Surprisingly, two resonances were observed without using shift reagents and assigned to intra- and extracellular Cs^+ pools.

CHAPTER II

STATEMENT OF THE PROBLEM

Most investigations have concentrated on establishing whether Li^+ transport rates and ratios can be used as genetic markers of bipolar disorder. However, very little attention has been given to investigating lithium interactions in RBCs. Although the pharmacological importance of lithium in psychiatry has been widely accepted, the mechanism of the biological action of Li^+ ion has remained an open question. Clearly, an understanding at the molecular level of how Li^+ ion affects phospholipid metabolism and membrane molecular dynamics in normal RBCs and in RBCs from bipolar patients are prerequisites to establishing the mode of action of Li^+ ion in RBCs.

The main objective of this study is to investigate Li^+ transport and binding in RBCs. Cell membrane dysfunction has been proposed to be one of the underlying biochemical defects in bipolar affective disorder or manic-depression (18). RBCs share Li^+ transport systems with neurons (7,13) and therefore may be a good system for

testing the link between bipolar disorder and cell membrane abnormality. In addition, Li^+ transport is more easily characterized in RBCs than in nerve cells because of the easier accessability and simple morphology of RBCs. Lithium carbonate is administered orally and is carried to the brain through the bloodstream; in order to comprehend the toxicity of this drug, it may be important to understand how lithium interacts with RBC and its components. There is still a controversy on the abnormalities reported for Li^+ transport in RBCs from manic depressive patients (23-29); if they indeed represent a characteristic of the disease.

In this dissertation, a novel approach using NMR spectroscopy, in particular ^7Li NMR, is used. The application of metal NMR to the direct study of binding and transport of Li^+ ions in RBCs reveals new and more reliable information about metal ion interactions in RBCs. One big advantage of the NMR method, as opposed to conventional analytical techniques, is that direct measurement of intracellular concentrations is possible. In the case of Na^+, radioactive labelling with ^{22}Na can be done with relative ease because of the long half-life of radioactive sodium. Since the radioactive half-life of Li is inconveniently short, the metal NMR approach poses a great advantage. Moreover, the standard analytical methods (flame photometry and atomic absorption) used cannot

provide any information about Li^+ interactions with the RBC membrane.

A number of reports on applications of NMR spectroscopy to the investigation of bipolar disorders and related lithium therapy have appeared in the literature (37,87-93,96,97,101-105). In this present study, several questions are addressed:

(1) Is it possible to use metal NMR to discriminate between the Li^+ pools in the intra- and extracellular compartments in RBC suspensions? Can ^7Li NMR be used to follow ionophore-induced passive Li^+ transport across the RBC membrane and Li^+ transport via the Na^+-Li^+ countertransport pathway in RBCs?

Two distinct noninvasive $^7Li^+$ NMR methods for discriminating between the intra- and extracellular Li^+ pools in Li^+ loaded red blood cells are used. One NMR method involves the use of a standard single pulse experiment and incorporation of a membrane impermeable shift reagent such as dysprosium (III) triphosphate, $Dy(PPP)_2^{-7}$ (93-98,101-105). The other NMR method does not require the use of shift reagents. Instead, it takes advantage of the difference in the ^7Li spin-lattice relaxation times (T_1) of the two lithium pools and uses a modified inversion recovery (MIR) pulse sequence. Similar methods have been used for to follow ion transport (106-108) and water diffusion (109) across membranes.

(2) If the metal NMR approach can distinctly show the two Li^+ pools in RBC suspensions, are the Li^+ pools 100% NMR visible?

To determine whether the observed ^7Li signals reflect the relative Li^+ populations in the two cell compartments, ^7Li NMR signals and AA data for intact and lysed RBCs are compared.

(3) Does the ^7Li NMR data provide any information about Li^+ interaction with RBC membranes? If there are indications of membrane interactions, what are the possible Li^+ binding sites in the RBC membrane?

If there is indeed an abnormality in the transport of Li^+ across the cell membrane, to what phenomena can this be attributed to? Lipids have been found to modulate the activity of membrane proteins (110). It is feasible that Li^+ may be exerting its biological action by interacting with the membrane phospholipids thereby causing changes in the molecular dynamics of the membrane, in turn affecting ion channels.

CHAPTER III

EXPERIMENTAL METHODS

A. Materials

1. Reagents

Lithium chloride (LiCl), dysprosium chloride ($DyCl_3$), triethylenetetraamine hexaacetic acid (TTHA), glucose, sodium triphosphate, deuterium oxide (99.8% D_2O), sucrose, sodium chloride (NaCl), potassium chloride (KCl), magnesium chloride ($MgCl_2$), calcium chloride ($CaCl_2$), cesium chloride (CsCl), choline chloride, sodium phosphate, potassium phosphate, ammonium sulfate and monensin were supplied by Aldrich (Wisconsin). HEPES [4-(2,hydroxyethyl)-1-piperazineethanesulfonic acid], TRITON X-100, Tris(hydroxymethyl)aminomethane, L-α-phosphatidylcholine (from bovine brain), L-α-phosphatidylserine (from bovine brain), L-α-phosphatidylinositol (from bovine liver), n-octyl-glucopyranoside, glycerol, hemoglobin and sialidase were obtained from Sigma (Missouri). Kryptofix C211 (4,7,13,18-tetraoxa-1,10-diazabicyclo-8.5.5)-eicosane and C221 (4,7,13,16,21-pentaoxa-1,10-diazabicyclo-8.8.5)-tricosane were obtained from VWR Scientific (Illinois).

Gramicidin was obtained from Calbiochem (Indiana). Phospholipase C was obtained from Boehringer Mannheim (Indiana). All chemicals were used as received except sodium triphosphate which was recrystallized three times from 40% ethanol. This is because the commercially available sodium triphosphate is only 85% sodium triphosphate.

2. Blood Samples

Packed red blood cells (RBCs) were supplied by the Chicago Chapter of Lifesource. Whole blood samples from bipolar patients and normal matched controls were obtained through the Department of Psychiatry, Loyola University Stritch School of Medicine. Bipolar patients were diagnosed according to Diagnostic and Statistical Manual of Affective Disorders (DSM-IIIR, 1987). The protocols for experiments involving human blood were approved by the Institutional Review Board for the Protection of Human Subjects (Loyola University of Chicago).

B. Instrumentation

1. NMR Instrument

^{7}Li, ^{23}Na and ^{31}P NMR measurements were made at 104.8, 71.2 and 109.3 MHz, respectively, on a JEOL FX-270 NMR spectrometer (Analytical Service Laboratory at Northwestern University). ^{7}Li NMR measurements were also made at 116.5 MHz on a Varian VXR-300 NMR Spectrometer

(Loyola University of Chicago). Both instruments were equipped with multinuclear probes. The spectra were recorded using 10 mm NMR non-spinning tubes to avoid settling of RBCs. Probe temperature was kept constant at 37° ± 0.1° C. The 90° pulse was 18 and 30 μs, for the JEOL 270 and VXR 300, respectively. T_1 measurements of ^{7}Li NMR resonances were done by the inversion recovery method while T_2 measurements of ^{7}Li NMR were done by the Carl-Purcell-Meiboom-Gill method (111).

For normal RBC suspensions, the T_1 of the intra- and extracellular ^{7}Li+ resonances were measured to be 5 and 16.5 s, respectively (105). In the presence of a shift reagent in the extracellular suspension medium, the T_1 of the extracellular ^{7}Li NMR resonance is 0.1 s (93). This difference in T_1's was taken into account in choosing the flip angle and repetition time. For experiments involving shift reagents, ^{7}Li NMR spectra were taken every $1.5T_1$ (repetition rate 7.5 s) with a flip angle of 45° or $3T_1$ (repetition rate 18 s) with a flip angle of 60°. In some samples 17% D_2O was used for field frequency lock, otherwise NMR measurements were run unlocked.

The shift reagent method described above employs a standard single pulse sequence. The alternative ^{7}Li NMR method does not require the incorporation of shift reagents in the suspension medium and employs a modified inversion recovery (MIR) pulse sequence (D1-180°-D2-60°-Acquire)

(104). Figure 4 shows the pulse sequence used for both the shift reagent and MIR methods. Table 5 shows the ^{7}Li MIR parameters used in the experiments. All NMR experiments were run under the same gain and absolute intensity conditions.

2. **Atomic Absorption Studies**

AA studies were carried out on a Perkin-Elmer spectrophotometer Model 5000, equipped with a graphite furnace. AA determinations of Na^{+}-Li^{+} exchange rates, and transmembrane Li^{+} or Na^{+} distributions were adapted from published procedures (73a,77).

3. **Refrigerated Centrifuge**

A Dupont Model RC-5B Refrigerated centrifuge equipped with a Sorvall SS-34 rotor was used for blood processing and preparation of RBC resealed right-side out white ghosts, at 4°C. Other blood washing procedures were also done using a Savant Refrigerated High Speed Model HSC10000 centrifuge.

4. **Vapor Pressure Osmometer**

The osmolarity of all RBC suspension media were adjusted with glycerol and measured to be approximately 300 $\pm$ 10 mOsm, with a Wescor Vapor Pressure Osmometer.

5. **Viscometer**

The viscosity of RBC, ghost, phospholipid vesicle, spectrin-actin and hemoglobin suspensions were

Figure 4. (A) Standard single pulse sequence, and (B) Modified inversion recovery pulse sequence.

A

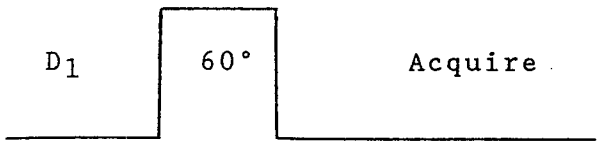

B

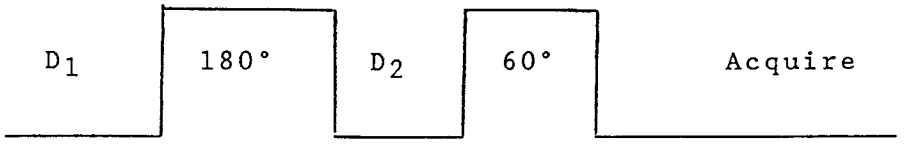

Table 5

^{7}Li MIR Parameters

Probe Temperature	37°C
60° Pulse width/μs	20
180° Pulse width/μs	60
D_1 delay/s	60(3 x longest T_1)
D_2 delay/s	11.5
Pre-acquisition Delay Array[a]/s	0,300,300,300,300,300,300

[a] In some MIR experiments pre-acquisition delays of 600 s each were used instead.

adjusted with glycerol and measured with a Brookfield Cone plate Viscometer, equipped for low viscosity samples, using an 8° CP-40 cone, at 12 rpm.

6. **Cell Volume Measurements**

To monitor the cell volume, hematocrit measurements by the capillary method were done using a IEC Hemofuge or using a Coulter Counter, Model ZM. For the Coulter counter measurements, the same Na^+, choline and Mg^{+2} suspension media were used to perform 1:20,000 dilution. All reported data took into account this dilution factor.

C. Li^+ Loading of Packed Red Blood Cells

Fresh packed RBCs or whole blood samples were washed three times by centrifugation at 2000 g for 6 minutes with isotonic 5 mM sodium phosphate - 150 mM NaCl buffer, pH 7.4 (5PBS7.4), in a Savant refrigerated centrifuge at 4°C. The cells were separated from the plasma and the buffy coat by aspiration. Li^+ loading of RBCs was achieved by incubating the cells with 150 mM LiCl, 10 mM glucose, 10 mM HEPES, pH 7.5 at 37°C for 0-12 hours at 50% hematocrit. Typically the intracellular Li^+ concentrations after 3 and 12 hour incubation times are approximately 1 and 3.5 mM, respectively. The Li^+ loaded RBCs were then washed at least four times by centrifugation at 2000 g for 6 min with washing buffer, containing 112.5 mM choline chloride, 85 mM

sucrose, 10 mM glucose, 10 mM HEPES, pH 7.5 at 4°C. This washing step removes all extracellular Li^+. Immediately before the NMR measurements the cells were washed in the appropriate NMR suspension buffer prior to final resuspension at 13% hematocrit, in the same NMR buffer. The NMR buffer contained glucose, sucrose, HEPES, pH 7.5 and chloride salts of Li^+, Na^+, K^+, Mg^{+2}, Ca^{+2} or choline. The exact composition of the RBC suspension media varied depending on whether or not the experiments involved the use of shift reagents.

D. Preparation of Shift Reagents

Dysprosium (III) triphosphate ($Na_7Dy(PPP)_2.3NaCl$) was prepared from $DyCl_3$ and sodium triphosphate. 0.25 M sodium triphosphate was added dropwise to 0.25 M $DyCl_3$, while vortexing, until a ratio of 2.5:1 was achieved, and a clear solution was obtained. The K^+ form of the shift reagent, $K_7Dy(PPP)_2.3KCl$ was obtained by first converting sodium triphosphate to potassium triphosphate by passing it down a Chelex-100 column loaded with K^+.

Dysprosium (III) triethylenetetraamine hexacetate ($Na_3DyTTHA$) was prepared from dysprosium hydroxide and the acidic form of the ligand according to published procedures (112).

E. Visibility of the ^{7}Li and ^{23}Na Resonances

Washed packed RBCs were loaded with approximately 3.5 mM Li^{+} as described above (III.C). RBCs were suspended in isotonic 10 mM TRIS buffer, pH 7.5 containing 112.5 mM choline chloride, 85 mM sucrose and 10 mM glucose. Hematocrit was 13%. A small aliquot of the shift reagent $Dy(PPP)_2^{-7}$, was added to the RBC suspension for confirmation that the extracellular compartment was Li^{+} free. ^{7}Li NMR spectra were obtained from: (1) the RBC suspension; (2) an RBC sample of the same hematocrit, except that 10% Triton X-100 was incorporated in the suspension medium to lyse the cells; and, (3) an RBC sample of the same hematocrit, treated with 0.1 μM gramicidin, prior to suspension in the medium containing 10% Triton X-100. ^{23}Na NMR spectra were obtained from: (1) non-Li^{+} loaded RBCs suspended in the same isotonic TRIS buffer used above; (2) non-Li^{+} loaded RBCs suspended in the same buffer except that 10% Triton X-100 was included in the suspension medium and, (3) non-Li^{+} loaded RBCs treated with 0.1 μM gramicidin, prior to suspension in the medium containing 10% Triton X-100.

F. ^{7}Li NMR Determination of Li^{+} Concentrations

In the NMR experiments involving shift reagents, the ^{7}Li resonance intensities were measured directly. With MIR, the intracellular Li^{+} resonance intensity was measured

directly from the spectrum while the resonance intensity of the extracellular Li^+ signal was taken from the difference spectrum obtained from the standard single pulse and MIR spectra of the same sample.

The resonance intensities measured in the NMR experiment can be expressed in terms of intracellular Li^+ concentrations according to the following expressions:

$$I = I_{obs} / (f_{in} \times C_1) \quad [1]$$

$$f_{in} = I_{in} / (I_{std} \times C_1) \quad [2]$$

$$f_{out} = I_{out} / (I_{std} \times C_2) \quad [3]$$

where f_{in} and f_{out} represent the fractional intra- and extracellular NMR windows, I_{in} and I_{out} are the intensities of known intra- and extracellular Li^+ concentrations (in mM) in isotonic RBC suspensions, and I_{std} is the intensity for the same Li^+ concentrations as for I_{in} and I_{out} but in the suspension medium alone. I_{in} was measured by MIR while I_{out} and I_{std} were measured using a standard single pulse sequence. The delay between pulses in the MIR spectrum is only sufficient to provide for partial relaxation of the magnetization of the intracellular Li^+ signal. The intracellular Li^+ intensities, I_{obs} and I_{in}, represent only 80% of the total intensities and thus, the origin of the correction factor "C_1" in the equation above. The intracellular Li^+ resonance intensities obtained by MIR is therefore underestimated by approximately 20% while the extracellular Li^+ resonance intensities obtained by

spectral subtraction from the MIR experiment is overestimated by approximately 20% and thus, the origin of the correction factor "C_2' The value of C_2 for the single pulse experiments is equal to 1.

The values for f_{in} and f_{out} were measured for RBC suspensions at different hematocrits. The fractional NMR windows, f_{in} and f_{out} are dependent on the apparent hematocrit within the NMR window as shown in a plot of f_{out} versus hematocrit (Figure 5). For the 13% hematocrit used in the experiments, f_{in} and f_{out} were measured to be 0.49 and 0.51, respectively. Thus, the NMR determined hematocrit is considerably higher than that measured by a hemofuge. When a RBC suspension is placed in an NMR tube, an initial rapid sedimentation takes place which modifies the ratio of the intra- to extracellular volumes along the height of the NMR sample (113). However, a time dependent study of f_{out} (Figure 6) shows that this rapid sedimentation occurs within the first 5 min and slows down within the next 60 min during which the ^7Li NMR measurements were made. Any change in hematocrit is taken into account by equations 1 through 3 since the fractional NMR window is directly and simultaneously determined for each sample at each time interval.

The observed intracellular Li^+ resonance intensities for the RBC suspensions, I_{obs}, are corrected, I, for the intracellular volume according to the equation:

Figure 5. A plot of f_{out} at different hematocrits. Non-Li^+ -loaded packed RBCs were suspended in isotonic buffer containing 112.5 mM choline chloride, 85 mM sucrose, 10 mM glucose and 10 mM Tris-Cl, pH 7.5, containing in addition 1.5 mM LiCl. Hematocrits were measured in triplicates on an IEC hemofuge. f_{out} for each RBC suspension was determined from the ratio of ^7Li resonance intensity of the RBC suspension to ^7Li resonance intensity of an aqueous isotonic choline chloride medium alone containing the same LiCl concentration.

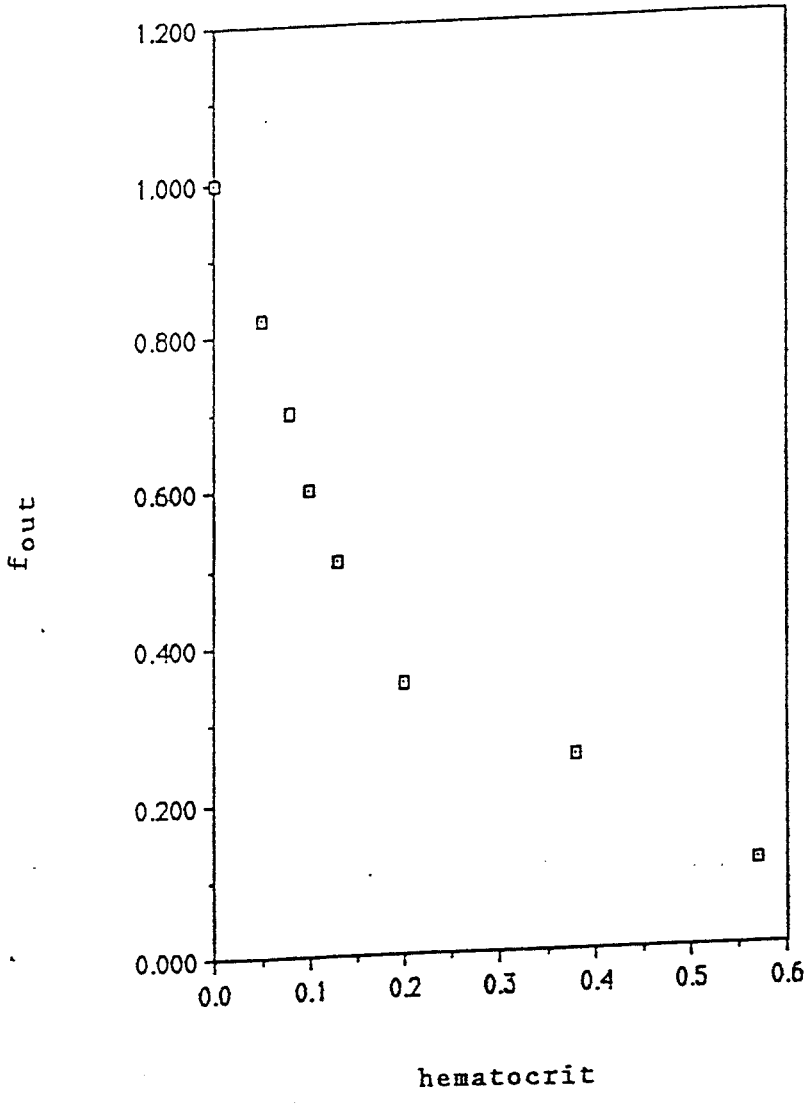
1.200
1.000
0.800
0.600
0.400
0.200
0.000
f_{out}
0.0
0.1
0.2
0.3
0.4
0.5
0.6
hematocrit

Figure 6. A plot of f_{out} versus time. f_{out} was determined from the ratio of $^{7}Li^{+}$ resonance intensities of non-Li^{+} loaded RBCs suspended in an isotonic choline chloride buffer containing 1.5 mM Li^{+} to that of the Li^{+}- containing medium alone. ^{7}Li NMR measurements were conducted using a standard single pulse sequence.

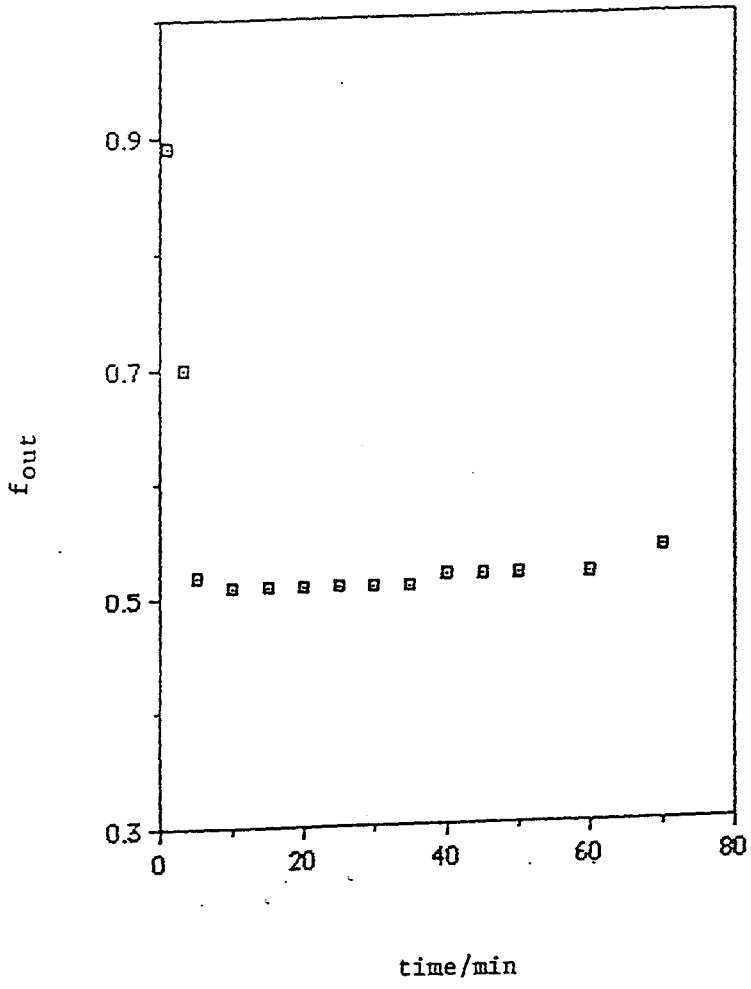
0.9
0.7
0.5
0.3
f_{out}
0
20
40
60
80
time/min

$$I = I_{obs} \times (Istd / I_{in}) \quad [4]$$

The actual Li^+ concentration corresponding to I was extrapolated from a calibration curve of Li^+ resonance intensities against Li^+ concentrations in mM in suspension medium alone. The Li^+ concentration range in the different suspension media used for the calibration curve was 0.1-3.5 mM. It is important to note that the MIR method outlined above for determination of Li^+ concentrations is self-correcting since the final value of I (equation 4) is independent of the correcting factor "C".

RBCs were loaded with different concentrations of intracellular Li^+ using the procedure described in III.C., and suspended in the isotonic choline buffer at 13% hematocrit. The ^7Li NMR resonance intensities for the RBC samples containing 0.2-3.5 mM intracellular Li^+ were compared with standard aqueous solutions of LiCl, of the same Li^+ concentrations. A plot of ^7Li NMR intensities obtained for the Li^+-loaded (intracellular Li^+ calibration) and non-loaded RBC suspensions (extracellular Li^+ calibration) versus ^7Li NMR resonance intensities of the aqueous LiCl solutions was constructed (Figure 7). The slope of the graph indicates the fractional intra- (0.49 $\pm$ 0.02, n =3) and extracellular (0.51 $\pm$ 0.02, n = 3) NMR window.

The intracellular Li^+ concentrations were determined

Figure 7. A plot of ^{7}Li NMR intensities, I, obtained for the Li^{+}-loaded (I_{in} = open squares) and non-loaded RBC suspensions (I_{out} = closed diamonds) versus ^{7}Li NMR resonance intensities (I_{std}) of the aqueous LiCl solutions, for 0.2, 0.4, 0.6, 0.8, 1.0, 1.5, 2.0 and 3.5 mM Li^{+} concentrations. I_{in} was obtained by MIR and I_{std} and I_{out} were obtained using a standard single pulse sequence.

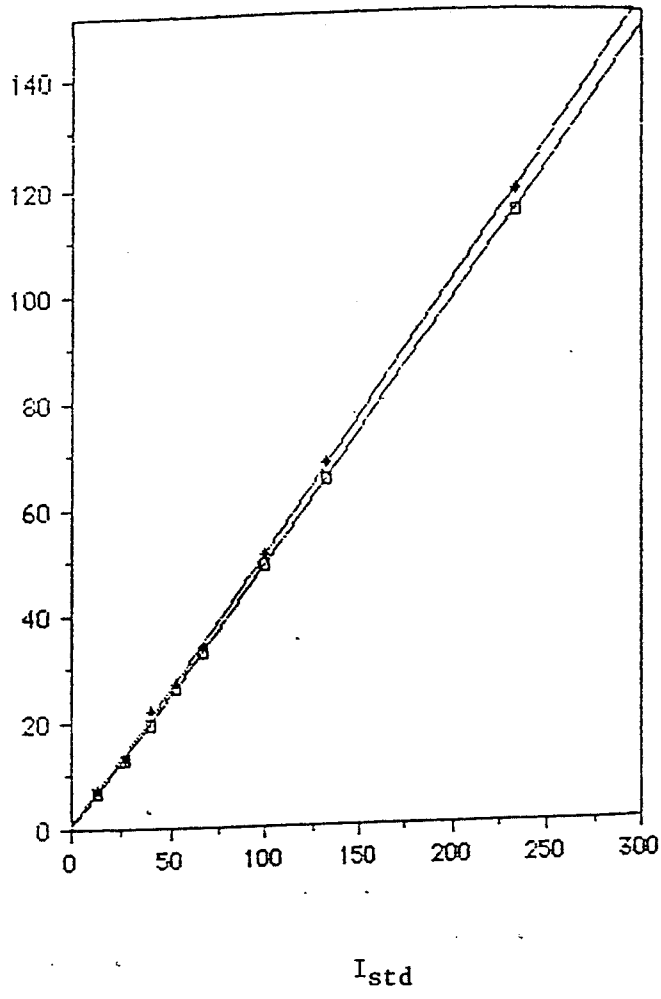
I
140
120
100
80
60
40
20
0
0
50
100
150
200
250
300
I_{std}

by AA and compared with those measured by ^{7}Li NMR.

It is important to note that flip angles of 60° were also used in the Li^{+} calibration curves.

G. ^{23}Na NMR Determination of Na^{+} Concentrations

The ^{23}Na NMR experiments only involved the use of the shift reagent method. The ^{23}Na intracellular resonance intensities were converted into Na^{+} concentrations after taking into account the 20% NMR invisibility of the intracellular Na^{+} signal. The Na^{+} concentration was read directly from a calibration plot of $^{23}Na^{+}$ resonance intensities of Na^{+} standards of RBC suspensions (containing no shift reagent) versus Na^{+} concentrations (2-100 mM). RBCs were loaded with Na^{+} using a similar procedure described in III.C, to load the cells up to 100 mM Na^{+}. A calibration plot of ^{23}Na resonance intensities of the Na^{+}-loaded RBCs versus intracellular Na^{+} concentrations determined by AA. The ^{23}Na extracellular resonance intensities were converted into extracellular Na^{+} concentrations by extrapolation from a calibration plot of $^{23}Na^{+}$ intensities of $^{23}Na^{+}$ aqueous standards versus Na^{+} concentrations (0-150 mM). The $^{23}Na^{+}$ aqueous standards contained the same concentration of shift reagents used in the RBC experiments.

H. AA Determination of Li^+ and Na^+ Concentrations

The AA instrument equipped with a graphite furnace was set up for lithium and sodium determinations using the parameters shown in Table 6.

RBCs and supernatant were isolated by centrifugation at 2000 g for 4 min at 4°C. A 50 μL aliquot of the packed RBCs (98 ± 2 hematocrit) was taken and lysed by dilution with deionized water up to 25 times its original volume, prior to analysis by AA. The supernatant was used as is or diluted as necessary with deionized water.

Li^+ standards were prepared in isotonic buffers approximating the RBC lysate and the supernatant solution. For determination of intracellular Li^+, the standards were prepared by taking 50 μL aliquot of the non-Li^+ loaded packed RBCs (98 ± 2 hematocrit) and lysed as before, except that the resulting lysate contained, in addition, 0.2-42 μg/mL LiCl. For determination of Li^+ in the supernatant, the standards were prepared in the appropriate medium (choline or Na^+ rich buffer) and contained, in addition, 0.2-42 μg/mL LiCl. An aliquot of 10 μL from the prepared samples was injected into the graphite furnace chamber and absorption readings taken. The samples were prepared in duplicate and an average of three independent absorption measurements were taken for each sample.

For AA determinations of intracellular Na^+, 50 μL aliquots were taken from the packed RBC and lysed by 100 x

Table 6

Lithium and Sodium Parameters for AA

	Lithium	Sodium
Detection Mode	Absorption	Absorption
Wavelength	670.8 nm	589 nm
Integration Time	7.0 s	7.0 s
Sample Volume	10 μL	10 μL
Ashing Temperature	700°C	700°C
Solvent Removal Temperature	110°C	110°C
Atomization Temperature	1500°C	1500°C
Purge Temperature	2000°C	2000°C

dilution with deionized water. Similarly, 50 μL aliquots were taken from the isolated supernatant and appropriately diluted with deionized water. Similarly, an aliquot of 10 μL from the prepared samples were injected into the graphite furnace chamber and absorption readings taken as described for Li^+ determinations. Calibration plots for Na^+ were prepared as described in III.G.

The calibration curve for each buffer medium was constructed by plotting the absorbance versus the Li^+ concentrations. The Li^+ concentrations in the unknown RBC lysate or supernatant were extrapolated from the appropriate calibration curves, taking into account the hematocrit and dilution factors, using the equations below:

$$[Li^+]_{RBC} = \frac{[Li^+]_u \times \text{dilution factor}}{(\text{hematocrit}) \times (\text{M.W. of LiCl})} \quad [5]$$

$$[Li^+]_{ext} = \frac{[Li^+]_u \times \text{dilution factor}}{(1 - \text{hematocrit})_s \times (\text{M.W. of LiCl})} \quad [6]$$

where $[Li^+]_{RBC}$ = intracellular Li^+ concentration, hematocrit = 0.98 (isolated packed cells), $[Li+]_u$ = Li^+ concentration from AA calibration curve, $[Li^+]_{ext}$ = extracellular Li^+ concentration and $(1 - \text{hematocrit})_s$ = 1-0.13 = 0.87, which represents the extracellular volume

fraction in the original RBC suspension with 0.13 hematocrit.

I. Determination of Transmembrane Li^+ and ^{23}Na Distribution

Washed packed RBCs were loaded with Li^+, up to an intracellular Li^+ concentration of 1.0 mM, as described in III.C. The protocol used was a modification of a published procedure (114). The Li^+-loaded RBCs were then resuspended in a Na^+-rich or choline-rich buffer medium, pH 7.5, containing in addition 1.5 mM Li^+, to a final hematocrit of 13%. The cell suspensions were incubated for 4 h at 37°C. For Na^+ ratios, Li^+-loaded RBCs were also used. The equilibrium intra- and extracellular Li^+ and Na^+ concentrations were determined by both AA and NMR, as described in III.F - III.H.

J. Determination of Na^+-Li^+ Countertransport Rates

For the determination of Na^+-Li^+ countertransport rates, washed packed RBCs either from manic-depressive patients or normal matched controls, that have been previously loaded with Li^+ to approximately 1 mM Li^+, were suspended in either a Na^+ rich medium (150 mM NaCL, 10 mM glucose, 0.1 mM ouabain, 10 mM TRIS-Cl, pH 7.5) or choline medium (112.5 mM choline chloride, 85 mM sucrose, 10 mM glucose, 0.1 mM ouabain and 10 mM TRIS-Cl, pH 7.5) to 13% hematocrit. Ouabain was added to inhibit any Li^+ transport

through the (Na^+,K^+)-ATPase. The choline suspension medium allows determination of the contribution of the leak pathway toward Li^+ efflux. The rate of Li^+ transport in the Na^+ rich medium is made up of two components: the Na^+-Li^+ countertransport pathway and the leak pathway. Thus the reported rates of Na^+-Li^+ countertransport were obtained by subtracting the measured rates in the Na^+ and choline media.

For the AA experiments, the Li^+ loaded cells were suspended in either the Na^+ rich or choline media, to 13% final hematocrit. The samples were incubated at 37°C in a water bath. Aliquots were taken from each sample at 15 min intervals over a 75 min period and collected into pre-cooled polyethylene tubes. The aliquots were centrifuged at 2000 g for 4 min at 4°C, and the supernatants collected and analyzed directly for Li^+ concentration. Li^+ standards (0.2-42 μg/mL Li^+) were prepared in both Na^+ and choline rich media and calibration curves constructed accordingly.

For the NMR experiments, 2.5 mL of the Na^+ rich and the choline media transferred into 10 mm NMR tubes and preincubated in a 37°C water bath. The Li^+ loaded cells were then suspended in the Na^+ rich or choline media, to 13% final hematocrit, immediately before NMR measurements were taken. The ^7Li NMR parameters used are summarized in Table 5. Time dependent ^7Li NMR measurements were taken over a 75 min interval, by using a pre-acquisition delay

array every 10 min. Each spectrum took 9.7 min.

For both AA and NMR experiments, plots of Li^+ concentration versus time were constructed, for the Na^+ and choline media, and the rates determined from the slopes of the curves. The Na^+-Li^+ countertransport rates were determined from the difference in the rates of Li^+ efflux in the two media. To determine the Na^+-Li^+ countertransport rate constants, plots of $\ln\{[Li^+]_t/[Li^+]_0\}$ versus time were constructed, and the rate constants determined from the slopes.

K. Preparation of Resealed Red Cell Ghosts

Packed RBCs were washed at least three times by centrifugation at 2000 g for 4 min, with isotonic buffer containing 150 mM NaCl and 5 mM sodium phosphate, pH 8 (5PBS8 buffer) at 4°C. The plasma and buffy coat was removed by aspiration. The resealed ghosts were prepared by hypotonic lysis according to reference 115. To describe the method briefly, one volume of washed RBCs was diluted to four times its volume with 5 mM sodium phosphate buffer, pH 8 (5P8 buffer). The ghosts were isolated by washing at least five times with 5P8, and centrifugation at 38720 g for 8 min at 4°C, on a Sorvall RC-5B high speed centrifuge. When the white ghosts pellet was obtained, it was then washed at least twice with 5P8 buffer containing 1 mM Mg^{+2} (5P8-1Mg buffer).

Resealing and Li^+ loading of the ghosts were accomplished by incubating the ghosts with 5P8 buffer, containing in addition four times the desired intracellular Li^+ concentration, for 90 min at 37°C. This resealing procedure has been found to result in about 90% resealed ghosts. For example, in order to load the resealed ghost with 0.5 mM Li^+, the incubating medium contained 2.0 mM Li^+. The resealed Li^+-loaded ghosts were then washed with 5P8-1Mg buffer, at least three times, by centrifugation, as before. The ghosts were isolated and resuspended in 5P8-1Mg buffer and kept in ice, prior to NMR analysis.

L. Isolation of the 0.5% Triton-X-100 Shell from Red Cell Ghosts

Resealed ghosts were prepared as outlined in III.K. The resealed ghosts were then incubated with 0.5% Triton X-100, in 55 mM sodium borate buffer, pH 8, for 20 min at 37°C (116). The suspension was then centrifuged at 38720 g in a Sorvall RC-5B, for 30 min at 4°C. The supernatant was decanted and the opalescent residue was collected. This gel like substance is the spectrin-actin matrix in Triton X-100.

The spectrin-actin was resuspended in 55 mM sodium borate buffer, pH 8, containing in addition 0.2-1.5 mM Li^+. The viscosity of the resulting suspension was adjusted by addition of glycerol, to approximate the intracellular viscosity in RBCs.

It is important to emphasize that this 0.5% Triton X-100 residue is not a pure spectrin-actin matrix but also contains 41% of the total phospholipid found in ghosts. The composition of the phospholipid contaminants are as follows: 6% phosphatidylcholine, 4% phosphatidylethanolamine, 0.8% phosphatidylserine and 12.8% sphingomyelin (116).

M. Preparation of Spectrin-depleted Inside-Out Vesicles

Ghosts were prepared from packed RBCs as in III.K and resuspended in 30 volumes of 0.3 mM sodium phosphate buffer, pH 7.6 (0.3P7.6) per 5 ml of packed RBCs used. The ghosts suspension were then incubated for 30 min at 37°C (117). This incubation releases spectrin and actin from the membranes and converts the ghosts to small inside-out vesicles (1μm). The suspension was centrifuged for 40 min at 18000 rpm (on an SS-34). The supernatant was discarded and the pellet washed at least three times with 0.3P7.6 buffer. An aliquot of 500 μL of the pellet was resuspended in 0.3P7.6 buffer containing 0.5 - 3.5 mM Li^+. The viscosity of the resulting solution was adjusted to about 5 cP with glycerol.

The vesicle preparations should be approximately 90% inverted and contaminated with about 15% of the ghost membranes. However, the samples were not analyzed for percent sealed vesicles.

N. Preparation of Hemoglobin

Packed RBCs were washed by centrifugation as described in III.C and hemoglobin was isolated according to published procedures (118). The washed cells were then suspended in 2 volumes of cold distilled water (40 mL deionized water/ 20 mL cells), and gently stirred for 30 min at 4°C to lyse the cells and release hemoglobin. 20 mL of neutral saturated ammonium sulphate solution (76.7 g/100 mL H_2O, adjusted to pH 7 with NaOH) was added to every 80 mL of hemoglobin solution. The resulting solution was gently stirred for 30 min at 4°C. The solutions were centrifuged at 38720 g using an SS34 rotor for 10 min, and the pellet discarded. The hemoglobin solution was transferred into dialysis tubing and dialyzed against 5 mM sodium phosphate buffer, pH 7.4, at a volume ratio of 1:1000 for 12 h. The concentration of hemoglobin was determined by the method of Drabkin (119). To describe the method briefly, small aliquots of the hemoglobin solution and hemoglobin standards were transferred into culture tubes containing 1.0 and 0.1 mL of 3.035 mM $K_3Fe(CN)_6$ and 38.4 mM KCN, respectively. The resulting solutions also contained 10 mM KH_2PO_4 and were made up to 5 mL total volume. Hemoglobin standards were prepared from a stock solution of the commercially available lyophilized hemoglobin (Sigma). The absorbance measurements were taken at 540 nm. The concentration of hemoglobin was determined

from a calibration plot of absorbance versus concentration of hemoglobin standards.

O. Preparation of Liposomes

Phosphatidylserine:phosphatidylcholine (PS:PC), phosphatidylinositol:phosphatidylcholine (PI:PC) and pure phosphatidylcholine vesicles were prepared by the detergent dialytic removal procedure (120). To describe the method briefly, 100 μL of a 10 mg/mL stock solution of PS or PI, in $CHCl_3/CH_3CH_2OH$, is mixed with 900 μL of a 10 mg/mL stock solution of PC in a septum capped vial. In the case of pure PC vesicles 1000 μL of the 10 mg/mL PC stock solution was used, instead. Solvent removal was accomplished by rapid purging with N_2 gas. An aqueous solution of 0.2-1.5 mM LiCl, containing n-octyl-glucopyranoside detergent, was added to the phospholipid mixture. The samples were transferred into dialysis tubings. Detergent removal was accomplished by dialyzing the samples twice against 2000 mL of 0.1 M NaCl (previously purged with N_2 gas for 12 h), for 12 h at 40°C, under N_2 atmosphere. The samples were taken out of the dialysis tubings and transferred to 10 mm septum capped NMR tubes previously purged with N_2 gas, prior to NMR analysis. The resulting vesicles are reported to be large unilamellar vesicles with an average diameter of 450 nm (120).

To prepare small unilamellar vesicles (SUV), the

phospholipid mixtures were prepared as outlined above, except no n-octyl-glucopyranoside was added to the aqueous LiCl solution. The samples were then sonicated for 30 min, in an ultrasonic water bath, under N_2 atmosphere (121). The SUVs were then transferred to 10 mm septum capped NMR tubes, previously purged with N_2, prior to NMR analysis.

Neither LUVs and SUVs preparations were checked by transmittance electron microscopy (TEM). Thus, it is possible that the preparations may be mixtures of unilamellar vesicles of a wide range of sizes or of multilamellar vesicles.

P. Protein Determination

The Coomasie Blue method was used for protein determination using the "Pierce Protein Assay Reagent" (122). This method is an adaptation of the Bradford method which utilizes the absorbance shift from 465 to 595 nm when Coomasie Blue G250 binds proteins in acidic solution. The protein assay reagent is composed of Coomasie Blue G250, phosphoric acid, methanol, water and a solubilizing agent. The assay procedure used was as follows. The reagent was mixed thoroughly prior to use. A known protein concentration series was made by diluting a stock solution of bovine serum albumin standard in the same diluent as the protein sample whose concentration was to be determined. The protein standard series used was 150-1500 μg/mL. An

aliquot of 0.1 mL of diluted standard or unknown protein sample was pipeted into disposable polyethylene cuvettes. An aliquot of 5 mL of the protein assay reagent was added to each sample. Mixing was accomplished by covering the cuvettes with paraffin film and inverting the cuvettes several times. Absorbance was taken at 595 nm versus deionized water. A standard curve was obtained by plotting the average absorbance (from duplicate samples) versus concentration for each dilute standard. The protein concentration for each unknown sample was extrapolated from the calibration curve.

For protein determination of membrane solutions, 20 μL of the membrane solution was transferred into a disposable cuvette containing 80 μL of deionized water. The protein assay reagent was then added and the protein concentration determined as described above.

Q. Determination of Inorganic Phosphate

Inorganic phosphate and the amounts of phospholipid in the membrane or phospholipid vesicles were determined after treatment with heat and strong acid (123). The protocol used is described as follows. An aliquot of 0.5 mL of the phospholipid or membrane solution was added to 9.5 mL of ethanol:ether (3:1) mixture. The solutions were placed in a hot water bath, set at 80°C, until boiling. The samples were allowed to cool and readjusted to 10 mL

volume with the ethanol:ether solvent. An aliquot of 5 mL of the ethanol:ether solution was transferred into a test tube and the solvent removal was accomplished by passing N_2 gas over the solution at 30°C. To the test tube containing the dried lipid sample, 4 drops of 6 N H_2SO_4 was added. The sample was allowed to sit in a hot sand bath until white SO_3 fume appeared. Digestion of the sample was accomplished by addition of 2 drops of 72% perchloric acid to the sample and heating the sample over a Bunsen flame until the solution clarified. The solution was allowed to cool and the volume adjusted to 25 mL with distilled water.

One part of a solution of Reagent B (containing 2.5% $(NH_4)_6Mo_7O_{24}$ and 10% ascorbic acid) was mixed with four parts of a solution of Reagent A (containing 1:2:1 of 6 N H_2SO_4:distilled water:2.5% $(NH_4)_6Mo_7O_{24}$) and labelled as Reagent C. Diluted solutions of the KH_2PO_4 standards and the lipid extracts were prepared and the volumes adjusted to 4 mL. An aliquot of 4 mL of Reagent C was added to each standard and lipid sample and incubated at 37°C for 1 h. The samples were allowed to cool, and the absorbance read at 820 nm. The phosphate content of the unknown phospholipid was determined from the calibration plot of absorbance versus phosphate concentration of the KH_2PO_4 standards.

R. Studies of Li^+ Interactions Sites

To determine if Li^+ interacts with the cell membrane, a systematic study of possible interactions was conducted. This entailed measurements of the intra- and extracellular ^7Li spin-lattice (T_1) and spin-spin (T_2) relaxation times using inversion-recovery and Carl-Purcell-Meiboom-Gill pulse sequences, respectively (111).

RBCs were loaded with LiCl to contain approximately 0.2-3.5 mM intracellular Li^+ as described in III.C. The Li^+-loaded RBCs were then washed with isotonic buffer containing 112.5 mM choline chloride, 85 mM sucrose, 10 mM glucose and 10 mM TRIS-Cl, pH 7.5, by centrifugation at 2000 g for 4 min at 4°C. Hemoglobin-depleted resealed red cell ghosts were also prepared and loaded to contain 0.2-3.5 mM intracellular Li^+, as described in III.K. ^7Li T_1 and T_2 relaxation times were then measured for intracellular Li^+ at 37°C.

The negatively charged sialic acid residues on the surface of the outer leaf of the red cell membrane provide potential interaction sites. To determine whether this is true, RBCs were incubated with sialidase enzyme (124) for 30 min at 37°C. These sialidase treated RBCs were washed with isotonic buffer containing 112.5 mM choline chloride, 85 mM sucrose, 10 mM glucose and 10 mM TRIS-Cl, pH 7.5, at least three times by centrifugation at 2000 g for 4 min at 4°C. The RBCs were then resuspended in isotonic choline

buffer, pH 7.5, containing in addition 0.2-3.5 mM Li^+. ^7Li T_1 and T_2 relaxation times were then measured for the extracellular Li^+ and compared with those obtained for the suspension medium alone.

Cs^+ was also used to probe Li^+ binding in RBCs. This was accomplished by looking at ^{133}Cs chemical shifts and ^7Li relaxation times (T_1 and T_2) for Cs^+-, Cs^+-Li^+ and Li^+- loaded RBCs and resealed ghosts. RBCs were loaded with Cs^+ by incubating washed packed cells in a medium containing 140 mM NaCl, 10 mM CsCl, 10 mM glucose and 10 mM Tris-Cl, pH 7.5, for 12 h, at 37°C, at 50% hematocrit. Cs^+-Li^+ loading of cells was accomplished by incubating washed packed cells in a similar medium, except that 40 mM LiCl replaced 40 mM NaCl. Li^+ loading of cells was done the same way except that the incubating medium contained 110 mM NaCl and 40 mM LiCl, instead.

PS is a negatively charged phospholipid found predominantly in the inner leaf of the cell membrane. In addition to PS, phosphatidylinositol (PI) may also provide possible sites of interaction for Li^+. In order to isolate this effect, LUVs were prepared from PS:PC and PI:PC mixtures, as described in III.O, and loaded with 0.2 -3.5 mM Li^+. The viscosities of the LUV suspensions were not adjusted to 5 cP. ^7Li T_1 and T_2 relaxation times were then measured for the intravesicular Li^+ and compared with those obtained for pure PC LUVs.

LUV preparations usually vary considerably in vesicle size and may be complicated with the formation of multilammelar vesicles (125). On the other hand, SUVs can be easily prepared and investigation of Li^+ binding to the phospholipids are simpler because no correction for intravesicular binding is required since the volume of the buffer medium was at least 100-fold greater than the intravesicular volume (121). SUVs were prepared from PS:PC and PI:PC mixtures, as described in III.N, and suspended in 5P7.4 buffer, containing in addition 0.2-3.5 mM Li^+. ^7Li T_1 and T_2 relaxation times were then measured for the extravesicular Li^+ and compared with those obtained for pure phosphatidylcholine vesicles. The viscosity of the SUV suspensions were adjusted to 5 cP with glycerol.

Lithium treatment has been found to affect intracellular choline levels (69,70). The mechanism by which Li^+ ion exerts this effect is not understood. It is possible that Li^+ may be modulating the activity of phospholipases responsible for the hydrolysis of phosphatidylcholine. To investigate this phenomenon, PC SUVs were prepared. The PC SUVs were further incubated with 10 units of phospholipase C (126) for 30 min at 37°C. These treated PC SUVs were then resuspended in 0.3P8 buffer containing 0.2-3.5 mM Li^+. ^7Li T_1 and T_2 relaxation times were measured for the phospholipase C treated PC SUVs and compared with those obtained for non-treated PC SUVs.

Relaxation times are dependent on temperature and viscosity. The viscosity of the intracellular aqueous medium has been reported to be 5 centipoise (105). Hemoglobin and the spectrin-actin matrix inside RBCs also contribute to this observed intracellular viscosity. However, the spectrin-actin matrix may also provide additional binding sites for the Li^+ ion. To look at these types of interactions, spectrin-actin and hemoglobin solutions were prepared in 50 mM sodium borate, pH 8 and 5P7.4 buffers, respectively, containing 0.2-3.5 mM Li^+. The viscosity of the spectrin-actin suspensions were adjusted with glycerol to approximate that of RBC suspensions. The viscosity of the hemoglobin solutions were not adjusted so that comparison can be made with previous Li^+-hemoglobin studies (105). ^7Li T_1 and T_2 relaxation times in these solutions were then measured at 37°C.

Resealed RBC ghosts (III.K), resealed ATP-depleted ghosts, 0.5% Triton X-100 shell containing the spectrin-actin matrix [III.L] and spectrin-depleted inside-out vesicles (ISO) [III.M] were prepared as described before. The resealed ghosts were loaded with 1.5 mM Li^+ while spectrin-depleted ISO vesicles were suspended in 0.3P7.4 buffer containing 0.5-3.5 mM LiCl. The intracellular viscosities of the resealed ghosts were not adjusted while the viscosities of the ISO vesicle suspensions were

adjusted to 5 cP with glycerol. ^{7}Li T_1 and T_2 relaxation times in these suspensions were then measured at 37°C and compared with that obtained for intact RBCs loaded to the same Li^{+} concentration.

CHAPTER IV

RESULTS

A. ^{7}Li NMR Method using the shift reagent, $Dy(PPP)_2^{-7}$

1. Resolution of the intra- and extracellular Li^+ pools in Normal Human RBCs by ^{7}Li NMR

Figure 8A indicates that the intra- and extracellular ^{7}Li resonances are not resolved in the ^{7}Li NMR spectrum of RBCs suspended in a medium containing 140 mM NaCl, 5 mM KCl, 3.5 mM LiCl, 10 mM glucose, and 50 mM HEPES, pH 7.5, at 13% hematocrit, to which no shift reagent was added. Similar observations were reported for ^{23}Na and ^{39}K NMR studies of RBCs (94,95,98). The reason for this observation is that the alkali metal NMR chemical shifts are almost independent of solvation and ligation (9). Moreover, lithium is believed to exist predominantly in the form of free hydrated ions in both the intracellular and extracellular compartments in RBC suspensions. Separation of the two ^{7}Li NMR signals (Figure 8B) can be achieved by incorporation of the highly negatively charged shift reagent dysprosium (III) triphosphate, $Dy(PPP)_2^{-7}$ in the

Figure 8. (A) ^{7}Li NMR spectrum (104.8 MHz, 37°C) of gently packed RBCs in a medium containing 140 mM Na^{+}, 5 mM K^{+}, 3.5 mM Li^{+}, 10 mM glucose, and 50 mM HEPES, pH 7.5. Li^{+} - loaded RBCs were prepared by incubating packed cells with 150 mM LiCl, 10 mM glucose and 10 mM Hepes, pH 7.5 for 12 h at 37°C. 17% D_2O was present for field frequency lock. Hematocrit was 13%. (B) ^{7}Li NMR spectrum of the same RBC suspension as in part A with the exception that 5 mM $Na_7Dy(PPP)_2.3NaCL$ was present in the medium instead of 50 mM NaCl. (C) ^{7}Li NMR spectrum of a concentric sample (5-mm inner tube containing 20 mM LiCl in distilled water, inside a 10 mm outer tube). The outer tube contained the same suspension medium as in part B. All spectra were obtained in 1.1 min. Line broadening of 2.0 Hz was applied to accumulated free induction decays to improve the signal-to-noise ratio. a and c represent inner pools of Li^{+} while b and d represent outer pools of Li^{+}.

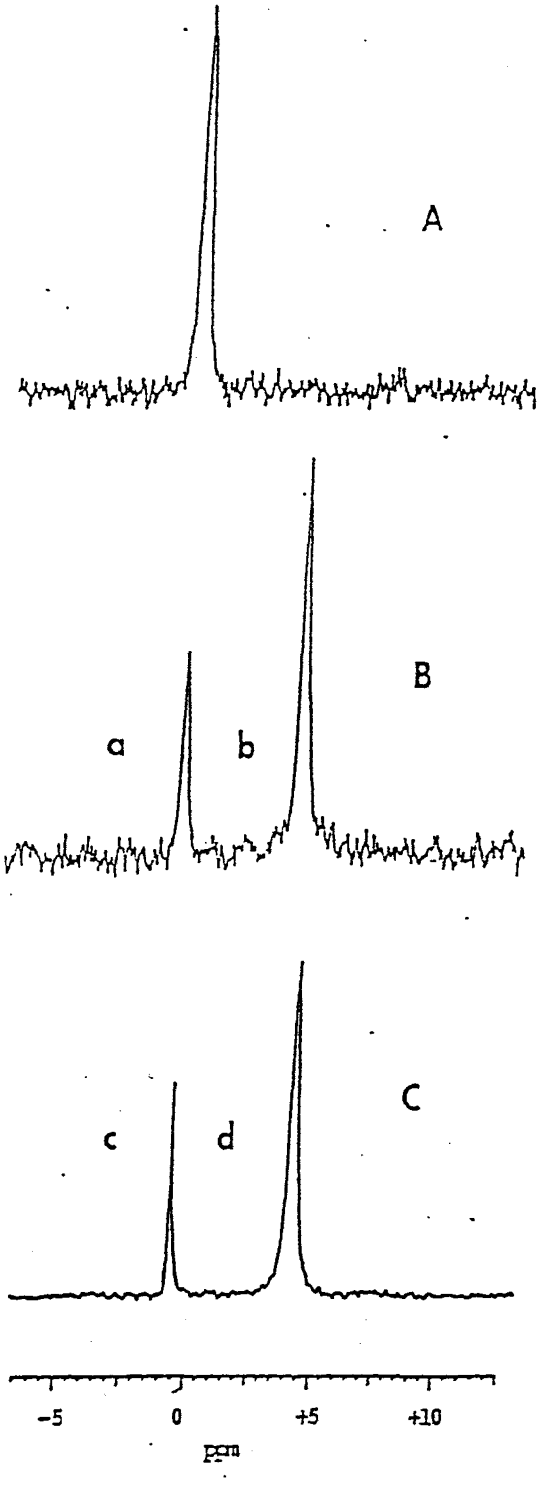
A
B
a
b
C
c
d
-5
0
+5
+10
ppm

suspension medium. RBCs were suspended in a medium as in (8A), except that 5 mM $Na_7Dy(PPP)_2$ was present in the medium instead of 50 mM NaCl. The ^7Li NMR spectrum of a concentric sample (5 mm inner tube inside a 10 mm outer tube) containing 20 mM LiCl in distilled water in the inner tube while the outer tube contained the same suspension medium as in (8B) was recorded and is shown in Figure 8C. The same chemical shift separation for the RBC suspension shown in Figure 8B, indicates that (1) the shift reagent does not cross the cell membrane and (2) the upfield resonance is due to extracellular Li^+, which is in contact with the shift reagent, while the downfield resonance corresponds to intracellular Li^+.

The T_1 values for the extracellular $^7Li^+$ signal in the presence and absence of the shift reagent were 0.1 and 16.5 s, respectively, while the T_1 value for the intracellular $^7Li^+$ was 4.9 s (93). Since the spin-lattice relaxation rates for the two lithium resonances were very different in magnitude, the ^7Li NMR spectra reported in Figure 8 were acquired in such a way that the relative intensities of the two measured NMR resonances reflect the relative amounts of the two lithium pools. This was accomplished by employing a flip angle of 45° and a repetition rate of 60 s (spectrum 8A) and 7.5 s (spectrum 8B and 8C). This ensures that in each spectrum the $^7Li^+$ resonance with the longer relaxation time undergoes full

relaxation between successive radio frequency pulses.

All the spectra were recorded using a standard single pulse sequence in 1.1 min. Since the relaxation times of the two Li^+ pools were very different in magnitude, ^7Li NMR spectra were taken every $1.5T_1$ (repetition rate 7.5 s), using a 45° pulse.

2. Effect of the Molar Ratio of Shift Reagent to Metal Cation, on the $^7Li^+$ and $^{23}Na^+$ Chemical Shift Separation

The effect of increasing the molar ratio of shift reagent to metal ion, on both ^7Li and ^{23}Na chemical shift separation were investigated. The Li^+ or Na^+ concentrations were kept at 5 mM while the concentration of the shift reagent, $Dy(PPP)_2^{-7}$, was varied from 0 to 25 mM. All samples were made in 50 mM HEPES buffer, pH 7.5 and contained 17% D_2O for field frequency lock. Figure 9 shows a comparison of the effect of increasing the molar ratio of shift reagent to metal cation on the observed $^7Li^+$ and $^{23}Na^+$ chemical shift separation. ^7Li and ^{23}Na NMR measurements were taken on two separately prepared samples at room temperature (20°C). The average of the ^7Li and ^{23}Na NMR chemical shift separations (Δ_{ppm}) relative to LiCl and NaCl solutions, respectively were then plotted against the [Shift Reagent]/[Cation] molar ratios. In order to compare $^7Li^+$ and $^{23}Na^+$ chemical shifts induced by the shift reagent, dysprosium (III) triphosphate, the K^+ form of the

Figure 9. Plots of ^{7}Li (filled squares) and 23Na (open squares) chemical shift separation as a function of the molar ratio of shift reagent to lithium or sodium cation, respectively. Data points shown represent the average of NMR measurements taken on two separately prepared samples.

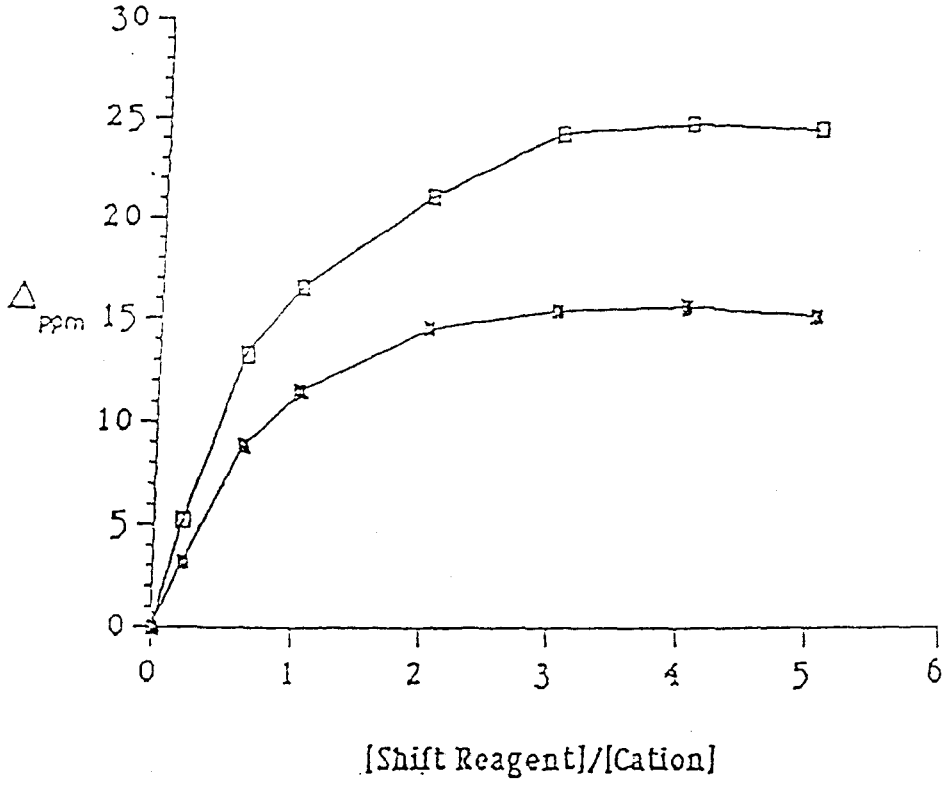
30
25
20
15
10
5
0
Δ ppm
0
1
2
3
4
5
6
[Shift Reagent]/[Cation]

the shift reagent was used. For [shift reagent]/[cation] ratios greater than or equal to 3, both the $^{7}Li^{+}$ and $^{23}Na^{+}$ chemical shift separations level off and remain approximately constant. Although the chemical shift separation for ^{23}Na is larger than that of Li^{+} at physiologically relevant concentrations of Na^{+}, it is still possible to obtain a clear separation of the two $^{7}Li^{+}$ pools using $Dy(PPP)_2^{-7}$. The chemical shift separations between the two $^{7}Li^{+}$ NMR resonances of Li^{+}-loaded RBC suspensions containing 1, 3, 5, 10, 15 and 20 mM shift reagent (in the Na^{+} form) and 1 mM Li^{+} in the extracellular compartment were found to be 0.2, 1.7, 3.7, 7.8, 10.7 and 10.8 ppm, respectively. Thus for the therapeutic levels of Li^{+} used in the United States, i.e, where the plasma [Li^{+}] concentration varies between 0.5 and 1.2 mM, a minimal concentration of 3 mM $Dy(PPP)_2^{-7}$ is enough to resolve the two $^{7}Li^{+}$ NMR resonances. The largest possible $^{7}Li^{+}$ chemical shift separation between the two $^{7}Li^{+}$ pools in RBC suspensions from manic-depressive patients can be achieved using 15 mM concentration of the shift reagent. However, a significant amount of broadening (>200 Hz) of the extracellular $^{7}Li^{+}$ resonance is observed under these conditions.

3. Competition between Li^{+} and other Metal Cations for the Shift Reagent, $Dy(PPP)_2^{-7}$

Table 7 shows the results of the study of the

competition for dysprosium (III) triphosphate between Li^+ and Na^+, K^+, Mg^{+2} and/ or Ca^{+2}, at their physiologically relevant concentrations. The ^7Li chemical shift separation was measured for concentric samples (5 mm inner tube containing 5 mM LiCl in distilled water inside a 10 mm outer tube containing the sample medium). The sample medium was composed of 10 mM glucose, 5 mM $Na_7Dy(PPP)_2.3NaCl$, 17% D_2O and 50 mM HEPES, pH 7.5. The concentrations of the metal cations used are indicated in Table 7.

Table 7 indicates that divalent cations compete more effectively with Li^+ than monovalent cations. Figure 10 shows the solution structure of the shift reagent, $Dy(PPP)_2^{-7}$. Multinuclear NMR studies on dysprosium (III) triphosphate carried out at pH 7.5 suggest a solution structure where the alkali countercations are present in the second coordination sphere of the complex thereby neutralizing its -7 charge (Figure 10). Because of the difference in charges, a smaller number of divalent cations are needed to counterbalance the negative charges on the triphosphate ligands relative to monovalent cations. Divalent cations have also been found to replace the lanthanide in the complex at higher divalent cation concentrations (112). Moreover, experiments carried out in the presence of two or more competing cations show that the decrease observed in the $^7Li^+$ chemical shift separation is

Table 7

Competition between Li^+ and other Metal Cations for the Shift Reagent, $Dy(PPP)_2^{-7}$

ion concentration[a] (mM)					7Li Chemical Shift Separation[b] (ppm)
Na^+	K^+	Mg^{+2}	Ca^{+2}	Li^+	
50				1	11.16[c]
140				1	5.89
50	5			1	10.84
50		1		1	9.66
50			2	1	6.11
140	5			1	5.16
140	5	1		1	4.48
140	5	1	2	1	2.93

[a] The sample medium contained, in addition to the ions indicated above, 10 mM glucose, 5 mM $Na_7Dy(PPP)_2.3NaCl$, 17% D_2O, and 50 mM HEPES at pH 7.5 and 37°C. [b] The ^7Li chemical shift separation was measured for concentric samples (5-mm inner tube containing 5 mM LiCl in distilled water inside a 10 mm outer tube containing the sample medium described in footnote a). [c] The [shift reagent]/[Li^+] ratio in this experiment is 5, and the chemical shift separation is 11.16 ppm.

Figure 10. The postulated solution structure of the shift reagent $Dy(PPP)_2^{-7}$ is shown on the right (adpated from ref. 127). Dy (III) is coordinated to two triphosphate ligands and one water in the first coordination sphere while seven alkali counterions (Na^+ or Li^+) are present in the second coordination sphere. Triphosphate is coordinated to Dy (III) via two oxygens of one PO_3 group, one oxygen of the other PO_3 group, and one oxygen of the PO_2 moiety.

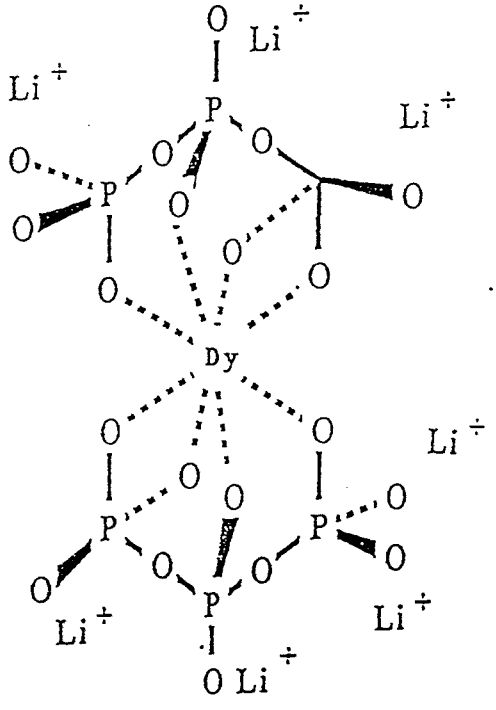
O
Li ÷
Li ÷
P
O
Li ÷
O
P
O
O
O
O
O
O
O
Dy
O
O
Li ÷
O
O
O
P
P
O
O
O
O
P
O
Li ÷
Li ÷
O Li ÷

is not additive. It is important to note that the two $^{7}Li^{+}$ NMR resonances in RBC suspensions are separated by approximately 3 ppm even in the presence of physiologically relevant concentrations of Na^{+}, K^{+}, Mg^{+2} and Ca^{+2}.

4. Monensin-induced Passive Li^{+} Transport in RBCs

A small volume of a stock solution of the ionophore monensin dissolved in methanol was added to Li^{+} loaded RBCs suspended in isotonic K^{+} rich buffer (99 mM KCl, 10 mM glucose, 1 mM LiCl, 5 mM $K_7Dy(PPP)_2.3KCl$, 5 mM phosphate, pH 7.5, 17% D_2O) to 0.06 mM final concentration, at 13% hematocrit. Addition of the lithium ionophore, monensin, to an RBC suspension in a K^{+}-only medium (Figure 11) induces passive Li^{+} transport. It was found that the gain in peak area of the extracellular $^{7}Li^{+}$ NMR resonance was exactly matched by the loss in peak area of the intracellular $^{7}Li^{+}$ resonance. Addition of different concentrations of monensin, 0.06, 0.09, and 0.23 mM, to Li^{+}-loaded RBC suspensions led to apparent k values of 0.013, 0.017 and 0.049 min^{-1}, respectively. The apparent rate constants were determined from a linear regression analysis of a plot of $\ln([Li^{+}]_t/[Li^{+}]_0)$ versus time ($r = 0.90$), where $[Li^{+}]_0$ and $[Li^{+}]_t$ represent the initial Li^{+} concentration and that after time t. The ratio k/[monensin] was approximately constant and equal to 206 $\pm$ 15 M^{-1} min^{-1}. Thus the pseudo-first order rate constants

Figure 11. Time dependence of the ^{7}Li NMR (104.8 MHz, 37°C) spectrum of a suspension of RBCs that have been incubated overnight with 150 mM LiCl, 10 mM glucose and 5 mM HEPES, pH 7.5. The suspension medium contained 1 mM LiCl, 149 mM KCl (including shift reagent and phosphate contribution), 10 mM glucose, 5 mM $K_7Dy(PPP)_2.3KCl$ and 5 mM potassium phosphate, at pH 7.5. 17% D_2O was present for field frequency lock and the hematocrit was 13%. Spectra A - D are labeled with the time elapsed after the RBC suspension was made 0.06 mM in monensin (ethanol solution). The time labels represent midpoints of the accumulation periods. The normalized percentage areas of the inner and outer pools of Li^+ are indicated on the plot. At the end of 75 min, all of the intracellular Li^+ had been transported out to the extracellular medium.

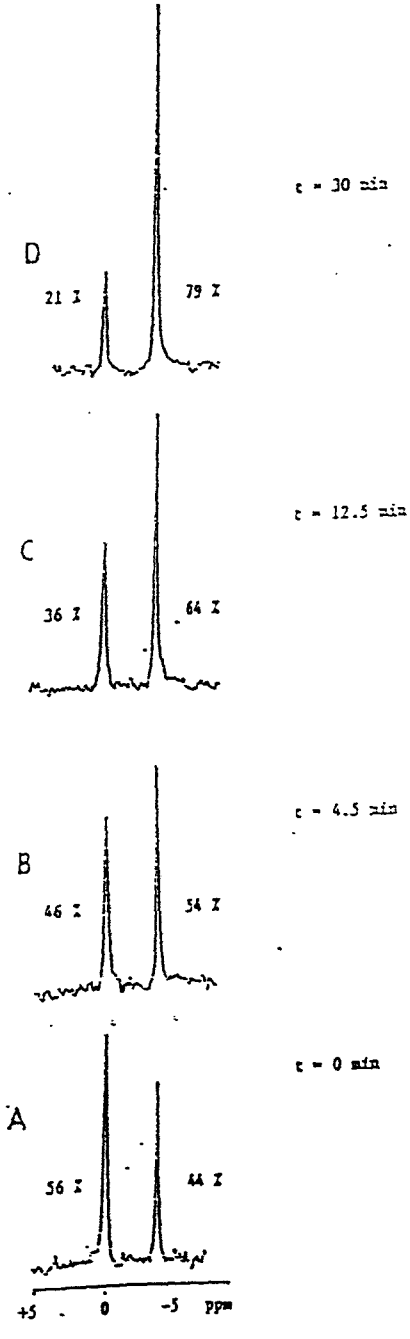
t = 30 min
D
21 %
79 %
t = 12.5 min
C
36 %
64 %
t = 4.5 min
B
46 %
54 %
t = 0 min
A
56 %
44 %
+5
0
-5
ppm

for Li^+ transport across RBC membranes are dependent on monensin concentration, indicating that the $^7Li^+$ NMR resonance intensity changes observed in Figure 11 are indeed due to Li^+ transport.

^{31}P NMR studies of inorganic phosphate present in the RBC suspension medium indicate that no pH change occurs as a result of the monensin-induced Li^+ transport. However, the chemical shift separation afforded by the shift reagent dysprosium (III) triphosphate is strongly pH dependent, particularly around pH 7.5 (112). Since no changes in the chemical shift separation between the two $^7Li^+$ NMR resonances or the position of the inorganic phosphate ^{31}P NMR resonance were observed, no Li^+ - H^+ exchange is taking place. Monensin is known to have a higher affinity for Na^+ than for Li^+ (5) and thus a Na^+-Li^+ exchange could in principle be occurring. However, a Na^+-Li^+ exchange mechanism is not probable because in this case the cells are suspended in a K^+-only medium and virtually no intracellular Na^+ is present in RBCs (as measured by ^{23}Na NMR spectroscopy), as a result of extensive Li^+ loading of red cells. Experiments similar to that described in Figure 11 have also been tried, where K^+ in the suspension medium was partially or completely replaced by Na^+ and it was found that no Li^+ transport occurred. Absence of monensin-induced Li^+ transport in RBCs suspended in a Na^+ medium is probably a result of

strong Na^+ binding to monensin. In the case of Figure 11, a Li^+-K^+ exchange mechanism is probably taking place. Direct evidence for the proposed mechanism is difficult to obtain by metal NMR spectroscopy because of the inherently low sensitivity of the ^{39}K nucleus and the unavailability of a K^+ probe.

C221 and C211 were also briefly tested as potential lithium ionophores (5) by ^7Li NMR spectroscopy. In a K^+-only suspension medium, addition of C221 led to slow Li^+ transport. Equilibrium of the two Li^+ pools took more than one day (Figure 10), in the case of C221 as opposed to 75 min for monensin. At C221 concentrations of 0.12, 0.36, 0.60 and 1.2 mM, the RBC/plasma Li^+ ratios at t = 24 h were found to be 0.14, 0.12, 0.14 and 0.15 respectively. It was also found that addition of C211 to a RBC suspension induced slow lithium transport as well as lithium binding to C211. It is important to note that the chemical shift position of the ^7Li resonance shown in Figure 12A does not exactly match the shifted ^7Li resonances shown in Figure 12B - 12D. Although the C221 binds Li^+, it is in fast exchange such that the observed ^7Li resonance is the weighted average of the bound and free Li^+ ions. With both cryptands, however, the unfacilitated Li^+ transport (obtained without addition of cryptand) amounted to approximately 50% of that induced by ionophores. Atomic absorption studies carried out on similar Li^+-loaded RBC

Figure 12. Time dependence of the ^{7}Li NMR (104.8 MHz, 37°C) spectrum showing passive Li^{+} transport induced by addition of C221 to RBCs which have been incubated overnight with 150 mM LiCl, 10 mM glucose and 5 mM HEPES, pH 7.5. The suspension medium contained 10 mM LiCl, 140 mM KCl (including contribution from the shift reagent), 10 mM glucose, 5 mM $K_7Dy(PPP)_2.3KCl$ and 5 mM HEPES, pH 7.5. The hematocrit was 13% and 17% D_2O was present for field frequency lock. Spectra B - D are labeled with the time elapsed after a small aliquot of an ethanolic stock solution of C221 was added to the RBC suspension, to a final concentration of 0.6 mM. A is a ^{7}Li NMR spectrum of a control sample containing the suspension medium alone.

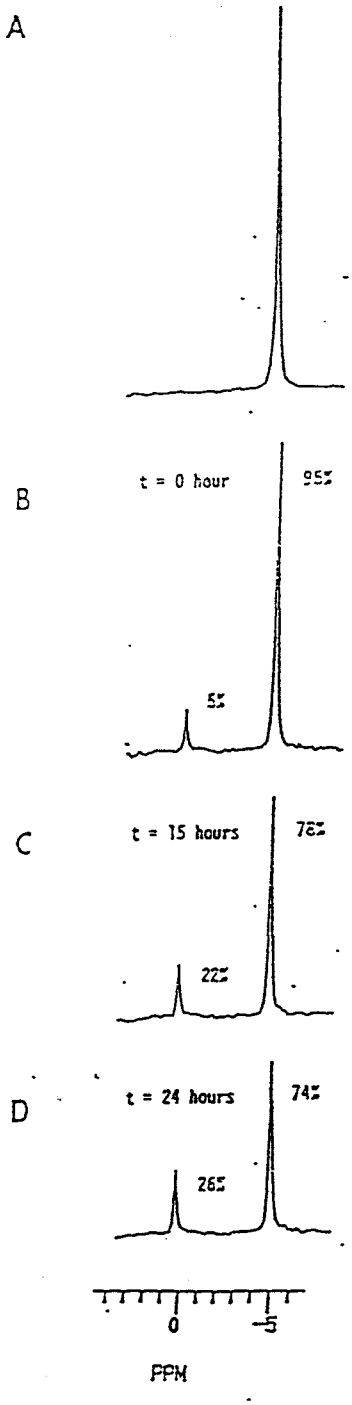
A
B
t = 0 hour
95%
5%
C
t = 15 hours
78%
22%
D
t = 24 hours
74%
26%
0
-5
PPM

suspensions that had been incubated with either cryptand, but in the absence of the shift reagent, confirmed that C221 and C211 can induce slow Li^+ transport in a K^+ -only RBC suspension.

B. Visibility of the ^7Li NMR Resonance

Before converting the signal intensities obtained in the NMR experiments into concentrations, it is important to establish whether or not the observed $^7Li^+$ resonances reflect the entire population of the two lithium pools. This control experiment is particularly important in the case of ^7Li NMR since the $^7Li^+$ nucleus has a quadrupole moment (9) and as a result, quadrupolar broadening could render part of the Li^+ invisible in the ^7Li NMR experiment. Li^+-loaded RBC samples (Figure 13A) suspended in a Li^+-free medium were subjected to hemolysis (Figure 13B). Cell hemolysis was achieved by incorporating 10% Triton X-100 in the RBC suspension medium. The hematocrit and total suspension volume are the same for all the samples depicted in Figures 13A and 13B. Thus there is no need for a dilution correction with this cell hemolysis procedure to compare the intensities of the resonances in the two experiments. The RBC membrane was totally solubilized by the detergent and thus, any Li^+ complexed to membrane phospholipids will also be measurable by this procedure. It was found that the intensity of the $^7Li^+$ NMR resonance

Figure 13. (A) ^{7}Li NMR (116.5 MHz, 37°C) spectrum of Li^{+}-loaded RBCs suspended in isotonic TRIS buffer, pH 7.5 containing 112.5 mM choline, 85 mM sucrose and 10 mM glucose. Hematocrit was 13%. Addition of shift reagent did not result in separation of two resonances confirming that the medium was Li^{+} free. Thus the observed resonance represents intracellular Li^{+}. (B) ^{7}Li NMR spectrum of an RBC solution with the same hematocrit as sample A except that 10% Triton X-100 is also present. Total sample volume is 3 mL as for the sample used in A. No change in intracellular Li^{+} intensity is observed relative to A. (C) ^{23}Na NMR (79.4 MHz, 37°C) spectrum of packed RBCs suspended in the same medium as in A. (D) ^{23}Na NMR spectrum after lysing RBCs with Triton X-100 as in B. The intracellular Na^{+} intensity increased by 20% relative to C. While the addition of 0.1 μM gramicidin had no effect on the intensity of the intracellular $^{7}Li^{+}$ resonance observed in A, it caused an increase in the intensity of the intracellular $^{23}Na^{+}$ resonance in C of approximately 10%. Total accumulation time for ^{7}Li and ^{23}Na NMR spectra were 3 and 1 hours, respectively.

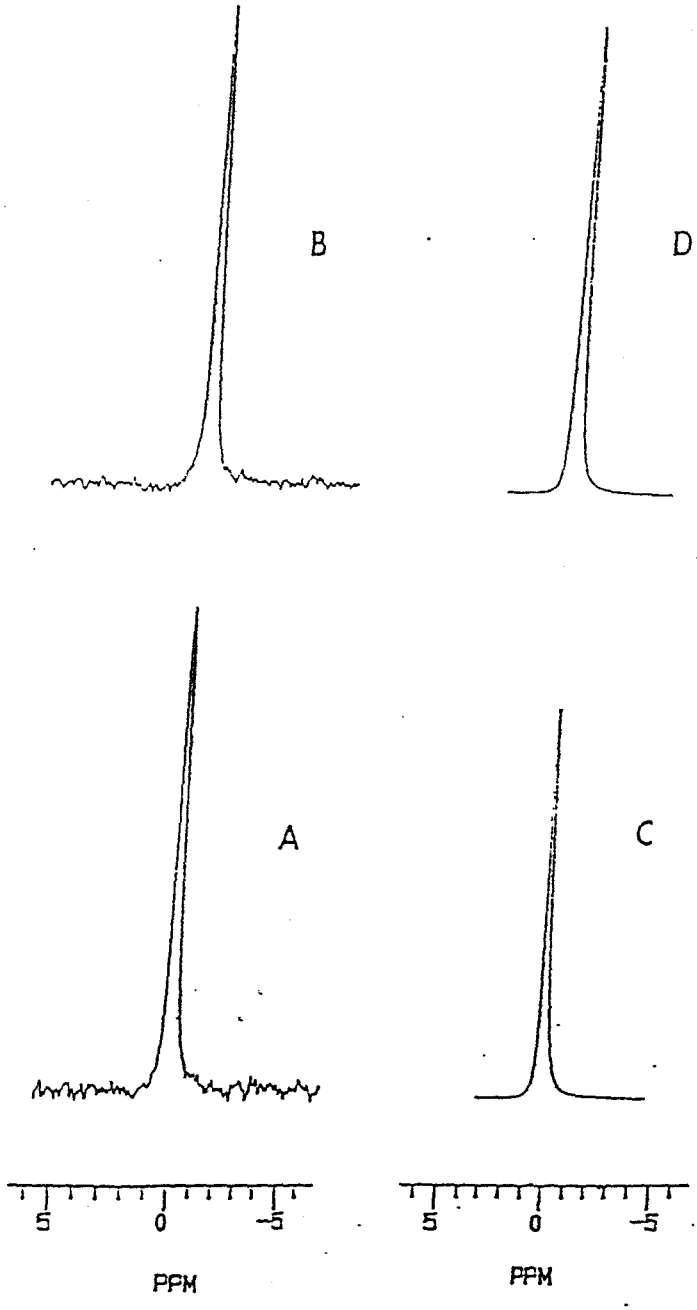
B
D
A
C
5
0
-5
PPM
5
0
-5
PPM

did not change after cell hemolysis indicating that lithium is 100% (98 ± 2, n=5) visible in the NMR experiment.

Similar experiments were carried out on intracellular Na^+ by ^{23}Na NMR (94b) have shown that the intracellular sodium pool in RBCs is only 80% visible in the ^{23}Na NMR experiment. However, addition of the Na^+ ionophore gramicidin resulted in depolarization of RBCs and rendered the Na^+ resonance 100% NMR visible. The results confirming this previous observations are shown in Figure 13C and 13D. The visibility of the $^{23}Na^+$ NMR resonance was 80% (80 ± 5, n=3). The $^{23}Na^+$ NMR results can be interpreted as evidence of a subpool of intracellular Na^+ ions experiencing quadrupolar broadening large enough to cause the disappearance of the corresponding resonance. The existence of this sodium pool is dependent upon the presence of a negative membrane potential, as demonstrated by the effect of gramicidin on the intensity of the intracellular Na^+ resonance. The NMR invisible Na^+ may be interacting with negatively charged phospholipids on the cytoplasmic side of the RBC membrane, such as phosphatidylserine, and may be in chemical exchange with free intracellular Na^+ ions. Treatment with Triton X-100 is disrupting specific Li^+- and Na^+-membrane interactions and thus, it ensures 100% NMR visibility of $Li^+$and Na^+ ions.

Although a subpool of intracellular Li^+ ions may

also be present in RBCs, it does not lead to partial NMR invisibility. Several reasons may account for the different behaviors of Li^+ and Na^+ ions in the corresponding NMR experiments. It may be that the lower quadrupole moment of the ^7Li nucleus (relative to that of the ^{23}Na nucleus) would result in smaller quadrupolar broadening for membrane-bound Li^+ ions. This relaxation mechanism may not be large enough to cause invisibility of the intracellular ^7Li NMR resonance. However, the observation of bound Li^+ ions would be expected to result in broadening of the intracellular $^7Li^+$ resonance in RBCs. Li^+ concentrations from three samples of RBC suspensions which have been loaded with different Li^+ levels were determined by both AA and NMR methods. The RBCs were found to contain 0.29, 0.50 and 0.90 mM Li^+ by AA and 0.31, 0.49 and 0.88 mM Li^+ by NMR (MIR). Determinations were done in triplicates and the values obtained by the two methods are in very good agreement. Thus, comparison of Li^+ concentrations in Li^+-loaded RBCs determined by AA and NMR confirms 100% NMR visibility of intracellular Li^+ ions. The different relaxation behavior of the intracellular $^7Li^+$ resonances in RBCs and the site of interaction of these metal cations with the cytoplasmic side of the RBC membrane are discussed in the section on Li^+ membrane interactions (IV.F).

C. ^{7}Li NMR Method involving a Modified-Inversion Recovery (MIR) Pulse Sequence

By using a modified inversion recovery method (MIR) previously described for $^{39}K^{+}$ NMR studies (106), it was possible to differentiate between the two pools of lithium in RBC without the use of shift reagents (Figure 14). The pulse sequence takes advantage of the large difference in T_1 values for the intra- and extracellular $^{7}Li^{+}$ ions (4.9 and 16.5 s, respectively). The standard one-dimensional ^{7}Li NMR spectrum (D-60°-Acquire) of the RBC suspension depicted in Figure 14A contains only one signal that represents the overlapped intra- and extracellular $^{7}Li^{+}$ NMR resonances. A 60° flip angle and a delay D_1 between single pulses $\geq$ 60 s were found to achieve complete relaxation of both lithium signals. Figure 14B shows the ^{7}Li NMR spectrum of the intracellular lithium resonance obtained by the MIR method (D_1-180°-D_2-60°-Acquire). Since the T_1 value of intracellular $^{7}Li^{+}$ is about 5 s, its magnetization component which was originally placed along the -z axis after a 180° pulse will have sufficient time to relax back to the +z axis after a delay of D_2 of 11.5 s. The intracellular $^{7}Li^{+}$ resonance can therefore be detected along the y-axis after a 60° pulse. Figure 15 shows the effect of varying D_2 on the $^{7}Li^{+}$ resonance intensities of a Li^{+}-loaded RBC suspension and of the medium alone. At D_2 = 11.5 s, the $^{7}Li^{+}$ signal is nulled for the suspension medium alone while the $^{7}Li^{+}$ resonance for the Li^{+}-loaded RBC

Figure 14. (A) ^{7}Li NMR (116.6 MHz, 37°C) spectrum of a Li^{+}-loaded control RBC suspension as for Figure 6A. A single pulse sequence was employed and the spectrum represents the overlapped intra- and extracellular lithium pools. (B) ^{7}Li NMR spectrum of the same RBC suspension as in A except that MIR pulse sequence was used. The spectrum represents the intracellular $^{7}Li^{+}$ resonance. (C) The difference spectrum of Figures A and B. The spectrum represents the extracellular $^{7}Li^{+}$ resonance. (D) ^{7}Li NMR spectrum of the suspension medium alone (no RBCs) using the same MIR method as in B. A total of 8 scans were taken for each spectrum with a total accumulation time of approximately 9.7 min, except for spectrum 14A which took 8 min.

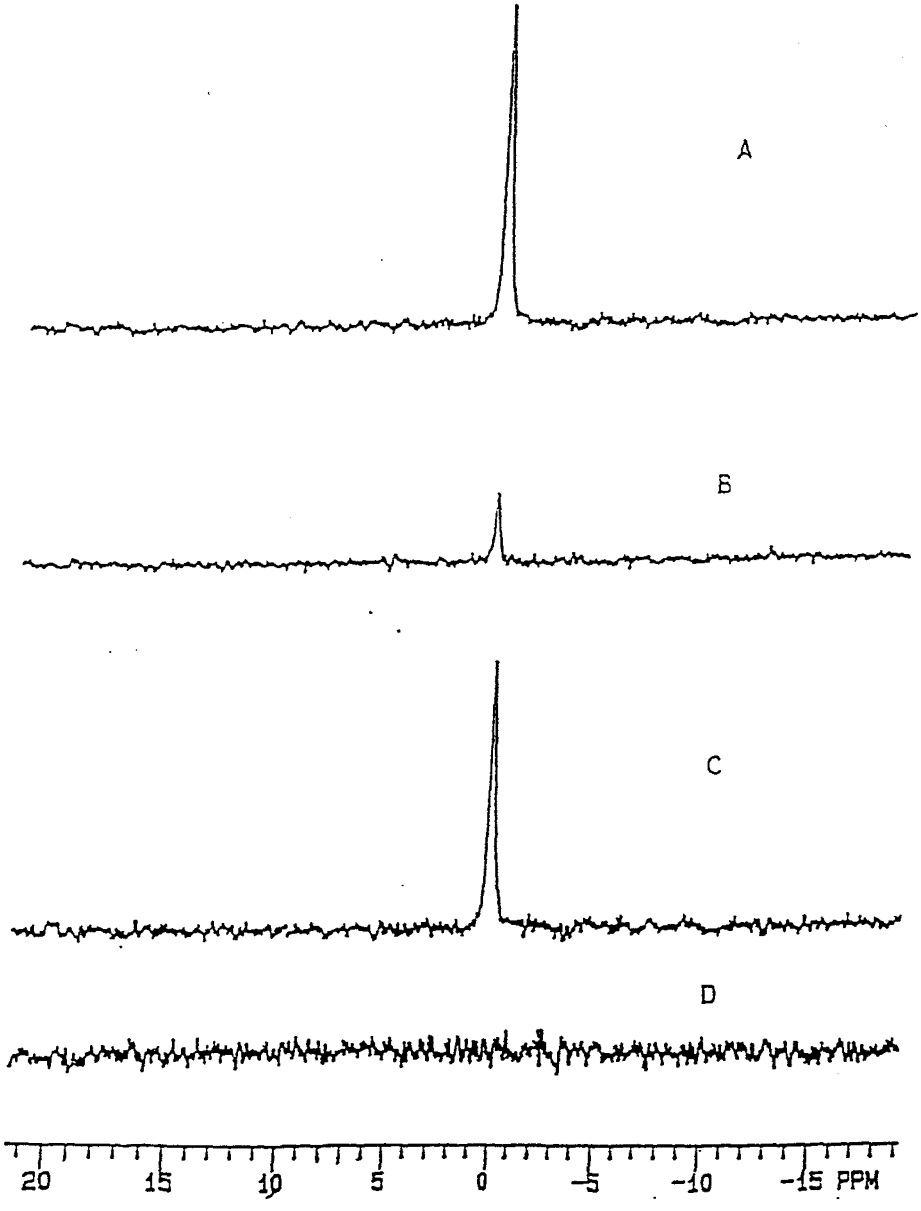
A
B
C
D
20
15
10
5
0
-5
-10
-15 PPM

Figure 15. Plot of $^{7}Li^{+}$ resonance intensities of a Li^{+} loaded RBC suspended in a non-Li^{+} containing medium (diamonds), Li^{+}-free RBC in Li^{+}-containing suspension medium (triangles) and Li^{+}-loaded RBC suspended in a Li^{+}-containing suspension medium (squares) as a function of delay time D_2 using the MIR pulse sequence. Acquisition parameters are the same as in Figure 14B. The Li^{+} -free and Li^{+} containing suspension media used were the isotonic choline chloride buffer used before except that 1.5 mM Li^{+} is present in the latter case. The inset is a plot of observed Li^{+} intensity versus D_2 and is an expansion of the D_2 = 0-18 s region of the full plot.

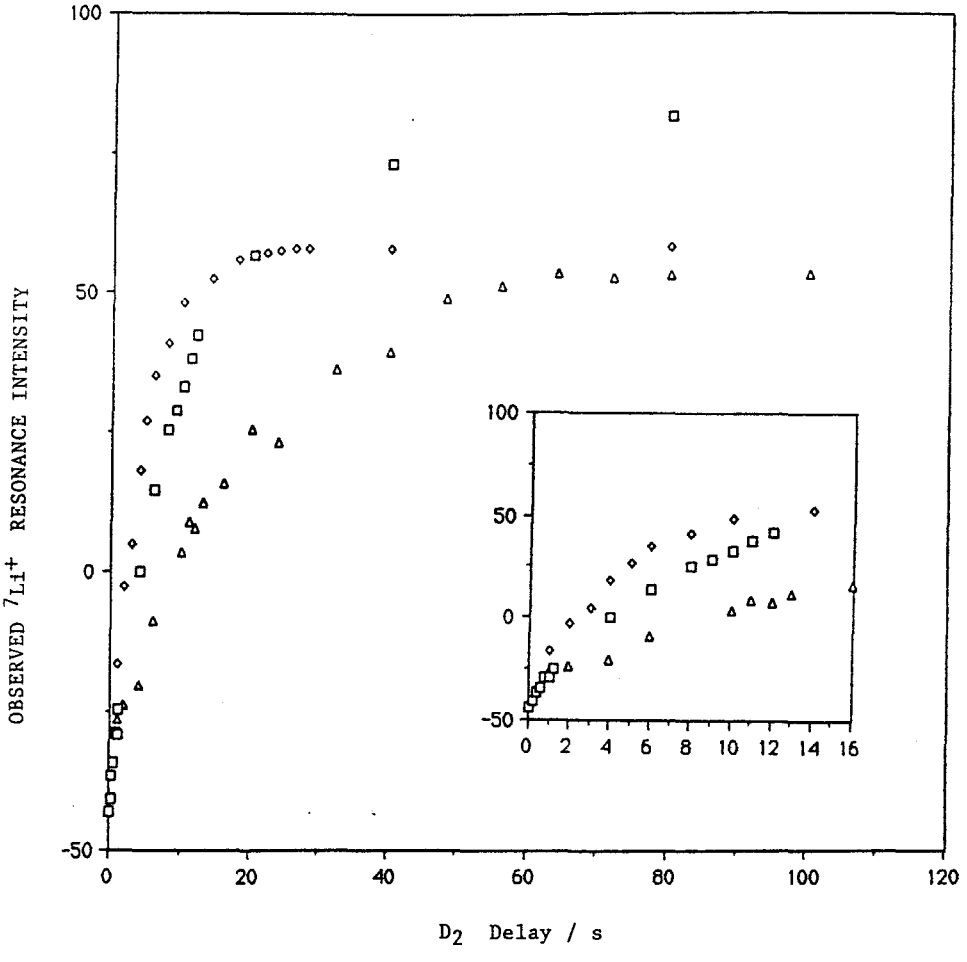
100
50
0
-50
0
20
40
60
80
100
120
OBSERVED $^{7}Li^{+}$ RESONANCE INTENSITY
D_2 Delay / s
100
50
0
-50
0
2
4
6
8
10
12
14
16

suspended in a non-Li^+ containing medium has reached 80% of its maximum intensity. All extracellular Li^+ in a Li^+-free RBC suspension has a T_1 identical to that of Li^+-containing medium, and therefore all extracellular Li^+ in a Li^+-loaded RBC suspension is expected to be at a null in the MIR experiment for D_2 = 11.5 s (Figure 14D and 15). The observed signal in Figure 14B is therefore only due to the intracellular Li^+ and not to a combination of intra- and extracellular signals. This means that at a D_2 of 11.5 s followed by a 60° pulse, the magnetization component of extracellular $^7Li^+$ along the y-axis is vanishingly small and its resonance disappears. To confirm this, a ^7Li NMR spectrum of the suspension medium alone using the modified pulse sequence was collected and is shown in Figure 14D. The difference spectrum shown in Figure 14C represents the extracellular lithium pool.

It is important to note that the delay time D_2 used for suppressing the extracellular $^7Li^+$ resonance and the spin-lattice relaxation time (T_1) are dependent on the suspension medium being used. Thus, for the experiments using whole blood and choline suspension medium, these parameters were remeasured. Table 8 shows the D_2 and ^7Li T_1's for the different suspension media and for whole blood plasma. All experiments involving the MIR technique were conducted at a constant temperature of 37°C, since T_1 and D_2 are highly temperature dependent.

Table 8

T_1 and D_2 Parameters for Different Buffer Media and Whole Blood Plasma

Medium	T_1/s n = 12	D_2/s n = 12
Na^+ rich buffer	16.5 ± 0.50	11.5 ± 0.10
Choline rich buffer	17.1 ± 0.50	11.5 ± 0.10
Whole blood plasma	11.3 ± 0.20	7.50 ± 0.30

D. Measurement of Rates of Na^+-Li^+ Countertransport in RBCs and Transmembrane Li^+ Distribution by ^7Li NMR and Atomic Absorption

Cell volume changes during the time course of Na^+-Li^+ countertransport measurements by NMR and AA were analyzed by Coulter Counter and hematocrit determinations for Li^+-loaded RBCs with an intracellular Li^+ concentration of 1.0 mM. During the time period of Li^+ transport in both the Na^+- or choline containing media used in this study, the hematocrit reading was fairly constant at 0.13 $\pm$ 0.01 (n=3) and the mean cell volume determined by the Coulter Counter was 89 $\pm$ 0.2 fL (n=3). Therefore, no significant changes in cell volume are observed during the time period that rates of Na^+-Li^+ countertransport are being monitored by either NMR or AA methods.

1. Transmembrane Li^+ and Na^+ Distribution by MIR and AA

Table 9 shows a comparison of transmembrane Li^+ and Na^+ distributions in control RBCs determined by AA and the two NMR methods. It is important to note that the NMR experiments were carried out in intact RBC suspensions while the AA measurements were carried out on lysed cells. For purposes of comparison, the ^7Li NMR measurements were also carried out on lysed RBCs (as for the AA determinations).

One of the NMR methods involve the incorporation of a shift reagent in the extracellular suspension medium to discriminate between the two Li^+ pools, thus AA

Table 9

Comparison of Li^+ and Na^+ ratios from control RBCs obtained by atomic absorption (AA) and two NMR methods, one involving the use of shift reagents (SR) and the other, a modified-inversion recovery pulse sequence (MIR)

	$[Li^+]_{in}/[Li^+]_{ex}$		$[Na^+]_{in}/[Na^+]_{ex}$	
	Intact	Lysed	Intact	Lysed
1. Atomic Absorption				
No SR (n=3)		0.36 ± 0.02		0.042 ± .004
With SR				
$Dy(TTHA)^{-3}$ (n=12)		0.34 ± 0.02		0.041 ± 0.004
$Dy(PPP)_2^{-7}$ (n=12)		0.46 ± 0.02		0.026 ± 0.004
2. NMR				
MIR (n=12)	0.34 ± 0.04			
With SR				
$Dy(TTHA)^{-3}$ (n=12)	0.34 ± 0.03	0.35 ± 0.02	0.042 ± 0.002	
$Dy(PPP)_2^{-7}$ (n=12)	0.47 ± 0.01	0.48 ± 0.03	0.028 ± 0.003	

A student t-test was applied to the data, and the difference between the Li^+ and Na^+ ratios measured in the presence or absence of 7 mM $Dy(PPP)_2^{-7}$ is significant up to a 99.9% confidence level. Aliquots of the same blood sample were analyzed by the three methods. The composition of the suspension media are: 1) for MIR samples, 140 mM NaCl, 10 mM glucose, 1.5 mM LiCl and 10 mM Tris-Cl, pH 7.5; 2) for the SR containing samples, the same as for the MIR suspension medium except that 7 mM $Dy(PPP)_2^{-7}$ replaced 70 mM NaCl or 7 mM $Dy(TTHA)^{-3}$ instead of 21 mM NaCl. The integrated $^{23}Na^+$ intensities were converted into Na^+ concentrations after taking into account the 20% invisibility of the intracellular $^{23}Na^+$ signal.

measurements were also taken for RBC samples which had been treated with shift reagent. For the MIR experiments, packed RBCs were suspended in isotonic medium containing 140 mM NaCl, 10 mM glucose, 1.5 mM LiCl and 10 mM Tris-Cl, pH 7.5 while for the shift reagent experiments packed RBCs were suspended in a similar isotonic media except that 7 mM $Dy(PPP)_2^{-7}$ replaced 70 mM NaCl or 7 mM $Dy(TTHA)^{-3}$ instead of 21 mM NaCl. All samples were prepared at 13% hematocrit. The RBC/plasma Li^+ and Na^+ ratios for these suspensions were then determined after incubation for 4 h at 37°C. The values obtained for transmembrane Li^+ and Na^+ distribution in control RBCs by AA, MIR and shift reagent method using dysprosium (III) tetraethylenehexacetate ($Dy(TTHA)^{-3}$) NMR, agree very well. However, those obtained by AA or the shift reagent method using $Dy(PPP)_2^{-7}$ are different. The latter shift reagent, $Dy(PPP)_2^{-7}$ is known to have a higher affinity for metal cations compared to $Dy(TTHA)^{-3}$ (97,112). Thus, the incorporation of the shift reagent, $Dy(PPP)_2^{-7}$, in the suspension medium leads to complexation of extracellular Na^+ ions which in turn causes a redistribution of the ions across the membrane resulting in an efflux of extracellular Na^+ and an influx of extracellular Li^+ (see Table 9).

2. Determination of Rates of Na^+-Li^+ Countertransport in RBCs by ^7Li NMR and Atomic Absorption

Figure 16 represents the changes in intracellular Li^+ intensities observed by the MIR method when Li^+-loaded

Figure 16. Time dependence of intracellular $^{7}Li^{+}$ NMR resonances of Li^{+}- loaded RBCs suspended in either a Na^{+}- rich medium (A) or a choline-rich medium (B). The time labels represent the midpoints of the accumulation periods. ^{7}Li NMR spectra were recorded using the MIR method described in Figure 14B. The coresponding changes in the linewidths of the $^{7}Li^{+}$ spectra are due to the dynamic exchange process during Li^{+} transport.

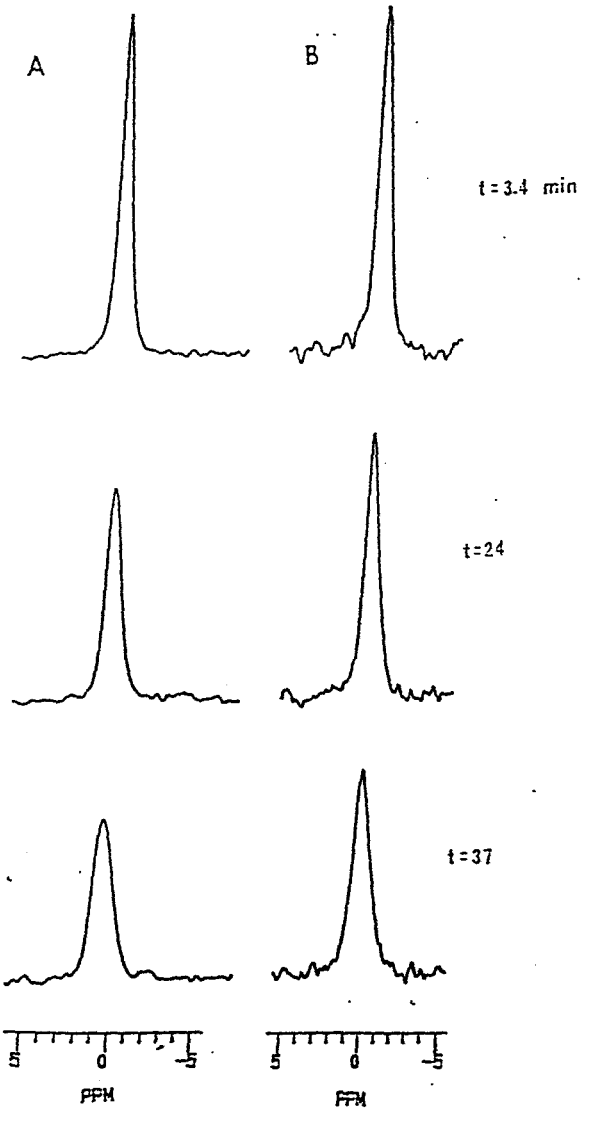
A
B
t = 3.4 min
t=24
t=37
5
0
-5
PPM
5
0
-5
PPM

RBCs from healthy donors are suspended in either a Na^+- or choline- containing medium. The changes in intracellular Li^+ concentration with time are shown in Figure 17. The rate of Na^+-Li^+ countertransport can be calculated by subtracting the slope of the curve obtained in the choline medium from that obtained in the Na^+ medium. To rule out any specific effect of choline (37), the rate for the leak pathway was also measured in a Mg^{+2} medium by AA and MIR. In both cases, the rates measured in a Mg^{+2} medium agreed well with those determined in a choline medium (data not shown). The Na^+-Li^+ countertransport rate constants was determined from the difference in the slopes of the plot of $\ln([Li^+]_t/[Li^+]_0)$ versus time (Figure 18) for the Na^+- and choline-rich media as in Figure 16 and 17. For this particular normal control, the rate and rate constants are 0.18 mmoles Li^+/(L RBCs x h) and 0.33 h^{-1}, respectively.

The rate constants and rates of Na^+ - Li^+ countertransport in RBCs from manic-depressive patients and normal matched controls were measured by AA and MIR methods, and the results are summarized in Table 10. The observed rates measured by MIR have been found to be lower for the manic-depressive patients relative to normal controls (0.13 ± 0.02 vs. 0.23 ± 0.03, mean $\pm$ std. dev., df = 14, one-tailed student t test, $t = -12.62$, $p < 0.0005$). These results are in agreement with earlier reports on rates of Na^+-Li^+ countertransport (Table 11). Moreover,

Figure 17. Time dependence of intracellular Li^+ concentration in Na^+- rich (open squares) and choline-rich (closed diamonds) media. Points 1, 4 and 6 in each curve correspond to the spectra displayed in Figure 16.

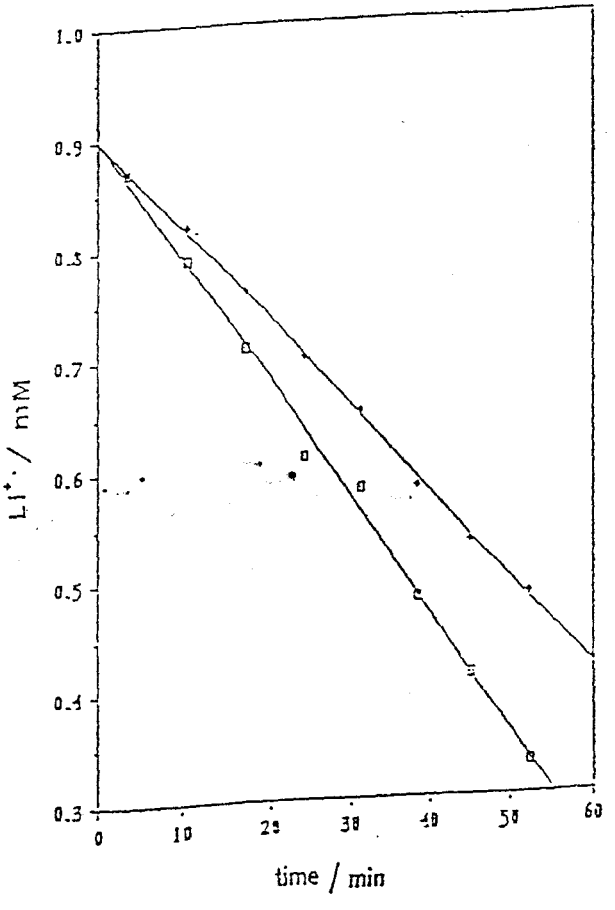
1.0
0.9
0.8
0.7
0.6
0.5
0.4
0.3
Li+ / mM
0
10
20
30
40
50
60
time / min

Figure 18. Plot of $\ln\{[Li^+]_t/[Li^+]_0\}$ versus time, where $[Li^+]_0$ and $[Li^+]_t$ represent the initial Li^+ concentration and that after time t. Open squares and closed diamonds represent transport measurements in Na^+- and choline-rich media, respectively. The Na^+-Li^+ countertransport rate constant is calculated from the difference of the slopes of the plot for Na^+- and choline-rich media.

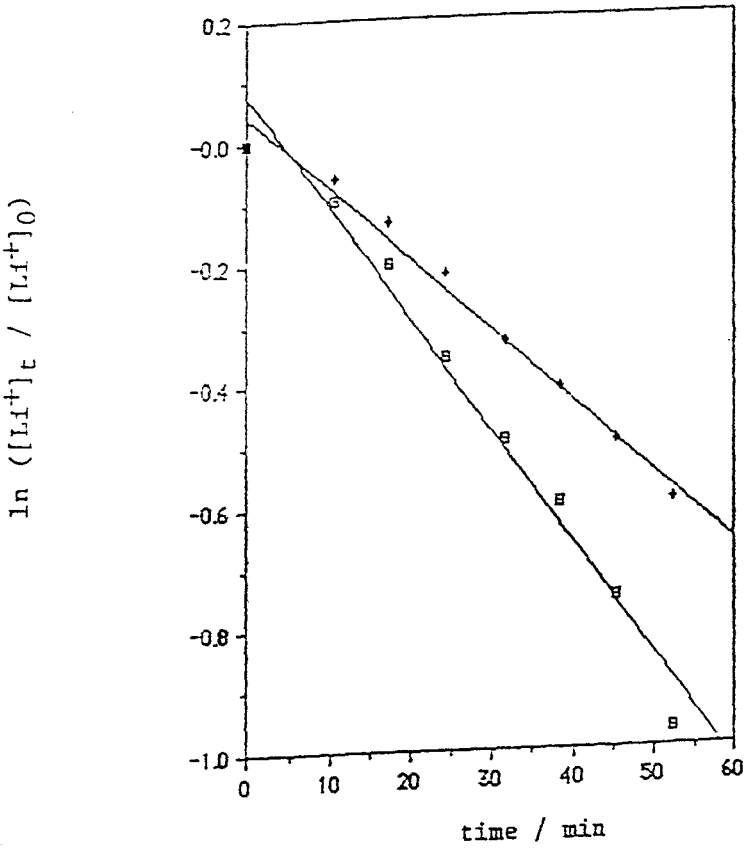
ln ([Li+]t / [Li+]0)
0.2
-0.0
-0.2
-0.4
-0.6
-0.8
-1.0
0
10
20
30
40
50
60
time / min

Table 10

Comparison of Na^+-Li^+ Countertransport Rates in mmoles of Li^+ / (L RBCs x h) obtained by Atomic Absorption (AA) and MIR

No.	Age, Race and Sex		Rates				Rate Constant	
			AA		MIR		MIR	
	Bipolar	Normal	Bipolar	Normal	Bipolar	Normal	Bipolar	Normal
1	24WM	30WM	0.10	0.23	0.11	0.22	0.09	0.18
2	30BM	35BM	0.13	0.19	0.14	0.20	0.11	0.29
3	34WM	31WM	0.13	0.19	0.12	0.20	0.09	0.16
4	35WM	33WM	0.15	0.23	0.15	0.23	0.15	0.19
5	35WM	45WM	0.12	0.20	0.13	0.23	0.17	0.19
6	36WM	50WM	0.15	0.25	0.16	0.26	0.11	0.20
7	28WF	28WF	0.10	0.20	0.11	0.21	0.07	0.20
8	29WF	29WF	0.10	0.22	0.11	0.24	0.09	0.36
9	30WF	32WF	0.11	0.20	0.12	0.23	0.16	0.33
10	31WF	36WF	0.11	0.24	0.12	0.27	0.13	0.33
11	33WF	35WF	0.11	0.20	0.11	0.21	0.17	0.17
12	60WF	37WF	0.12	0.21	0.13	0.21	0.12	0.17
13	60WF	57WF	0.11	0.18	0.12	0.19	0.19	0.28
14	63WF	60WF	0.14	0.29	0.15	0.32	0.13	0.32
Ave	38±13	38±10	0.12±0.03	0.22±0.03	0.13±0.02	0.23±0.03	0.12±0.04	0.24±0.07

W=white, B=black, F=female, M=male; A one-tailed student t-test was applied to the data and the measured rates and rate constants are significant to a 99.95% confidence level ($p < 0.0005$). The values shown at the bottom of the table are mean ± standard deviation.

Table 11

Comparison of data on Na^+- Li^+ Countertransport Rates

Bipolar Patients	Matched Controls	References
$0.13 \pm 0.05^{a,e}$ n=15	0.16 ± 0.03 n=15	23
$0.16 \pm 0.08^{a,e}$ n=11	0.28 ± 0.09 n=11	26
$0.12 \pm 0.04^{b,e}$ n=52	0.19 ± 0.04 n=58	27
$0.24 \pm 0.17^{a,d,e}$ n=6	0.35 ± 0.14 n=28	34
$0.20 \pm 0.11^{a,d,e}$ n=46	0.26 ± 0.11 n=20	52
$0.13 \pm 0.02^{a,d,e}$ n=14	0.23 ± 0.03 n=14	this study[g]
$0.39 \pm 0.17^{a,d,f}$ n=10	0.36 ± 0.13 n=8	32
$0.36 \pm 0.17^{a,d,f}$ n=12	0.35 ± 0.14 n=28	33
$0.10 \pm 0.04^{c,d,e}$ n=8	0.10 ± 0.04 n=52	34
$0.32 \pm 0.14^{a,d,e,f}$ n=42	0.29 ± 0.11 n=238	31a

[a] expressed as millimoles Li^+/l RBC x 4 hr; [b] expressed as millimoles Li^+/l RBC x hr; [c] expressed as microequivalents Li^+/ ml RBC x 30 min; [d] maximal rates; [e] lithium treated bipolar patients; [f] lithium free bipolar patients; [g] data was collected by NMR, all other data in this table were collected by AA.

the results determined by MIR agree very well with AA data (Table 10). Most of the studies on Li^+ transport in RBCs employed conventional techniques (85) like flame emission and atomic absorption. These techniques are invasive in nature. Thus, sample processing may have problems like nonspecific ion binding and additional ion transport. It should be noted that intraindividual variations (66) measured by AA were not found to be caused by the method used for Li^+ determination since most measurements have been carried out at least in duplicate and are highly reproducible. Thus, it appears that a methodological problem is not the cause for the overlap in the data from manic-depressive patients and normal controls reported previously (30,31,66,67). The Na^+-Li^+ countertransport rate constants had not been determined in previous studies. In this dissertation, the rate constants were determined and found to be significantly lower for manic-depressive patients relative to normal controls. It is possible that this parameter may be a better biological marker for manic-depression since it takes into account the variations in intracellular Li^+ levels.

E. Application of the ^{7}Li NMR Methods to Whole Blood of Bipolar Patients

The concentration of Li^+ in the plasma (0.5-1.2 mM) of bipolar patients undergoing lithium therapy is much lower than that of Na^+ or K^+ ions (11). In addition,

divalent cations like Mg^{+2} and Ca^{+2} are present in the plasma but not in the packed RBC suspension media used in most of these studies. Competition between Li^{+} and other cations, particularly Mg^{+2} and Ca^{+2}, for the shift reagents, could result in insufficient separation of the two $^{7}Li^{+}$ NMR signals (93). ^{7}Li NMR spectra of whole blood from three bipolar patients, to which an aliquot of isotonic 30 mM $Dy(PPP)_2^{-7}$ was added resulting in a final concentration of 5 mM of shift reagent in the plasma, showed clear separation of the two lithium pools. Figure 19A and 19B show the ^{7}Li MIR spectra of whole blood from one manic-depressive patient (patient 1 in Table 12). Figure 19C shows the ^{7}Li NMR spectrum of whole blood from the same patient obtained after addition of $Dy(PPP)_2^{-7}$. For one patient sample, the intracellular Li^{+} concentration determined by the MIR method was 0.38 mM while that obtained by the shift reagent method was 0.44 mM. Using a lower concentration of $Dy(PPP)_2^{-7}$, direct addition of 3 mM shift reagent to the RBC suspension medium caused the transmembrane Li^{+} ratio to increase to 0.81 (rather than 0.47). Direct addition of $Dy(PPP)_2^{-7}$ to the whole blood sample results in a 30 or 50 mM increase in Na^{+} in the plasma, for the 3 and 5 mM $Dy(PPP)_2^{-7}$, respectively. Water presumably leaked from the cells due to increase in the osmolarity of the extracellular media resulting in

Figure 19. (A) ^{7}Li NMR (117 MHz, 37°C) spectrum showing the intracellular Li^{+} pool of a whole blood suspension from a manic-depressive patient, obtained by MIR using a D_2 = 7 s. (B) ^{7}Li NMR spectrum of the extracellular Li^{+} from the same whole blood suspension as in (A). The spectrum is the difference spectrum as described in Figure 14C. (C) ^{7}Li NMR spectrum of a whole blood suspension from a manic-depressive patient, after addition of a small aliquot of isotonic $Dy(PPP)_2^{-7}$ solution to yield a final concentration of 5 mM shift reagent. A and B were obtained by MIR while C was obtained using the same single pulse sequence used for experiments involving shift reagents. A line broadening of 100 Hz was applied to A and B for better signal to noise ratio. A line broadening of 10 Hz was applied to C. The intensity scale for A and B is 6.7 x that of C. The RBC/plasma Li^{+} ratio were 0.38 and 0.44 as determined by MIR and SR methods, respectively.

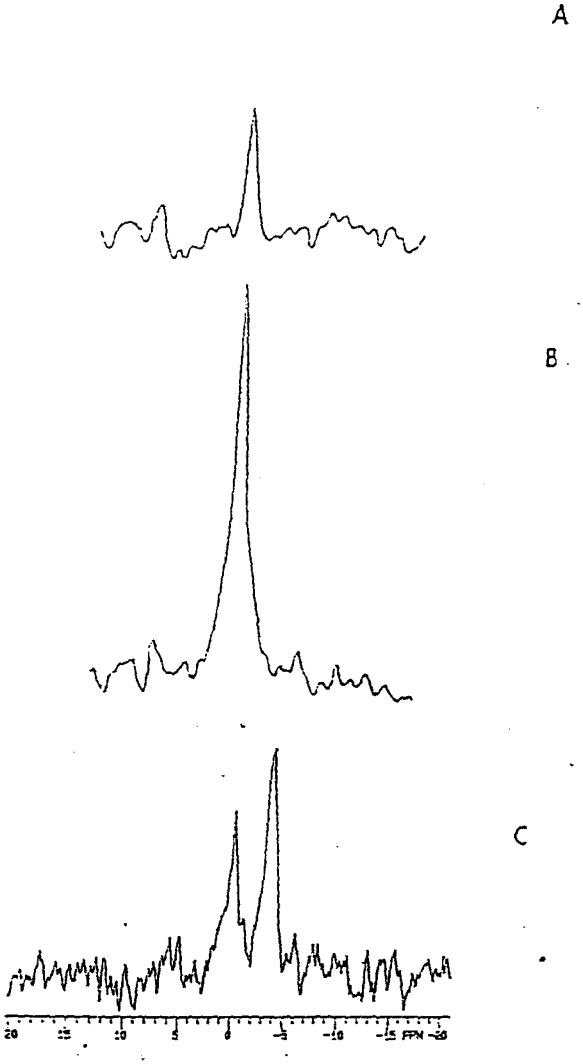
A
B
C
20
15
10
5
0
-5
-10
-15 PPM -20

Table 12

Comparison of Transmembrane Li^+ Distribution in Whole Blood samples from Bipolar Patients as measured by the Shift Reagent (SR) and MIR methods

	$[Li^+]_{in}/[Li^+]_{ex}$		
Patient No.	5 mM $Dy(PPP)_2^{-7}$	50 mM NaCl	MIR
1	0.44	0.37	0.38
2	0.47	0.35	0.35
3	0.45	0.38	0.37

abnormally high intracellular and low extracellular Li^+ concentrations. It is important to find out whether the redistribution of the Li^+ ions across the membrane was caused by this increase in Na^+ in the plasma or by the shift reagent itself. To check for this, an aliquot of an isotonic 150 mM NaCl solution was added to the whole blood sample of the same patient resulting in a 50 mM final NaCl concentration and the transmembrane Li^+ distribution was measured by the MIR technique. It was found that the addition of NaCl had no significant effect on the intracellular Li^+ concentration (0.37 mM). This same trend was observed in similar experiments with whole blood samples obtained from two other manic-depressive patients. The results are summarized in Table 12.

Thus, the changes observed are indeed due to the specific shift reagent effect. Transmembrane Li^+ ratios are likely to be overestimated if a shift reagent is added, rather than incorporated, in the RBC suspension medium. Both ^7Li NMR methods present sensitive approaches to discrimination of the two lithium pools in RBC suspensions, at therapeutic levels of lithium. Although the shift reagent approach shows easy visualization of the two lithium pools, it must be used with caution as it may change the transmembrane Li^+ distribution.

F. Interactions of Li^+ with RBCs and RBC Membrane

1. Measurement of Intracellular $^7Li^+$ T_1 and T_2 relaxation times and $\Delta\nu_{1/2}$ of Li^+-loaded RBCs

Packed RBCs were loaded to contain intracellular Li^+ levels from 0.2 - 3.5 mM. This was accomplished by varying the loading times from 0.5 - 12 h. $^7Li^+$ T_1 and T_2 measurements were obtained by using inversion-recovery and Carl-Purcell-Meiboom-Gill pulse sequences, respectively. All relaxation measurements were conducted at 37°C. Linewidths at half heights ($\Delta\nu_{1/2}$) were calculated from the corresponding ^7Li NMR spectra. The results are summarized in Table 13. The large difference in relaxation times is indicative of specific Li^+ interactions in RBCs.

The outer leaf of the RBC membrane is negatively charged due to the sialic acid residues and could be a possible binding site for the Li^+ ion. Non-Li^+ loaded RBCs were incubated with 0.1 μM sialidase for 45 min at 37°C, to cleave off the sialic acid residues. The RBCs were washed at least three times with isotonic choline buffer and resuspended in the isotonic choline buffer containing in addition 1.5 mM LiCl. $^7Li^+$ T_1 and T_2 measurements were obtained for extracellular Li^+ in sialidase treated and non-treated RBCs and compared to that of 1.5 mM aqueous LiCl solution. No changes on the $^7Li^+$ relaxation times (T_1 = 17.0 $\pm$ 0.20 and T_2 = 16.5 $\pm$ 0.30 s, n = 3, for treated and non-treated RBCs) were observed indicating the $^7Li^+$ ion

Table 13

Intracellular ^{7}Li T_1 and T_2 of Li^+-loaded RBCs

Sample	T_1/s n = 6	T_2/s n = 6	$\Delta\nu_{1/2}$/Hz n = 6
Li^+-loaded RBCs			
[Li^+] in mM			
0.2	4.5 ± 0.5	0.07 ± 0.02	100
0.5	5.2 ± 0.4	0.07 ± 0.03	65
1.0	5.4 ± 0.4	0.08 ± 0.02	33
1.5	5.6 + 0.6	0.09 ± 0.01	17
3.5	6.2 ± 0.5	0.17 ± 0.02	15

does not interact with the sialic acid residues. The amount of sialic acid residues released by the treatment of sialidase were not determined. It is possible that the treatment with the enzyme may not have cleaved all of the sialic acid residues. However, if specific Li^+-sialic acid interactions were present, an increase in $^7Li^+$ relaxation times should have been observed upon treatment with sialidase. Since this was not the case, Li^+-sialic acid interactions are apparently negligible. It is possible that the sialidase used was inactive and no sialic acid residues were cleaved. However, this is not the case because the sialidase enzyme has been used previously for membrane sidedness assays.

The problem of $^{23}Na^+$ NMR visibility arises from 20% bound Na^+ inside the red cells. These bound Na^+ ions become NMR visible only after disrupting the cell potential by addition of gramicidin (94b). In order to determine whether Li^+ binding is dependent on membrane potential (120), RBCs which have been loaded with 1.5 mM LiCl were suspended in an isotonic choline buffer containing 112.5 mM choline chloride, 85 mM sucrose, 10 mM glucose and 10 mM TRIS-Cl, pH 7.5, and incubated with 0.1 μM gramicidin for 30 min at 37°C. To differentiate between the two $^7Li^+$ pools, the shift reagent $Dy(PPP)_2^{-7}$ was added to the suspension to a final concentration of 3 mM. $^7Li^+$ T_1 and T_2 were measured for the intracellular Li^+ pool of the RBC

suspension described above, before and after gramicidin treatment. However, no significant change in the $^{7}Li^{+}$ relaxation times was observed after treatment with gramicidin.

^{133}Cs NMR was also used as a complimentary method to probe $^{7}Li^{+}$ binding to the RBC membrane. RBCs were loaded with Li^{+} alone, Cs^{+} alone and Cs^{+} - Li^{+}. RBCs were loaded with Cs^{+} by incubating packed RBCs with isotonic buffer containing 140 mM NaCl, 10 mM CsCl, 10 mM glucose and 10 mM TRIS-Cl, pH 7.4 for 3 h at 37°C. Cs^{+} - Li^{+} loading of RBCs was accomplished by incubating packed RBCs in a similar buffer medium except 40 mM NaCl was replaced by 40 mM LiCl. RBCs were loaded with Li^{+} by incubating the cells in a medium containing 110 mM NaCl, 40 mM LiCl, 10 mM glucose and 10 mM TRIS-Cl, pH 7.4 for 3 h at 37°C. The hematocrit for the RBC suspensions is 13%. The rate of Cs^{+} influx in RBCs is faster than Li^{+} influx, presumably because Cs^{+} may be mimicking K^{+}. After loading, the intracellular Cs^{+} and Li^{+} are approximately 6 and 1.0 mM, respectively. Evidence for interaction of Cs^{+} with intracellular Li^{+} binding sites come from $^{133}Cs^{+}$ NMR chemical shifts and ^{7}Li T_1 and T_2 measurements. The intracellular $^{133}Cs^{+}$ chemical resonance position shifted from -0.10 to 0.45 ppm for Cs^{+}-loaded RBCs alone versus Cs^{+} - Li^{+} loaded RBCs. The intracellular ^{7}Li T_1 and T_2 relaxation times were lower for Li^{+} - loaded relative to Li^{+} - Cs^{+} loaded cells (5.3 vs. 5.9, n = 3, and

0.13 vs. 0.5 s, n = 3, respectively). This can be explained in terms of Cs^+ competing for the Li^+ binding sites. Since the relative intracellular Cs^+ ion concentration is six times higher than that of intracellular Li^+, the Cs^+ ions are able to replace some of the bound Li^+ despite their lower ionic potential. The effective increase in the ^7Li relaxation times is due to an increase in free intracellular Li^+.

2. Measurement of Intracellular $^7Li^+$ T_1 and T_2 relaxation times of phospholipid vesicles

Phosphatidylserine:phosphatidylcholine (PS:PC), phosphatidylinositol:phosphatidylcholine (PI:PC) and pure phosphatidylcholine large unilamellar vesicles were prepared, using a 10:90% ratio for the phospholipid mixtures. The intravesicular Li^+ concentration was 1.5 mM. The viscosities of the resulting solutions were measured to be 0.90 $\pm$ 0.30 cP (n = 2, water reference set at 0 cP at 37°C). Intracellular $^7Li^+$ spin-lattice (T_1) and spin-spin (T_2) relaxation times of the vesicle preparations are shown in Table 14. The same large difference in relaxation times, as obtained for intact RBCs (Table 13) was observed for vesicles. The trend in the observed data indicate Li^+ interaction with the phospholipids, with PS and PI having relatively a higher affinity for Li^+ ions than PC.

The viscosity of the aqueous intracellular volume in RBCs is about 5 cP (105) and it had been postulated that

Table 14

Intravesicular ^{7}Li T_1 and T_2 of Phospholipid LUVs[a]

Sample	T_1/s n = 3	T_2/s n = 3
PS:PC	5.5 ± 0.20	0.67 ± 0.35
PI:PC	5.5 ± 0.30	0.91 ± 0.10
PC	9.4 ± 1.10	2.20 ± 0.38
Aqueous LiCl	17.2 ± 0.81	17.4 ± 1.10

[a] Transmittance electron microscopy (TEM) of these LUV samples was not done. Thus, it is possible that the phospholipid vesicle preparations were not pure LUVs but may be non-homogeneous mixtures of unilamellar and multilamellar vesicles or particles of a large size range.

the viscosity itself maybe contributing to the observed difference in intracellular $^{7}Li^{+}$ T_1 and T_2 (105). To isolate this viscosity effect, small unilamellar vesicles (SUVs) of PS:PC, PI:PC and PC phospholipids of the same composition as in the LUV preparations were made. Homogeneously sized LUVs are more difficult to prepare and are sometimes complicated by formation of multilammellar phospholipid layers (125). On the other hand, SUV preparation is easier and its smaller size range (25-50 nm) simplifies binding studies (121,128). Li^{+} concentration dependent studies of the extracellular ^{7}Li T_1's and T_2's were conducted for the SUVs. The phosphate content of each preparation was approximately the same (41 μg phosphate/mL) and the viscosities adjusted to 5 cP with glycerol. A plot of the ^{7}Li T_1's and T_2's for aqueous solutions of LiCl at different viscosities is shown in Figure 20. The trend in the observed data does not show any specific Li^{+} - glycerol interaction apart from viscosity effects as both T_1 and T_2 behave in the same fashion.

A plot of the ^{7}Li T_1's and T_2's at different extravesicular Li^{+} concentrations for the PS:PC, PI:PC, PC SUVs and aqueous LiCl solutions is shown in Figure 21. The T1's and T2's were normalized to take into account the vesicle size relative to RBC ghost by multiplying the relaxation times by RBC ghost/SUV diameter ratio. The average SUV diameter after 30 minute sonication is

Figure 20. A plot of ^{7}Li spin-lattice (T_1) (open squares) and spin-spin (T_2) (closed diamonds) relaxation times versus viscosity. The aqueous samples contained 1.0 mM LiCl and 0 - 80% glycerol vol/vol, to give 0 - 5 cP solution viscosities.

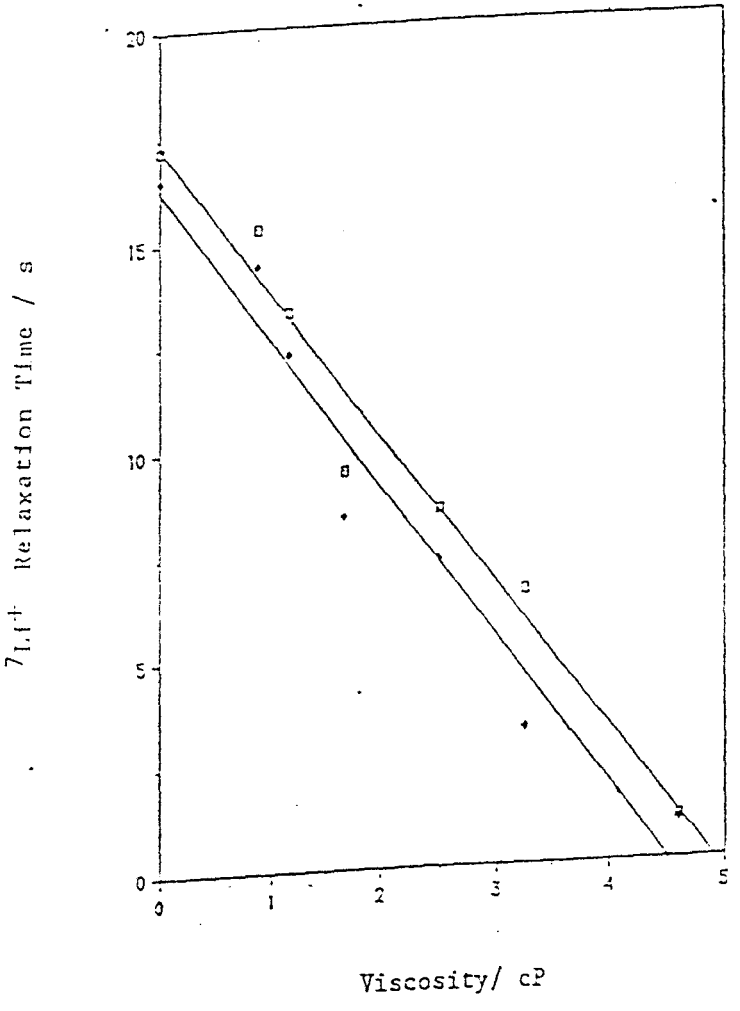
$\tau_{1,1}$ Relaxation Time / s
20
15
10
5
0
0
1
2
3
4
5
Viscosity/ cP

Figure 21. A plot of ^{7}Li T_1's and T_2's for PS:PC, PI:PC, PC SUVs suspended in an aqueous solution containing 0.5 - 3.5 mM Li^+. The viscosities of the solutions were adjusted to 5 cP with glycerol. The ^{7}Li T_1's and T_2's for aqueous controls containing 0.5 - 3.5 mM Li^+ were 0.90 -1.2 and 0.70 - 0.8 s respectively. Open and closed symbols are for ^{7}Li T_1's and T_2's, respectively. Triangles, squares, and diamonds are for ^{7}Li T_1's and T_2's, for PC, PS:PC and PI:PC SUVs, respectively. It is important to note that Li^+-(PI:PC) interactions are strongest as indicated by very low T_2's (0.004-0.098 s).

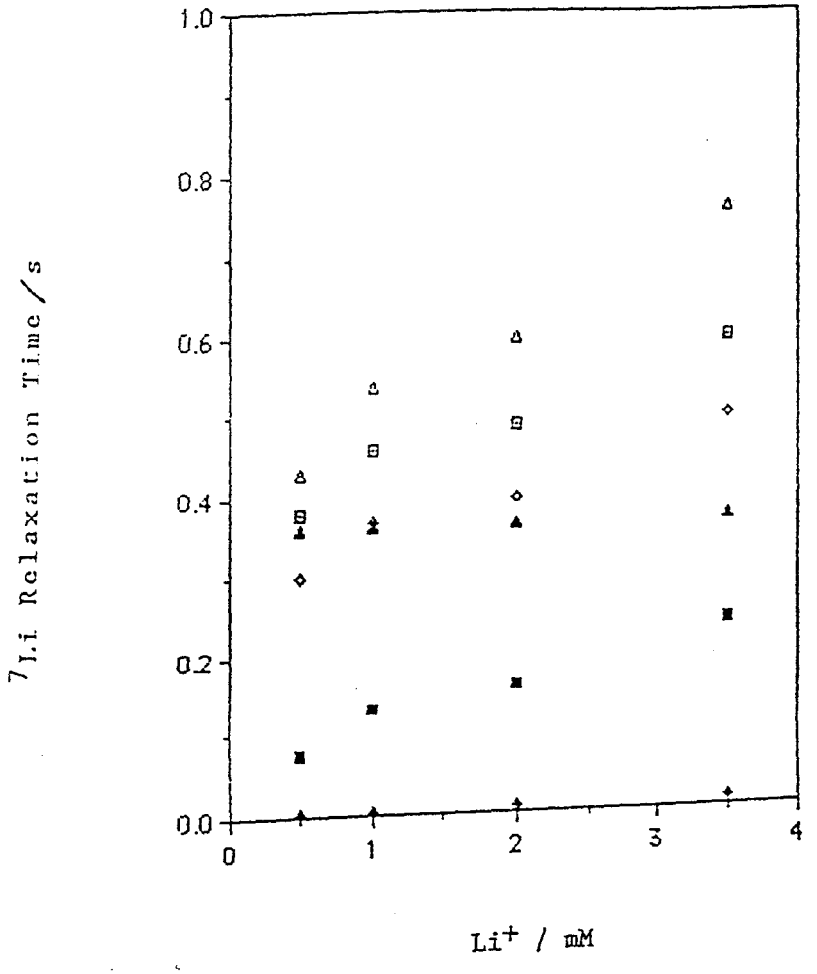
1.0
0.8
0.6
0.4
0.2
0.0
0
1
2
3
4
^{7}Li Relaxation Time / s
Li$^+$ / mM

Figure 22. A plot of [1/ΔR] versus [Li^+] for the: (A) PC; (B) PS:PC and (C) PI:PC SUV solutions. The aqueous samples contained 0.5 - 3.5 mM LiCl. The viscosities of the samples were adjusted to about 5 cP with glycerol.

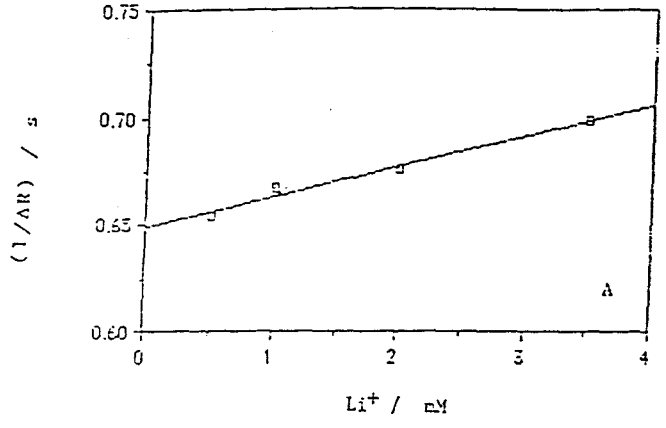
0.75
0.70
0.65
0.60
(1/ΔR) / s
A
0
1
2
3
4
Li+ / mM

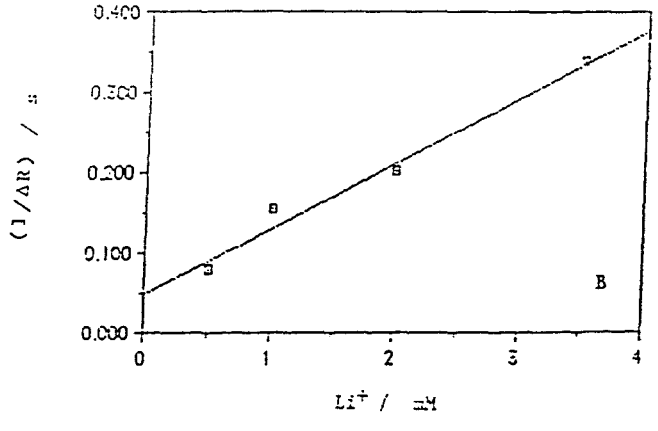
0.400
0.300
0.200
0.100
0.000
(1/ΔR) / s
B
0
1
2
3
4
Li+ / mM

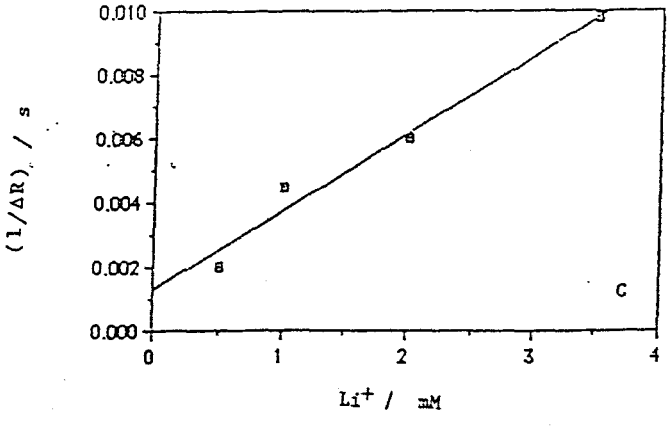
0.010
0.008
0.006
0.004
0.002
0.000
(1/ΔR) / s
C
0
1
2
3
4
Li+ / mM

approximately 30 nm (125) while the diameter of the RBC ghost is approximately 7400 nm (129). Thus, the RBC ghost/SUV diameter ratio is about 247.

To calculate the normalized Li^+ - phospholipid affinities, the spin-spin ($1/T_2$) relaxation rates were plotted against Li^+ concentrations and are shown in Figure 22. The binding constants were calculated from the slopes and intercepts of the plot using the James and Noggle equation (equation 14) (130). The assumption is that the observed relaxation rate is a weighted-average due to free and bound species.

$$R_{obs} = F_{free}\,(R_{free}) + F_{bound}\,(R_{bound}) \quad [7]$$

where

$$R_{free} = (1/T_2)_{free} \quad [8]$$

$$R_{bound} = (1/T_2)_{bound} \quad [9]$$

F_{free} = fraction of free Li^+

F_{bound} = fraction of bound Li^+

Since

$$F_{bound} = [PL\text{-}Li^+]/[Li^+] \quad [10]$$

$$F_{bound} = (K)[PL]/(1 + K([PL] + [Li^+] - [PL\text{-}Li^+])) \quad [11]$$

$$\Delta R = F_{bound}\,(\Delta R') \quad [12]$$

Combining equations [11] and [12] yields

$$\Delta R = ((\Delta R')(K)[PL])/(1 + K[PL]) \quad [13]$$

Under the conditions that $PL << Li^+$, this gives the linear form,

$$[1/\Delta R] = [1/(\Delta R')[PL]][Li^+] + [1/(\Delta R')[PL](K)] \quad [14]$$

where

$\Delta R' = R_{bound} - R_{free}$ [15]

$\Delta R = R_{obs} - R_{free}$ [16]

$[Li^+]$ = Li^+ concentration in mM

[PL] = phospholipid concentration, expressed in mM phosphate

$PL\text{-}Li^+$ = phospholipid - Li^+ complex

$$K = \text{binding constant} = \frac{[PL\text{-}Li^+]}{[PL][Li^+]} \quad [17]$$

The experimental conditions under which this equation was developed originally were that the total ligand concentration, PL, was held constant and the total substrate concentration, Li^+, was varied. Although the model is for a 1:1 binding, the interpretation is that [PL] is the molar concentration of the binding sites. The Li^+-phospholipid binding constants are summarized in Table 15. Intrinsic binding constants were determined by dividing the slope by the intercept of the James - Noggle plot. To calculate for the intrinsic binding constants of PS, K_{PS}, or PI, K_{PI}, the observed K for the phospholipid mixtures can be expressed as

$$K = (f_{PS})(K_{PS})(f_{PC})(K_{PC}) \quad [18]$$

or

$$K = (f_{PI})(K_{PI})(f_{PC})(K_{PC}) \quad [19]$$

where

Table 15

Li^+ - Phospholipid Binding Constants[a]

	Intrinsic K M^{-1}	Normalized K' M^{-1}
PC	2.00×10^{-5}	7.41×10^{-4}
PS:PC	1.60×10^{-3}	
PS	0.89	54.96
PI:PC	1.85×10^{-3}	
PI	1.02	3.54

[a] Transmittance electron microscopy (TEM) of these samples was not done. Thus, it is possible that the phospholipid vesicle preparations were not pure SUVs but may be non-homogeneous mixtures of unilamellar and multilamellar vesicles or particles of a large size range.

f_{PS} = fraction of PS in the mixture = 0.10

f_{PI} = fraction of PI in the mixture = 0.10

f_{PC} = fraction of PC in the mixture = 0.90

K_{PC} = intrinsic binding constant for Li^+-PC

The normalized binding constant K' is the binding constant normalized to that of the phospholipid concentration found in RBCs or RBC ghosts. To calculate for K', the intrinsic binding constants are multiplied by the RBC/vesicle size factor (7400 nm/30 nm) and by the fraction of PS, PI or PC found on the inner leaf of the RBC membrane, which are 0.25, 0.014 and 0.15, respectively, of the total inner leaf membrane phospholipids. Although the calculated binding constants seem to indicate the presence preferential Li^+ binding sites, it is important to point out that a more detailed characterization of the samples used in these studies is needed to ultimately identify specific phospholipid-Li^+ interactions.

Lithium treatment has been found to induce accumulation of choline in RBCs (37). It is feasible that Li^+ ions could activate phospholipase C and induce an increase in hydrolysis of PC. However, the Li^+ ion interacts weakly with PC (Table 15). To test this possibility, ^7Li T_1's and T_2's were determined for phospholipase C treated - PC SUVs and non-treated PC SUVs. Hydrolysis of PC would be expected to result in a decrease in the number of interaction sites and an increase in the

^7Li relaxation time would be observed. However, the relaxation measurements indicated the opposite (0.54 to 0.21 s, n = 2, for ^7Li T_1 and 0.36 to 0.02 s, n = 2, for ^7Li T_2). Therefore, the decrease in ^7Li may be indicative of Li^+ binding to phospholipase C. To test phospholipase C-Li^+ interaction, ^7Li T_1 and T_2 measurements were taken for solutions of phospholipase C and Li^+. The results were compared with ^7Li relaxation times for solutions of Li^+ alone. The ^7Li relaxation times decreased in the presence of phospholipase C (0.52 to 0.27 s, n = 2, for T_1 and 0.34 to 0.29 s, n = 2, for T_2), indicating interaction between phospholipase C and Li^+. It is important to note that treatment of vesicles with phospholipase C could also indirectly disrupt Li^+-RBC membrane interactions; phospholipase C could change membrane dynamics which in turn could change Li^+ interactions.

3. Measurement of $^7Li^+$ T_1 and T_2 relaxation times of normal RBC ghosts, ATP-depleted RBC ghosts, 0.5% Triton X-100 Shell containing spectrin-actin matrix, spectrin-depleted inside-out vesicles and hemoglobin

RBC ghosts were prepared as described before (III.K). ATP-depleted ghosts were prepared by incubating normal ghosts with 0.1 mM of the ionophore A23187 and 10 mM of EDTA. The ghosts were then washed with 5P8-1Mg buffer at least three times. They were resealed and loaded with 1.5 mM Li^+ by incubating the ghosts in 5P8-1Mg containing 6 mM Li^+ for 45 min at 37°C. The 0.5% Triton X-100 shell

which contains the spectrin-actin matrix was prepared as described in III.L. Spectrin-depleted vesicles were prepared as described in III.M. A detailed characterization of the ghosts, the 0.5% Triton X-100 shell and the spectrin depleted vesicles were not done. The resealing procedure for ghosts has been found to yield at most 90% resealed ghosts. Thus, the actual NMR sample contained only 90% resealed ghosts and the other 10% may be unsealed ghosts and membrane fragments or vesicles. The Triton X-100 shell containing the spectrin-actin matrix also contains about 41% of the total phospholipid found in RBC ghosts and is therefore not a pure spectrin-actin matrix. Similarly, the spectrin-depleted vesicle samples contained 15% of the membranes from the ghosts, and is not 100% spectrin-depleted vesicles.

Due to the diagonal relationship between Li^+ and Mg^{+2}, it is also possible for Li^+ to compete with Mg^{+2} binding sites. To test this, aqueous solutions containing 1:1 ATP:Mg^{+2} were prepared to give final 2.3 mM ATP-Mg^{+2} concentrations. These ATP-Mg^{+2} solutions were prepared to contain 0-3.5 mM Li^+. The ^7Li T_1 and T_2 data obtained for these samples are summarized in Table 16.

Studies on Li^+ binding to hemoglobin have been previously reported (105,131) and have shown a very weak Li^+ - hemoglobin interaction. ^7Li T_1 and T_2 relaxation times were measured for freshly prepared hemoglobin

solutions (72 mg hemoglobin/mL) containing 0.5-3.5 mM Li+. The observed results indicate that Li^+ does bind weakly to hemoglobin (Table 16). On the other hand, ^7Li T_1 and T_2 relaxation times were also measured for the 0.5% Triton X-100 shell and found to be approximately the same (Table 16). The intrinsic binding constants for Li^+ - spectrin actin matrix and Li^+ -hemoglobin were determined as before from the James - Noggle plots (Figure 23).

The normalized binding constant for Li^+ - 0.5% Triton X-100 shell containing the spectrin actin matrix in RBCs was determined by multiplying the intrinsic binding constant by the ratio of (SA in mg protein/mL of RBC ghosts)/(SA in mg protein/mL in the 0.5% Triton X-100 shell samples). The total protein content in RBCs is 52% by weight and SA represents 25% of this fraction (132). The protein content of a 0.5% Triton X-100 shell sample is about 45% of the total protein content of RBC ghosts, of which 56% represents the spectrin-actin matrix (116). The actual protein concentration of the 0.5% Triton X-100 shell sample used in the NMR experiments is 16.7 mg protein/mL solution. Thus, the concentration of spectrin-actin in the NMR sample is about 9.4 mg protein/ml solution. The normalized Li^+-spectrin-actin binding constant can be calculated by multiplying the intrinsic binding constant K by the normalization factor, F. The factor F is equal to

Table 16

Observed ^{7}Li T_1 and T_2 Relaxation Times for Spectrin-Actin, ATP-Mg^{+2} and Hemoglobin Solutions

Sample	T_1/s n = 3	T_2/s n = 3
Spectrin-actin matrix[a]		
0.5 mM Li^+	0.79 ± 0.01	0.62 ± 0.01
1.0	0.80 ± 0.01	0.63 ± 0.01
1.5	0.81 ± 0.01	0.64 ± 0.01
3.5	0.83 ± 0.02	0.68 ± 0.02
ATP-Mg^{+2}[a]		
0.5 mM	0.15 ± 0.02	0.021 ± 0.001
1.0	0.15 ± 0.01	0.024 ± 0.002
1.5	0.16 ± 0.02	0.028 ± 0.002
3.5	0.16 ± 0.01	0.043 ± 0.003
Hemoglobin solutions[b]		
1.0 mM Li^+	16.10 ± 0.53 (2.87)	2.40 ± 0.31 (0.43)
2.0	16.10 ± 0.49 (2.87)	3.30 ± 0.23 (0.59)
4.0	16.70 ± 0.63 (2.97)	5.10 ± 0.21 (0.91)
8.0	16.80 ± 0.79 (2.99)	8.70 ± 0.37 (1.55)

[a] sample viscosity adjusted to 5 cP with glycerol; [b] sample viscosity not adjusted (0.89 cP); data in parentheses after viscosity correction for 5 cP solutions.

Figure 23. A plot of [1/ΔR] versus [Li^{+}] for (A) 0.5% Triton X-100 shell solutions containing the spectrin-actin matrix, (B) hemoglobin solutions and (C) ATP-Mg^{+2}. The viscosity of the 0.5% Triton X-100 shell and ATP-Mg^{+2} solutions have been adjusted to 5 cP with glycerol. The concentration of hemoglobin for all the samples was maintained at 72 mg/ml. The viscosity of the hemoglobin solutions was about 0.89 cP.

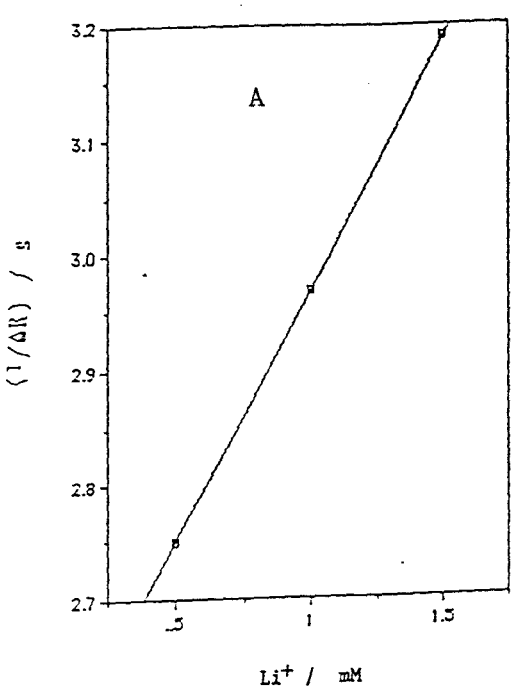
A
3.2
3.1
3.0
2.9
2.8
2.7
.5
1
1.5
(1/ΔR) / s
Li+ / mM

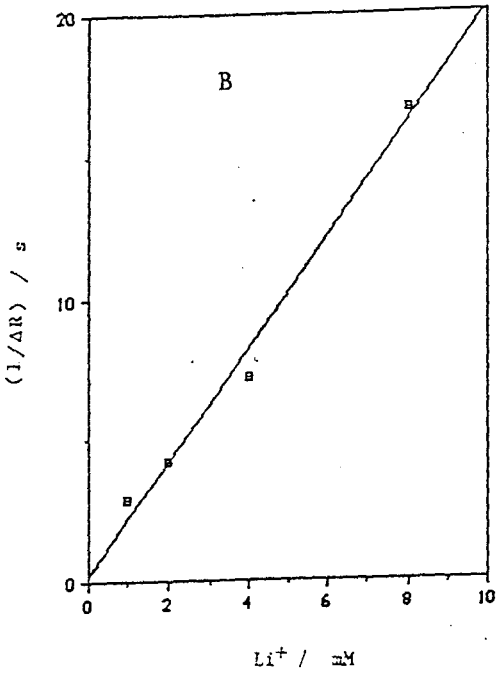
B
20
10
0
0
2
4
6
8
10
(1/ΔR) / s
Li+ / mM

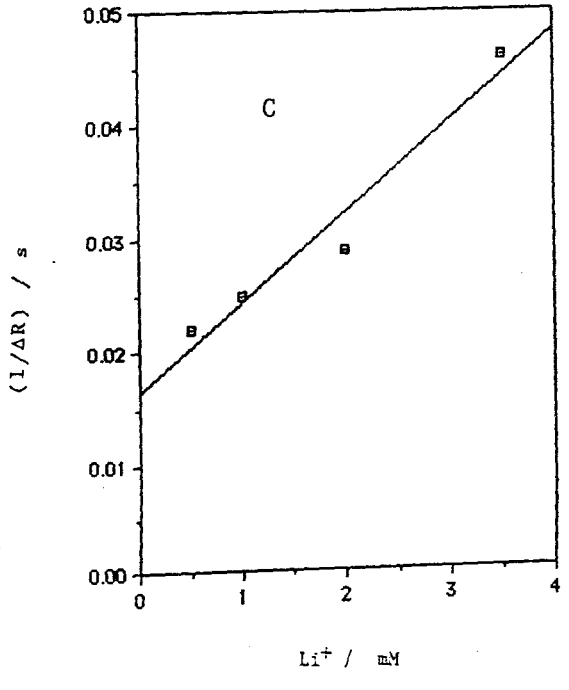
C
0.05
0.04
0.03
0.02
0.01
0.00
0
1
2
3
4
(1/ΔR) / s
Li+ / mM

{[(3.43 mg protein/mL RBC ghosts) x 0.25]/[9.4 mg spectrin-actin/mL 0.5% Triton X-100 solution]}, which yields a value of F = 0.09. Howvever, the protein concentration determined may be overestimated due to interference by Triton X-100.

The normalized binding constant for Li^+ -hemoglobin in RBCs was determined by multiplying the intrinsic binding constant by the ratio of hemoglobin in RBCs/hemoglobin in the sample. The concentration of hemoglobin in RBCs is 4.7 mM (133) while the hemoglobin solution used in this study is 1.13 mM.

Table 17 shows that Li^+ may be preferentially binding to the membrane phospholipids. The difference in ^7Li relaxation times between RBCs and ghosts is probably due to the difference in intracellular viscosities contributed by the globular hemoglobin protein which is present in RBCs but absent in ghosts. No significant difference in ^7Li T_1's and T_2's were observed for normal ghosts and ATP-depleted ghosts which indicates much weaker Li^+-ATP interactions in RBCs. Similarly, only weak Li^+-(spectrin-actin) interactions are present in RBCs. It is also possible that the dense cytoskeleton matrix contributes to the viscosity effects on the intracellular ^7Li relaxation rates.

Table 18 summarizes the intrinsic and normalized binding constants and the intrinsic ^7Li spin-spin

Table 17

Observed ^{7}Li T_1 and T_2 Relaxation Times

Sample	T_1/s n = 3	T_2/s n = 3
Li^+ -loaded RBCs with 1.5 mM Li^+	5.6 ± 0.60	0.09 ± 0.01
Li^+ -loaded Normal ghosts with 1.5 mM Li^+[a,b]	11.1 ± 0.90	0.17 ± 0.02
Li+ - loaded ATP-depleted ghosts with 1.5 mM Li^+[a,b]	12.1 ± 1.10	0.16 ± 0.01
Spectrin-depleted ISO vesicles[c,d] w/extracellular		
0.5 mM Li^+	0.55 ± 0.01	0.16 ± 0.01
1.0	0.58 ± 0.05	0.16 ± 0.01
1.5	0.59 ± 0.01	0.17 ± 0.01
3.5	0.62 ± 0.01	0.19 ± 0.01

[a] The viscosities of the resulting solutions were not adjusted to 5 cP with glycerol; [b] The ghosts samples contain 90% resealed ghosts and the other 10% may possibly be a mixture of unsealed ghosts and membrane fragments or vesicles; [c] The viscosities of the solutions were adjusted to 5 cP with glycerol; [d] These samples contain about 90% ISO and also contains 15% of the ghost membranes.

Table 18

Intrinsic and Normalized Binding Constants for Intracellular Li^+ Binding Sites

	$K(M^{-1})$	
	Intrinsic	Normalized
PS	0.89	54.96
PI	1.02	3.54
PC	2.00×10^{-5}	7.41×10^{-4}
Spectrin-actin	8.70×10^{-5}	7.83×10^{-6}
Hemoglobin	12.23×10^{-3}	3.42×10^{-4}
ATP-Mg^{+2}	4.60×10^{-4}	4.60×10^{-4}

relaxation rates for the different potential Li^+ binding sites inside the RBC.

It is generally accepted that the outer leaf of mature human RBC contains approximately 40-50% PC, 40-50% sphingomyelin (SM) and 10-15% phosphatidylethanolamine (PE) of the total outer leaf phospholipids while the inner leaflet contains approximately 10-20% PC, 10% SM, 40-50% PE, 20-30% PS and 1.4 % PI of the total inner leaf phospholipids (129,134,135). Both anionic phospholipids, PS and PI are found only in the inner leaflet.

The intrinsic binding constants for Li^+ - PS and Li^+ - PI are 0.89 and 1.023 M^{-1}, respectively. By comparison, the intrinsic binding constants for PS - Na^+, PS - Mg^{+2}, and PS - Ca^{+2} have been reported to be 0.8, 4.0 and 35 M^{-1}, respectively (128).

In summary, although the results seem to indicate the presence of preferential Li^+ binding sites (PS > PI > PC > ATP-Mg^{+2} > Hemoglobin > Spectrin-actin), a more detailed characterization of the samples used in these preliminary studies is needed to conclude the studies on Li^+ binding sites in RBCs.

Chapter V

DISCUSSION

^{7}Li NMR is a novel approach for addressing lithium transport and binding to RBCs. In Li^{+} - loaded RBC suspensions containing lithium in both the intra- and extracellular compartments, only one ^{7}Li NMR signal is observed. This signal is a composite of the two resonances from the two lithium pools. The ^{7}Li nucleus has a narrow chemical shift range and is not very sensitive to ligation because the paramagnetic and diamagnetic contributions cancel each other. Lithium is present in both compartments as hydrated species, thus only one signal is observed. However, incorporation of a paramagnetic shift reagent such as $Dy(PPP)_2^{-7}$ in the extracellular compartment results in a change in the magnetic environment of the extracellular lithium pool. The high negative charge of the shift reagent complex causes the shift reagent to be repelled by the RBC membrane phospholipids and renders it membrane impermeable. Thus, distinct ^{7}Li NMR signals are observed for the intra- and extracellular Li^{+} pools. The use of the

shift reagent allows for easy visualization of the Li^+ pools. However, the high negative charge of the shift reagent and its affinity for positively charged metal ions affects the distribution of these metal ions across the cell membrane. Consequently the amount of Li^+ complexed to the shift reagent will vary during an ion transport experiment and thus it will be difficult to correct for the effects of complexation. This problem of complexation appears to be eliminated when a shift reagent with a lower negative charge, like $Dy(TTHA)^{-3}$, is used.

A non-invasive ^7Li NMR method based on a MIR pulse sequence reported used in this dissertation is a better method for studying cell systems such as that of RBCs because it does not perturb the native metal cation transmembrane distribution. This technique does not suffer from the limitations introduced by AA and the use of shift reagents in ^7Li NMR in that there is no sample destruction, ion binding to cell membranes, and/or effect on transmembrane ion distribution. The method works very well for lithium ion transport studies because of the inherent large difference in intra- and extracellular spin-lattice (T_1) relaxation times, and will presumably work for other nuclei that exhibit this same property like ^{31}P, ^{35}Cl and ^{23}Na. One other advantage of ^7Li NMR is that the nucleus is 100% NMR visible. Thus the relative changes in the ^7Li resonance intensities directly reflect the lithium ion

distribution across the cell membrane. Other NMR methods for following membrane transport processes have also been used (107-109,120). However, they most often require complex multiple pulse sequence. The MIR method is simpler than these in that it only requires a two pulse experiment.

Since the MIR approach is totally non-invasive, allows for easy visualization of Li^+ pools and relatively time efficient, it is the method of choice for comparative study of Na^+-Li^+ countertransport rates and rate constants in blood samples from manic-depressive patients relative to normal matched controls. The results obtained in this study show a statistically significant difference in the Na^+-Li^+ countertransport rates and rate constants ($p < 0.0005$, $df = 14$), and are in agreement with previous reports (23,27). Overlapping trends in the rates of Na^+-Li^+ countertransport have been observed by several investigators (30,31,66,67). Thus the use of this parameter as a biological marker for manic-depression has been questioned. The rate constants observed for Na^+ -Li^+ countertransport in RBCs have also been found to be lower for manic-depressives relative to normal controls. Because the rate constants are normalized by taking into account the variations in the intracellular Li^+ levels, it appears to be a better parameter as a biological marker for manic-depression.

The proposed membrane abnormality for neurological

disorders is a widely accepted hypothesis (18). More research has been geared to identifying a marker for other disorders, in the cell membrane. In recent studies the focus has been on membrane phospholipids as they are now known to modulate the activities of membrane proteins and possibly be affecting ion transport processes. One study has reported a decrease in the PS levels in manic-depressives (35). In fact it is now known that PS is necessary to maintain the activity of (Na^+,K^+)-ATPase activity, while PI is important for Ca^{+2}-ATPase activity (110). It is important to note that Li^+ - PS interactions have been the subject of numerous studies (120,136,137). Although these investigations were aimed at characterizing Li^+ - phospholipid interactions, not much attention has been focused in RBCs, more importantly on intracellular Li^+ interactions.

Recently, Pettegrew and co-workers have made elegant applications of ^7Li NMR and fluorescence methods to normal RBCs (105,138). Fluorescence anisotropy (138) studies showed that the presence of Li^+ ion may have increased the mobility of RBC membrane surface molecules and the surrounding water structure. In model membrane studies, Li^+ has been found to bind to negatively charged phospholipids such as phosphatidylserine (120,137). Phosphatidylserine is found predominantly in the inner leaf of the RBC membrane. To address the question of possible

binding sites of Li^+ in RBCs, a systematic approach to discriminate between binding sites needed to be done. Thus, the interactions of Li^+ with spectrin-actin network, negatively charged sialic acid groups on the outer leaf of the cell membrane, the negatively charged phosphatidylserine and hemoglobin were studied in this dissertation. Li^+ treatment has been shown to result in the accumulation of choline in RBCs. Li^+ ion has also been shown to inhibit the enzyme inositol-1-monophosphatase, which results in the alteration of the phosphoinositide signal transduction (19-21). ^7Li NMR studies have also shown that the Li^+ ion interacts with phosphatidylcholine-phosphatidylglycerol liposomes (137). Thus, the interactions of Li^+ with phosphatidylcholine and phosphatidylinositol were similarly studied.

The previous studies with phospholipid vesicles were done using very high Li^+/PS ratios (120). In this dissertation, the Li^+ concentrations used are within therapeutically relevant concentrations (0.5-1.5 mM). These investigations involve ^7Li NMR T_1 and T_2 measurements using the inversion recovery and the Carl-Purcell-Meiboom-Gill pulse sequences. It is well established that slow motions contribute only to toward T_2 whereas fast motions such as those components of motions at the resonance frequency contribute to both T_1 and T_2 (111). The observation of the large difference between T_1 and T_2 is

indicative of some kind of interaction of Li^+ with a long correlation time (111). When lithium ions are subject to substantial electric field gradients or are immobilized in the membrane, the relaxation times of the ^7Li nucleus decreases - the lower the relaxation times, the stronger the interaction. ^7Li T_2 measurements show that this parameter is more sensitive and was thus used to study the different potential binding sites inside the red cell.

Figure 24 shows a schematic representation of RBCs and possible Li^+ binding sites. The glycophorins account for 90% of the total sialic acid residues and thus the outer cell surface has a negative charge (132). In principle these residues can interact or bind the positively charged lithium ion. However, a comparison of the ^7Li T_1's and T_2's of the extracellular Li^+ resonance for a suspension of sialidase treated and non-treated RBCs show that there is negligible interaction. The amount of sialic acid residues released by the treatment of sialidase was not conducted. Thus, it is possible that not all the silic acid residues were released by treatment with sialidase. However, if specific sialic acid - Li^+ interactions were present, one would expect an increase in ^7Li relaxation times after treatment with sialidase. Thus, the results indicate the absence of sialic acid - Li^+ interactions.

The red cell is most often thought of as a packet of

Figure 24. The topography of membrane protein, lipid and carbohydrate moieties and the spectrin-actin cytoskeleton in the fluid mosaic model of the erythrocyte membrane is shown.

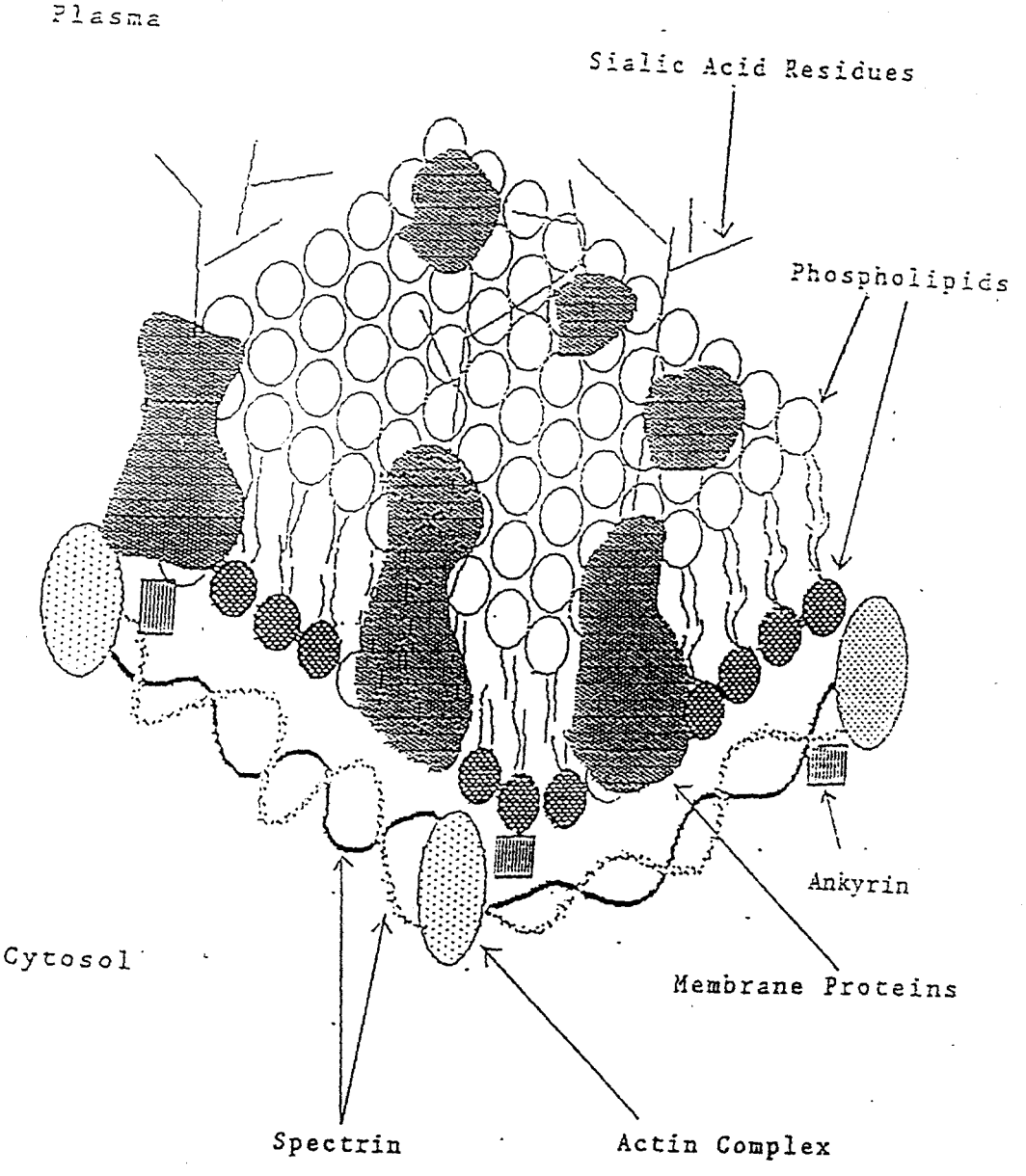
Plasma
Sialic Acid Residues
Phospholipids
Ankyrin
Cytosol
Membrane Proteins
Spectrin
Actin Complex

hemoglobin. Thus, intracellular Li^+ may also be interacting with hemoglobin. Li^+ - hemoglobin binding studies have been done by other workers and only very weak interactions were found (105,131). In the present study, Li^+ was also found to bind weakly to hemoglobin.

Pettegrew and coworkers (105) have measured by ^7Li NMR the spin-lattice (T_1) and spin-spin (T_2) relaxation times for intracellular Li^+ in normal RBCs and found them to be approximately 5 and 0.15 s, respectively. They speculated the large difference in relaxation times to diffusion of Li^+ across the heterogeneous electrostatic field gradients generated by the spectrin-actin network of the RBC membrane. However, no studies of Li^+-(spectrin-actin) have been reported as yet. From the observed ^7Li relaxation times of Li^+-(0.5% Triton X-100 shell) solutions presented in this dissertation, only weak interactions are present under therapeutic Li^+ levels in RBCs. It is important to note that the 0.5% Triton X-100 shell was not characterized in detail. The samples did not contain pure spectrin-actin matrix but also contained 41% of the ghost membranes. Thus, it is possible that the presence of these membranes may be inhibiting Li^+ from interacting directly with the spectrin-actin matrix. Future experiments on Li^+ binding need to be done on isolated spectrin, actin and spectrin-actin complex to determine if Li^+ interaction with the cytoskeleton is present.

The lipids of the erythrocyte membrane are asymmetrically distributed (134). Figure 25 shows the structures of phospholipids found in RBCs. The majority of the phospholipids that exhibit a net negative charge at physiological pH like phosphatidylserine and phosphatidylinositol are limited to the cytosolic half of the bilayer. Although this preliminary Li^+ binding study indicates the presence of preferential Li^+ binding sites, a more detailed characterization of the samples used in this study is needed to for a better understanding of the phenomenon of Li^+ binding in RBCs at the molecular level.

It is possible that alteration of these potential Li^+ binding sites may be responsible for the abnormal Li^+ transport properties in RBCs from bipolar patients. More experiments are needed to probe Li^+-RBC membrane interactions as they may provide a better understanding of the pharmacological properties of Li^+. Changes in the phospholipid composition (139-141) or activities of enzymes involve in phospholipid metabolism (142) and interconversion warrant more investigation since they may provide alternate biological markers of bipolar illness or other neurological diseases.

Figure 25. Structures of RBC Membrane Phospholipids (adapted from ref. 135).

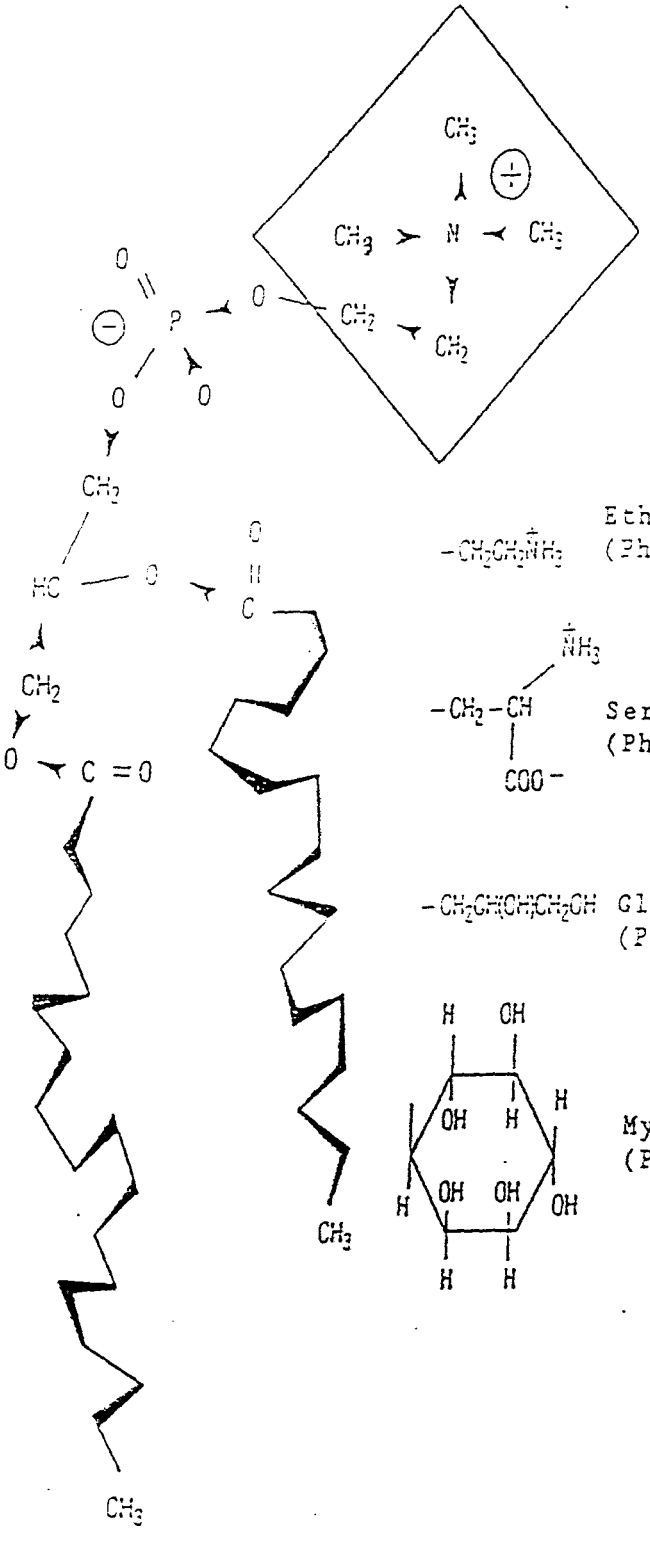

Phosphatidylcholine

Ethanolamine
(Phosphatidylethanolamine)

Serine
(Phosphatidylserine)

Glycerol
(Phosphatidylglycerol)

Myo-inositol
(Phosphatidylinositol)

REFERENCES

1. Hart WA and Beumel OF (1973) Lithium and its compounds. In Bailar JC, Emeleus HJ, Nyholm R and Trotman-Dickerson AF (eds.): "Comprehensive Inorganic Chemistry" vol. 1, Oxford: Pergamon Press, pp. 331.

2. Birch NJ (1978) Lithium in Medicine. In Williams RJP and Frausto Da Silva JRR (eds.): "New Trends in Bioinorganic Chemistry", New York: Academic Press, pp. 389-435.

3. Frausto da Silva JJR and Williams RJP (1976) Possible mechanisms for the biological action of lithium. Nature 263, 237-239.

4. Buschmann HJ (1986) The macrocyclic and cryptate effects. 5: Complexation of alkali ions by monocyclic and bicyclic ligands in methanol. Inorg Chim Acta 125, 31-35.

5. Burgermeister W and Winkler-Oswatitsh R (1977) Complex formation of monovalent cations with biofunctional ligands. In Boschke FL (ed.): "Topics in Current Chemistry", vol. 69, Berlin: Springer-Verlag, pp. 91-196.

6. Weber E and Vogtle F (1981) Crown-type compounds: an introductory overview. In Boschke FL (ed.): "Topics in Current Chemistry", vol. 98, Berlin: Springer-Verlag, pp. 1-42.

7. Birch NJ (1982) Lithium in Psychiatry. In Sigel MH (ed.):"Metal Ions in Biological Systems" vol. 14, New York: Marcel Dekker Inc., pp. 257-313.

8. Williams RJP (1973) The chemistry and biochemistry of lithium. In Gershon S and Shopsin B (eds.) "Lithium: Its Role in Psychiatric Research and Treatment", New York: Plenum Pub., pp. 15-31.

9. Detellier C (1983) Alkali metals. In Laszlo P (ed.): "NMR of Newly Accessible Nuclei", New York: Academic Press, pp. 105-151.

10. Brevard C and Granger P (1981) Handbook of High Resolution Multinuclear NMR. John Wiley and Sons, New York.

11. Jefferson JW, Greist JH and Baudhuin M (1985) Lithium in psychiatry. In Bach RO (ed.): "Lithium: Current Applications in Science, Medicine and Technology", New York: Wiley, pp. 345-352.

12. Pandey GN and Davis JM (1980) Biology of lithium. Adv Exper Med Bio 127, 15-60.

13. Ehrlich BE and Diamond JM (1980) Lithium, membranes and manic-depressive illness. J Memb Biol 52, 1981-2000.

14. Avissar S, Schreiber G, Danon A, Belmaker RH (1988) Lithium inhibits adrenergic and cholinergic increases in GTP binding in rat cortex. Nature 331, 440-442.

15. Egeland JA, Gerhard DS, Pauls DL, Sussex JN, Kidd KK, Allen CR, Hostetter AM, and Housman DE (1987) Bipolar affective disorders linked to DNA markers on chromosome X. Nature 325, 783-787.

16. Hodgkinson R, Sherrington R, Gurling H, Marchbanks R, Reeders S, Mallet J, McInnis M, Petursson H and Bynjolfsson J (1987) Molecular genetic evidence for heterogeneity in manic-depression. Nature 325, 805-806.

17. Baron M, Risch N, Hamburger R, Mandel B, Kushner S, Newman M, Drumer D and Belmaker RH (1987) Genetic linkage between X-chromosome markers and bipolar affective illness. Nature 326, 289-292.

18. Mendels J and Frazer A (1973) Toward a membrane theory of depression. J Psychiat Res 10, 9-18.

19. Worley PF, Heller W, Snyder SH and Baraban JM (1988) Lithium blocks a phosphoinositide mediated cholinergic response in hippocampal slices. Science 239, 1428-1429.

20. Drummond AH, Joels LA and Hughes PJ (1987) Lithium and phosphoinositide signal transduction. Biochem

Soc Trans 15, 32-35.

21. Ebstein RP, Newman ME, Bennett ER and Leres B (1989) Mechanism of action of lithium and ECS action in affective disorder: modulation of post-receptor second messenger function. In Tipton KE and Youdim MBH (eds.): "Biochemical and Pharmacological Aspects of Depression", London: Taylor and Francis, pp. 123-141.

22. Meltzer H (1986) Lithium mechanism in bipolar illness and altered intracellular calcium functions. Biol Psychiatry 21, 492-510.

23. Pandey GN, Dorus E, Davis JM and Tosteson DC. (1979) Lithium transport in human red blood cells: genetic and clinical aspects. Archs Gen Psychiat 36, 902-908.

24. Pandey GN, Ostrow DG, Haas M, Dorus E, Casper RC, Davis JM and Tosteson DC. (1977) Abnormal lithium and sodium transport in erythrocytes of a manic patient and some members of his family. Proc Nat Acad Sci, USA 74, 3607-3611.

25. Shaugnessy R, Greene SC, Pandey GN and Dorus E (1985) Red-cell lithium transport and affective disorders in multigeneration pedigree: evidence for genetic transmission of affective disorders. Biol Psychiatry 20, 451-460.

26. Ostrow DG, Pandey GN,Davis JM, Hurt SW and Tosteson DC. (1978) A heritable disorder of lithium transport in erythrocytes of a subpopulation of manic-depressive patients. Am J Psychiat 135, 1070-1078.

27. Szentistvanyi I, and Janka Z. (1979) Correlation between lithium ratio and Na dependent Li transport in red blood cells during lithium prophylaxis. Biol Psychiat 14, 973-977.

28. Ramsey TA, Frazer A, Mendels J and Dyson L (1979) The erythrocyte lithium plasma lithium ratio in patients with primary affective disorder. Archs Gen Psychiat 36, 457-461.

29. Frazer A, Mendels J, Brunswick D, London J, Pring M, Ramsey A, and Rybakowski J. (1978) Erythrocyte concentrations of lithium ion: clinical correlates and mechanisms of action. Am J Psychiat 135, 1065-1069.

30. Greil W, Eisenried F, Becker BF and Duhm J (1977) Interindividual differences in the Na^+ -dependent Li^+ countertransport system and in the Li^+ distribution ratio across the red cell membrane among Li^+ treated patients. Psychopharmacologia 53, 19-26.

31. (a) Richelson E, Snyder K, Carlson J, Johnson M, Turner S, Lumry A, Boerwinkle E, and Sing CF (1986) Lithium ion transport in erythrocytes of randomly selected blood donors and manic-depressive patients: lack of association with affective illness. Am J Psychiat 143, 457-462; (b) Mallinger AG and Hanin I (1981) Membrane transport processes in affective illness. In Usdin E and Hanin I (eds.): " Biological Markers in Psychiatry and Neurology ", New York: Pergamon Press, pp. 137-151.

32. Mallinger AG, Mallinger J, Himmelhoch JM, Rossi A and Hanin I (1983) Essential hypertension and membrane lithium transport in depressed patients. Psychiatry Res 10, 11-16.

33. Dagher G, Gay C, Brossard M, Feray JC, Olie JP, Garay RP, Loo H and Meyer P (1984) Lithium sodium and potassium transport in erythrocytes of manic-depressive patients. Acta Psychiatr Scand 69, 24-36.

34. Egeland JA, Kidd JR, Frazer A, Kidd KK and Neuhauser VI (1984) Amish study V: Lithium-sodium countertransport and catechol o-methyltransferase in pedigrees of bipolar probands. Am J Psychiatry 141, 1049-1054

35. Sengupta N, Datta SC and Sengupta D. (1981) Platelet and erythrocyte membrane lipid and phospholipid patterns in different types of mental patients. Biochem Med 25: 267-275.

36. Kuchel P, Hunt GE, Johnson GFS, Beilharz GR, Chapman BE, Jones AJ and Singh BS. (1984) Lithium, red blood cell choline and clinical state: a prospective study in manic-depressive patients. J Affect Disorder 6: 83-94.

37. (a) Domino EF, Sharp RR, Lipper S, Ballast CL, Delidow B and Bronzo MR (1985) NMR analysis of red blood cell constituents in normal subjects and lithium-treated psychiatric patients. Biol Psychiat 20: 1277-1283.; (b) Jones AJ and Kuchel PW (1980) Measurement of choline concentration and transport

in human erythrocytes by ^{1}H NMR: comparison of normal blood and that from lithium treated-psychiatric patients. Clin Chim Acta 104, 77-85.

38. Bunney WE and Garland BL (1984) Lithium and its possible modes of action. In Post RM and Ballenger JC (eds.): "Neurobiology of Mood Disorders", Baltimore: William and Wilkins, pp. 731-743.

39. Bunney WE and Murphy DL (1976) Neurobiological considerations on the mode of action of $LiCO_3^-$ in the treatment of affective disorder. Pharmakopsych 9, 142-147.

40. Aragon MC, Herrero E and Gimenez C (1986) Effects of systematically administered lithium on tryptophan transport and exchange in plasma membrane vesicles isolated from rat brain. Neurochem Res 12, 439-444.

41. Herrero E, Gimenez C and Aragon MC (1987) Chronic administration of lithium modulates tryptophan transport by changing the properties of the synaptosomal plasma membrane. Life Sciences 41, 643-650.

42. Duhm J (1982) Lithium transport pathways in red blood cells. Excerpta Medica 1, 1-19.

43. Kennedy BG, Lunn G and Hoffmann JF (1986) Effects of altering the ATP/ADP ratio on pump mediated Na/K and Na/Na exchanges in resealed human red blood cell ghosts. J Gen Physio 87, 47-72.

44. Dunham PB and Senyk O (1977) Lithium efflux through the Na+/K+ pump in human erythrocytes. Proc Nat Acad Sci, USA 74, 3099-3103.

45. Rodland KD and Dunham PB (1978) Kinetics of active lithium efflux in human erythrocytes. Fed Proc 37, 312-319.

46. Ehrlich BE and Diamond JM (1979) Lithium fluxes in human erythrocytes. Am J Physio 237, C102-C110.

47. Hokin-Neaverson M, Spiegel DA and Lewis WC (1974) Deficiency of erythrocyte sodium pump activity in bipolar manic-depressive psychosis. Life Sciences 15, 1739-1748.

48. El-Mallakh RS (1983) The Na,K ATPase hypothesis for manic-depression: II. The mechanism of action of lithium. Med Hypothesis 12, 269-282.

49. Glen AIM and Reading HW (1973) Regulatory action of Li^+ in manic-depressive illness. The Lancet 12, 1239-1241.

50. Alexander DR, Deeb M, Bitar F and Antun F (1986) Sodium-potassium, magnesium and calcium ATPase activities in erythrocyte membranes from manic-depressive patients responding to lithium. Biol Psychiat 21, 997-1007.

51. Pandey GN, Sarkadi B, Haas M, Gunn RB, Davis JM and Tosteson DC (1978) Lithium transport pathways in human red blood cells. J Gen Physio 72, 233-247.

52. Funder J, Tosteson DC and Wieth JO (1978) Effects of bicarbonate on lithium transport in human red cells. J Gen Physio 71, 721-746.

53. Canessa M, Bize I, Adragna N and Tosteson DC (1982) Cotransport of lithium and potassium in human red cells. J Gen Physio 80, 149-168.

54. Haas M, Schooler J and Tosteson DC (1975) Coupling of lithium to sodium transport in human red cells. Nature 258, 425-427.

55. Garay RP and Hannaert PA (1986) A kinetic analysis of Na-Li countertransport in human red blood cells. J Gen Physio 87, 353-368.

56. Sachs J (1971) Ouabain-insensitive sodium movements in the human red blood cell. J Gen Physio 57, 259-282.

57. Sarkadi B, Alifimoff JK, Gunn RB and Tosteson DC (1978) Kinetics and stoichiometry of Na dependent Li transport in human red blood cells. J Gen Physio 72, 249-265.

58. Duhm J, Eisenried F, Becker BF and Greil W (1976) Studies of lithium transport across the red cell membrane. I. Lithium uphill transport by the Na^+ dependent Li^+ countertransport system of human erythrocytes. Pflugers Arch 364, 147-155.

59. Zaremba D and Rybakowski J (1986) Erythrocyte lithium transport during lithium treatment in patients with affective disorders. Pharmacopsychiat 19, 63-67.

60. Cabantchik ZI and Rothstein A (1974) Membrane

proteins related to anion permeability of human red cell. I. Localization of disulfonic stilbene binding sites in proteins involved in permeation. J Memb Biol 15, 207-226.

61. Mullins LJ (1982) Ion transport in nerve membrane. In Martonosi AN (ed.): The Enzymes of Biological Membranes, vol. 3, New York: Plenum Press, pp 321-334.

62. Duhm J and Becker BF (1977) Studies on lithium transport across the red cell membrane. II. Characterization of ouabain sensitive and ouabain insensitive Li^{+} transport: effects of bicarbonate and dipyridamole. Pflugers Arch 367, 211-219.

63. Feray JC and Garay R (1986) A Na^{+}-stimulated Mg^{+2}-transport system in human red blood cells. Biochim Biophys Acta 856, 76-84.

64. Ramasamy R and Mota de Freitas D (1989) Competition between Li^{+} and Mg^{+2} for ATP in human erythrocytes. A ^{31}P NMR and optical spectroscopy study. FEBS Lett 244, 223-226.

65. Meltzer HL and Kassir S (1983) Abnormal calmodulin-activated Ca^{+2}-ATPase in manic-depressive subjects. J Psychiat Res 17, 29-35.

66. Werstiuk ES, Rathbone MP, and Grof P (1981) Phloretin-sensitive lithium transport in erythrocytes of affectively ill patients: intra-individual reproducibility. Prog Neuropsychopharmacol 5, 503-506.

67. Waters B, Thakar J, and Lapierre Y (1983) Erythrocyte lithium transport variables as a marker for manic-depressive disorder. Neouropsychobiology 9, 94-98.

68. Weder, A, Torreti, BA and Julius S (1984) Racial differences in erythrocyte cation transport. Hypertension (Dallas) 6, 115-123.

69. Ehrlich BE, Diamond JM, and Gosenfield L (1981) Lithium-induced changes in sodium-lithium countertransport. Biochem Pharmacol 30, 2539-2543.

70. Ehrlich BE, Diamond JM, Fry V, and Meier K (1983) Lithium erythrocyte cation transport involves a slow process in the erythrocyte membrane. J Memb Biol 75, 233-240.

71. Rybakowoski J, Potok E, and Strzyzewski W (1981) The activity of the lithium-sodium countertransport system in erythrocytes in depression and mania. J Affective Disord 3, 59-64.

72. Szentistvanyi I, Janka Z, and Szilard J (1980) Clinical significance of Na-dependent Li transport in affective psychoses. Psychiat Clin 13, 57-64.

73. (a) Canessa M, Adragna N, Solomon H, Connolly T and Tosteson DC. (1980) Increased sodium-lithium countertransport in red cells of patients with essential hypertension. N Engl J Med 302, 722-776.; (b) Canessa M, Brugnara C and Escobales N (1987) The Li^+-Na^+ exchange and Na^+-K^+-Cl^- cotransport systems in essential hypertension. Hypertension (Dallas) 10 (Suppl I), I4-I10.

74. Mallinger AG, Mallinger J, Himmelhoch JM, Rossi A and Hanin I (1983) Essential hypertension and membrane lithium transport in depressed patients. Psychiatry Res 10, 11-16.

75. Xie YX and Christian GD (1987) Measurement of serum lithium levels. In Johnson FN (ed):"Depression and Mania," Oxford: IRL Press, pp. 78-88.

76. Vartsky D, LoMonte A, Ellis KJ, Yasumura S and Cohn SH (1988) A method for in vivo measurement of lithium in the body. In Birch NJ (ed.): "Lithium: Inorganic Pharmacology and Psychiatric Use", Oxford, IRL Press, pp. 297-298, and references therein.

77. Trevisan M, Ostrow D, Cooper R, Kiang L, Sparks S, and Stamler J (1981) Methodological assessment of assays for red cell sodium concentration and sodium-dependent lithium efflux. Clin Chim Acta 116, 319-329.

78. Blijenberg BG and Leijinse B (1968) The determination of lithium in serum by atomic absorption spectroscopy and flame emission spectroscopy. Clin Chim Acta 19, 97-99.

79. Kimura K, Tanaka M, Kitazawa S and Shono T (1985) Highly-selective crown ether dyes for extraction photometry. Chemistry Lett 1239-1240.

80. Wheeling K and Christian GD (1984) Spectrofluorimetric determination of serum lithium using 1,8-dihydroxyanthraquinone. Anal Lett 17,

217-227.

81. Pacey GE, Wu YP, and Sasaki K (1987) Selective determination of lithium in biological fluids using flow injection analysis. Anal Biochem 160, 243-250.

82. Gadzepko VPY, Hungerford JM, Kadry AM, Ibrahim YA, Xie RY, and Christian GD (1986) Comparative study of neutral carriers in polymeric lithium ion selective electrodes. Anal Chem 58, 1948-1953.

83. Sakamoto H, Kimura K, and Shono T (1987) Lithium separation and enrichment by proton-driven cation transport through liquid membranes of lipophilic crown nitrophenols. Anal Chem 59, 1513-1517.

84. Metzger E, Dohener R, Simon W, Vonderschmitt DJ, and Gautschi K (1987) Lithium/sodium ion concentration ratio measurements in blood serum with lithium and sodium ion selective liquid membrane electrodes. Anal Chem 59, 1600-1603.

85. Xie RY and Christian GD (1986) Serum lithium analysis by coated wire lithium ion selective electrodes in a flow injection analysis dialysis system. Anal Chem 58, 1806-1810.

86. Thellier M, Wissocq J-C, and Monnier A (1988) Methods for studying the distribution and transport of lithium. In Birch NJ (ed.): "Lithium: Inorganic Pharmacology and Psychiatric Use", Oxford, IRL Press, pp. 271-274.

87. Rosenthal J, Strauss A, Minkoff L, and Winston A (1986) Identifying lithium-responsive bipolar depressed patients using nuclear magnetic resonance. Am J Psychiatry 143, 779-780.

88. Ranguel-Guerra RA, Perez-Payan H, Minkoff L, and Todd LE (1983) Nuclear magnetic resonance in bipolar disorders. A J N R 4, 229-231.

89. Diamond JM, Meier K, Gosenfeld LF, Jope RS, Jenden DJ and Wright SM (1983) Recovery of erythrocyte Li^+/Na^+ countertransport and choline transport from lithium therapy. J Psychiat Res 17, 385-393.

90. Renshaw PF, Haselgrove JC, Leigh JS, and Chance B (1985) In vivo nuclear magnetic resonance imaging of lithium. Magn Reson Med 2, 512.

91. Renshaw PF, Haselgrove JC, Bolinger L, Chance B, and

Leigh JS (1986) Relaxation and imaging of lithium in vivo. Magn Reson Imag 4, 193.

92. Renshaw PF and Wicklund S (1988) In vivo measurement of lithium in humans by nuclear magnetic resonance spectroscopy. Biol Psychiatry 23, 465-475.

93. Espanol MT and Mota de Freitas D (1987) ^{7}Li NMR studies of lithium transport in human erythrocytes. Inorg Chem 26, 4356-4359.

94. (a) Gupta RJ and Gupta P (1982) Direct observation of resolved resonances from intra- and extracellular sodium-23 ions in NMR studies of intact cells and tissues using dysprosium (III) tripolyphosphate as paramagnetic shift reagent. J Magn Reson 47, 344-350; (b) Gupta RK (1987) ^{23}Na NMR Spectroscopy of intact cells and tissues. In Gupta RK (ed.): "NMR Spectroscopy of Cells and Organisms," vol.2, Boca Raton: CRC Press, pp. 1-32.

95. Brophy PJ, Hayer MK, and Ridell FG (1983) Measurement of intracellular potassium concentrations by NMR. Biochem J 210, 961-963.

96. Mota de Freitas D, Espanol MT, and Ramasamy R (1988) ^{7}Li NMR studies of lithium transport in red cells of manic-depressive patients and normal controls. In Birch NJ (ed.): "Lithium: Inorganic Pharmacology and Psychiatric Use", Oxford, IRL Press, pp. 281-284.

97. Ramasamy R, Espanol MT, Long KM, Geraldes CFGC, and Mota de Freitas (1989) Aqueous shift reagents for ^{7}Li NMR transport studies in cells. Inorg Chim Acta, submitted for publication.

98. Ogino T, Shulman GI, Avison MJ, Gullans SR, Den Hollander JA and Shulman RG (1985) ^{23}Na and ^{39}K NMR studies of ion transport in human erythrocytes. Proc Nat Acad Sci USA 82, 1019-1033.

99. Peters JA and Kieboom APG (1983) Multinuclear magnetic resonance in the presence of lanthanide (III) as an analytical tool for structure determination in solution. Recl Trav Chim Pays-Bas 102, 381-392.

100. Davis DG, Murphy E and London RE (1988) Uptake of cesium ions by human erythrocytes and perfused rat hearts: a cesium-133 study. Biochemistry 27, 3547-3551.

101. Hughes MS, Flavell KJ, and Birch NJ (1988) Transport of lithium into human erythrocytes as studied by ^{7}Li NMR and atomic absorption spectroscopy. Biochem Soc Trans 16, 827-828.

102. Shinar H and Navon G (1986) Novel organometallic ionophore with specificity toward Li^{+}. J Am Chem Soc 108, 5005-5006.

103. Mota de Freitas D, Espanol MT, Ramasamy R, Silberberg JW, Dorus W, Bansal V, and Labotka R (1989) Measurement of rates of Na^{+}-Li^{+} countertransport and Li^{+} ratios in human erythrocytes by ^{7}Li NMR Spectroscopy (submitted to Biophysi J for publication).

104. Mota de Freitas D, Espanol M and Ramasamy R (1989) Measurement of lithium transport across human erythrocyte membranes by ^{7}Li NMR spectroscopy. In Butterfield A (ed): "Biological and Synthetic Membranes," New York: Alan Liss Inc., in press.

105. Pettegrew JW, Post JFM, Pangchalingam K, Withers G and Woessner DE (1987) ^{7}Li NMR study of normal human erythrocytes. J Magn Reson 71, 504-519.

106. Seo Y, Murakami M, Suzuki E, and Watari H (1987) A new method to discriminate intracellular and extracellular K by ^{39}K NMR without chemical shift reagents. J Magn Reson 75, 529-533.

107. Degani H and Elgavish GA (1978) Ionic permeabilities of membranes: ^{23}Na and ^{7}Li NMR studies of ion transport across the membrane of phosphatidylcholine vesicles. FEBS Lett 10, 357-360.

108. Andrasko J (1976) Measurement of membrane permeability to slowly penetrating molecules by a pulse gradient NMR method. J Magn Reson 21, 479-484.

109. Conlon T and Outhred R (1972) Water diffusion permeability of erythrocytes using NMR technique. Biochim Biophys Acta 288, 354-361.

110. Deutcke B and Haest CWM (1987) Lipid modulation of transport proteins in vertebrate cell membranes. Ann Rev Physio 49, 221-235.

111. Gadian DG (1982) NMR and its Applications to Living Systems. Clarendon Press, Oxford.

112. Chu SC, Pike MM, Fossel ET, Smith TW, Balschi JA and Springer CS Jr (1984) High resolution cationic NMR shift reagents. J Magn Reson 56, 33-43.

113. Boulanger Y, Vinay P and Desroches M (1985) Measurement of a wide range of intracellular sodium concentration in erythrocytes by ^{23}Na nuclear magnetic resonance. Biophys J 47, 553-561.

114. Pandey GN, Baker J, Chang S and Davis JM (1978) Prediction of in vivo red cell/plasma Li^+ ratios by in vitro methods. Clin Pharm Thera 24, 343-349.

115. Steck TL and Kant JA (1974) Preparation of impermeable ghosts and inside-out vesicles from human erythrocyte membranes. Methods in Enzymology 31, 172-180.

116. Yu J, Fischman DA and Steck TL (1973) Selective solubilization of proteins and phospholipids from red blood cell membranes by non-ionic detergents. J Supra Struc 254, 233-247.

117. Bennett V and Branton D (1977) Selective association of spectrin with the cytoplasmic surface of human erythrocyte plasma membrane. J Biol Chem 252, 2753-2763.

118. Fung LW-M (1981) Spin-label detection of hemoglobin membrane interaction at physiological pH. Biochem 20, 7162-7166.

119. (a) Waterman M (1978) Spectral characterization of human hemoglobin and its derivatives. Methods in Enzym 52, 456-459; (b) Drabkin DL (1946) Spectrophotometric studies XIV: the crystallographic and optical properties of the hemoglobin of man in comparison with those from other species. J Biol Chem 164, 703-710.

120. Ridell FG and Arumugam S (1988) Surface charge effects upon membrane transport processes: the effects of membrane surface charge on the monensin-mediated transport of lithium ions through the phospholipid bilayers studied by ^{7}Li NMR spectroscopy. Biochim Biophys Acta 945, 65-72.

121. Kurland R, Newton C, Nir S and Papahadjopoulos D (1979) Specificity of Na^+ binding to phosphatidylserine vesicles from a ^{23}Na NMR relaxation rate study. Biochim Biophys Acta 551, 137-147.

122. Bradford M (1976) A Coomasie blue assay for proteins. Anal Biochem 72, 248-254.

123. (a) Lowry OH and Lopez JA (1946) The determination of inorganic phosphate in the presence of labile phosphate esters. J Biol Chem 162, 421-428; (b) Chen PS Jr, Toribara TY and Warner H (1956) Microdetermination of phosphorus. Anal Chem 28, 1756-1758.

124. Eylar EH, Madoff MA, Brody OV and Oncley JL (1962) The contribution of sialic acid to the surface charge of the erythrocyte, J Biol Chem 237, 1992-1202.

125. Lichtenberg D (1988) Liposomes: preparation, characterization and preservation. Method Biochem Anal 33, 337-462.

126. Den Bosch HV (1982) Phospholipases. In Hawthorne JN and Ansell GB (eds.): "Phospholipids," Amsterdam:Elsevier Biomedical Press, pp.313-351.

127. Niewenhuizen MS, Peters JA, Sinnema A, Kieboom APG and Bekkum HV (1985) Multinuclear study of the complexation of lanthanide (III) cations with sodium triphosphate: induced shifts and relaxation enhancements. J Am Chem Soc 107,12-16.

128. Newton C, Pangborn W, Nir S and Papahadjoupoulos D (1978) Specificity of Ca^{+2} and Mg^{+2} binding to phosphatidylserine vesicles and resultant phase changes of bilayer membrane structure. Biochim Biophys Acta 506, 281-287.

129. Surgenor M (1974) The Red Blood Cell. New York: Academic Press.

130. Connors KA (1987) Binding Constants. John Wiley: New York, pp.189-215.

131. Bull TE, Andrasko J, Chiancone E and Forsen S (1973) Pulsed nuclear magnetic resonance studies on ^{23}Na, ^{7}Li and ^{35}Cl binding to human oxy- and carbon monoxyhemoglobin. J Mol Biol 73, 251-259.

132. Steck TL (1974) The organization of proteins in the human red blood cell membrane. J Cell Bio 62, 1-19.

133. Bolin RB and Venuto F (1983) Hemoglobin solutions as blood substitute. In Bolin RB, Geyer RP, Nemo GJ (eds.): " Advances in Blood Substitute Research,"New

York: Alan Liss, Inc., pp. 1-7.

134. Schwartz RS, Chiu DTY and Lubin B (1984) Studies on the organization of plasma membrane phospholipids in human erythrocytes. In Kruckeberg WC, Eaton JW, Aster J and Brewer GJ (eds.): " Erythrocyte Membranes 3: Recent Clinical and Experimental Advances," New York: Alan Liss, pp. 89-122.

135. Cullis PR and Hope MJ (1985) Physical Properties and functional roles of lipids in membranes. In Vance DE and Vance JE (eds.): "Biochemistry of Lipids and Membranes," California: Benjamin/Cummings Publ Co, pp. 25-72.

136. Casal HL and Mantsch HH (1987) Infrared studies of fully hydrated saturated phosphatidylserine bilayers. Effect of Li^{+} and Ca^{+2}. Biochemistry 26, 4408-4416.

137. Fossel ET, Sarasua MM and Koeler KA (1985) A lithium-7 NMR investigation of the lithium ion interaction with phosphatidylcholine-phosphatidylglycerol membrane. Observation of calcium and magnesium ion competition. J Magn Reson 64, 536-540.

138. Pettegrew JW, Short JW, Woessner RD, Strychor M, McKeag KW, Armstrong J, Minshew NJ and Rush AJ (1987) The effects of lithium on the membrane molecular dynamics of normal human erythrocytes. Biol Psychiatry 22, 857-871.

139. Hitzemann RJ and Garver DL (1982) Abnormalities in membrane lipids associated with deficiencies in lithium counterflow. In Usdin E and Hanin I (eds.): " Biological Markers in Psychiatry and Neurology," Oxford: Pergamon Press, pp. 177-182.

140. Henn FA and Henn SW (1982) Phospholipids as markers in schizophrenia. In Usdin E and Hanin I (eds.): " Biological Markers in Psychiatry and Neurology," Oxford: Pergamon Press, pp. 183-186.

141. Hanin I (1982) Red blood cell choline as a potential marker in psychiatric and neurologic disease. In Usdin E and Hanin I (eds.): " Biological Markers in Psychiatry and Neurology," Oxford: Pergamon Press, pp. 187-189.

142. Callahan J (1985) Phospholipids in disorders of the nervous system. In Eichberg J (ed.): "Phospholipids

in Nervous Tissues," New York: John Wiley, pp. 297-320.

APPROVAL SHEET

The dissertation submitted by Maryceline Tiausas Espanol has been read and approved by the following committee:

Dr. Duarte Mota de Freitas, Director
Assistant Professor, Chemistry, Loyola

Dr. David Crumrine
Professor, Chemistry, Loyola

Dr. Kenneth Olsen
Professor, Loyola

Dr. Leslie Wo-Mei Fung
Professor, Loyola

Dr. Thomas V. O'Halloran
Assistant Professor, Northwestern University

The final copies have been examined by the director of the dissertation and the signature which appears below verifies the fact that any necessary changes have been incorporated and that the dissertation is now given final approval by the committee with reference to content and form.

The dissertation is therefore accepted in partial fulfillment of the requirement for the degree of Doctor of Philosophy.

4/19/89
Date

Director's Signature